Vol. 55 • No. 7

July 2012

Microwave Journal

EXPERT TIPS, TRICKS & TECHNIQUES

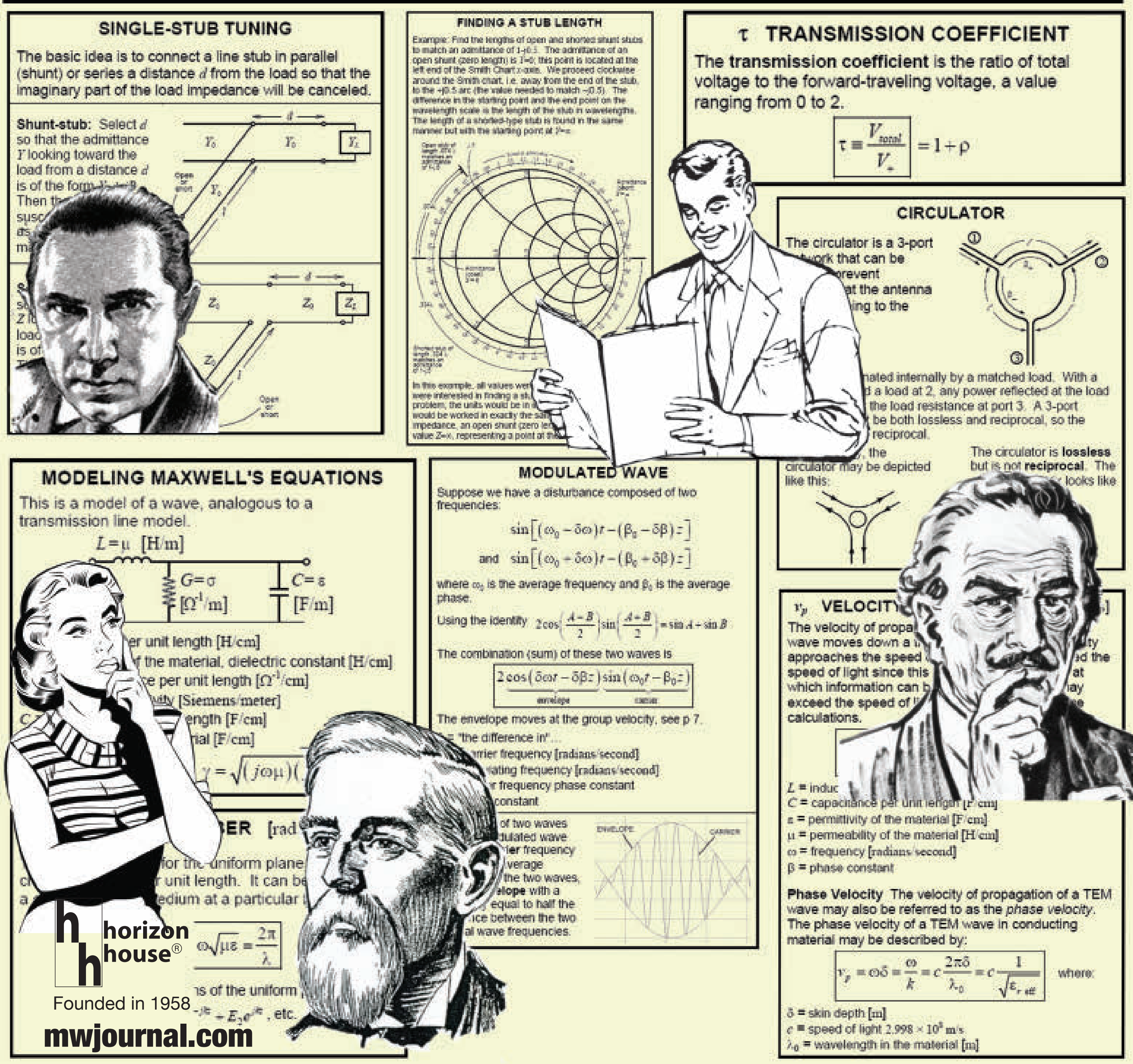

horizon house®

Founded in 1958

mwjournal.com

July 2012

Microwave Journal®

Software and Design

Vol. 55 • No. 7

DIRECT MODULATION MICROWAVE

FIBER OPTIC LINKS To 20 GHz

FEATURES:

- Low Noise Figure
- Low Signal Loss (Typ. RF Loss: 0.4 dB/km)
- Small Size And Low Power Consumption
- No External Control Circuits Required
- Variable Gain Control Option In Receiver
- High Reliability Models Available - HRL
- Custom Configurations Available
- Backed By A 3-Year Warranty*

WIDE RANGE OF APPLICATIONS:

- EMC Testing · Antenna Remoting · Radio Over Fiber
- Interfacility RF Communication Link · Radio Astronomy
- Radar Applications · Aircraft And Shipboard Applications
- SATCOM Applications · Links For Satellite Ground Stations
- ELINT, EW And EMC Applications · Tactical Common Data Links

Electrical Specifications (1 Meter of Fiber)

Series	Frequency	Gain (dB)	Noise Figure (dB)	Input Power @ P1dB (dBm, Min.)	Spurious Free Dynamic Range (dB/Hz, Typ.)	Phase Noise (dBc, Typ.)	Group Delay (ns)	VSWR (In/Out)	Available Wavelengths: Standard (nm)	Available Wavelengths: Optional Wavelengths
Transmitters and Receivers										
SLL	5 kHz - 2.5 GHz	12	18	-14	103	>100	0.2	2:1	1550/1310	18 CWDM Ch
	100 MHz - 2.5 GHz	12	18	-14	103	>100	0.2	2:1	1550/1310	18 CWDM Ch
LBL	50 KHz - 3 GHz	15	11	-14	106	>100	0.2	2:1	1550/1310	18 CWDM Ch, 45 DWDM Ch
	50 KHz - 4.5 GHz	15	11	-14	106	>100	0.2	2:1	1550/1310	18 CWDM Ch, 45 DWDM Ch
	10 MHz - 3 GHz	15	11	-14	106	>100	0.2	2:1	1550/1310	18 CWDM Ch, 45 DWDM Ch
	10 MHz - 4.5 GHz	15	11	-14	106	>100	0.2	2:1	1550/1310	18 CWDM Ch, 45 DWDM Ch
LBL-HD	950 MHz - 2.5 GHz	0	22	7	114	>100	0.2	2:1	1550/1310	18 CWDM Ch
SCML	50 kHz - 6 GHz	15	15	-14	103	>100	0.2	2:1	1550	1310/1490 nm
	100 MHz - 6 GHz	15	15	-14	103	>100	0.2	2:1	1550	1310/1490 nm
	100 MHz -11 GHz	15	15	-14	103	>100	0.2	2:1	1550	1310/1490 nm
	100 MHz -13 GHz	15	15	-14	103	>100	0.2	2:1	1550	1310/1490 nm
	100 MHz -15 GHz	15	15	-14	103	>100	0.2	2:1	1550	1310/1490 nm
	100 MHz - 18 GHz	15	15	-14	103	>100	0.2	2:1	1550	1310/1490 nm
	10 MHz - 18 GHz	15	15	-14	103	>100	0.2	2:1	1550	1310/1490 nm
HRL	50 KHz - 6 GHz	20	12	-14	103	>100	0.2	2:1	1550	1310/1490 nm
High Gain Broadband Receivers										
DR-125G-A	30 KHz - 12.5 GHz	35 O/E (or TIG = 2800 ohms)						2:1		1280-1580
SCMR-100K20G	100 KHz - 20 GHz	32 O/E (or TIG = 2000 ohms)						2:1		1280-1580

CWDM: Course Wavelength Division Multiplexing, DWDM: Dense Wavelength Division Multiplexing

Enclosures Are Available For Multiple Tx or Rx Combinations

For additional information or technical support, please contact our Sales Department at (631) 439-9220 or e-mail components@miteq.com

MITEQ

100 Davids Drive • Hauppauge, NY 11788
TEL.: (631) 436-7400 • FAX: (631) 436-7430
www.miteq.com

*3-year warranty applies to rack-mounted and indoor equipment


MCL B 744
ADP-2-10
MCL B 744
ADP-2-10
MCL B 744
ADP-2-10

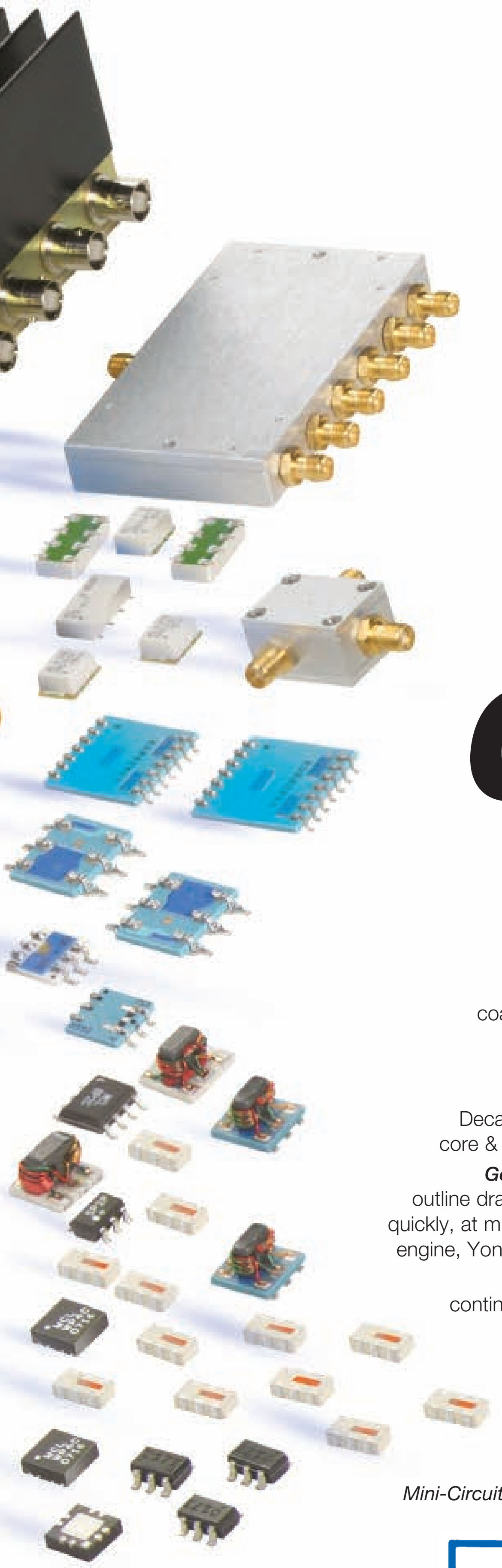

Your supplier of high performance, precise equipment for AWGN

NOISEWAVE
The new wave in NOISE

Ph. (973) 386-1119 • Fax (973) 386-1131 • info@noisewave.com • www.noisewave.com

Microwave Journal

JULY 2012 VOL. 55 • NO. 7

NOTE FROM THE EDITOR

20 **Eye on EDI CON**
David Vye, Microwave Journal *Editor*
Highlights the EDI CON 2013 conference and trade show that will take place in Beijing in 2013

COVER FEATURE

22 **Expert Tips, Tricks and Techniques**
Invited seasoned and well-respected professionals share their tips, tricks and techniques on a range of subjects covering areas such as testing, tweaking and troubleshooting

22 Dr. Ajay Poddar, Synergy Microwave
24 Ray Pengelly, Cree
26 Rafi Hershtig, K&L Microwave
28 Dr. Nickolas Kingsley, Auriga Microwave
30 David Hall, National Instruments
32 Dominic FitzPatrick, Principal Consultant
34 Liam Devlin, Plextek Ltd.
36 Andy Howard, Agilent Technologies
38 Chris Marki, Marki Microwave

SPECIAL REPORTS

56 **Testing Radar and EW Systems for the Real-World**
Dingqing Lu, Agilent Technologies
Presents a combination of COTS instrumentation and EDA software that makes it easier to create scenarios for testing radar and EW systems in a complex EM environment

64 **The 3D Smith Chart and Its Practical Applications**
Andrei Müller, Dan C. Dascalu, IMT-Bucharest; Pablo Soto, Vicente E. Boria, University Politécnica de Valencia
In-depth look at the 3D Smith chart and how the 2D and 3D Smith charts deal with the infinite regions, and advantages of using the 3D Smith chart to represent both active and passive loads using real example devices

Microwave Journal (USPS 396-250) (ISSN 0192-6225) is published monthly by Horizon House Publications Inc., 685 Canton St., Norwood, MA 02062. Periodicals postage paid at Norwood, MA 02062 and additional mailing offices.

POSTMASTER: Send address corrections to *Microwave Journal*, PO Box 3256, Northbrook, IL 60065-3256 or e-mail mwj@omeda.com. Subscription information: (847) 291-5216. This journal is issued without charge upon written request to qualified persons working in the RF & microwave industry. Other subscriptions are: domestic, $120.00 per year, two-year subscriptions, $185.00; foreign, $200.00 per year, two-year subscriptions, $370.00; back issues (if available) and single copies, $10.00 domestic and $20.00 foreign. Claims for missing issues must be filed within 90 days of date of issue for complimentary replacement.

Posted under Canadian international publications mail agreement #PM40612608

AWR

A National Instruments Company™

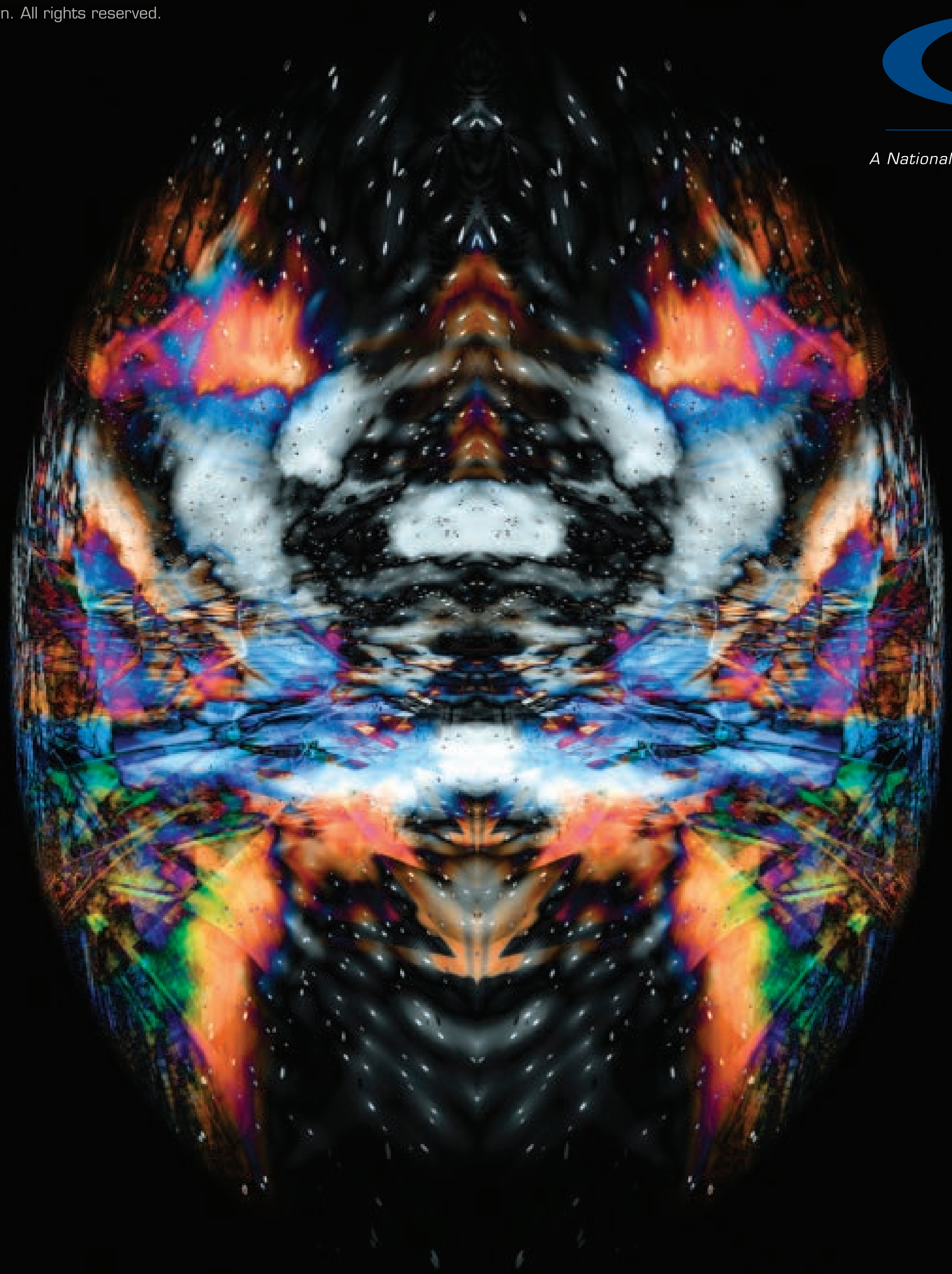

EM speed that will turbocharge your design creativity.

Stop waiting and wishing for an EM tool that keeps pace with your own creative ideas. AXIEM is capable of solving big problems fast — typically 10x faster than current alternatives for designs of 10K unknowns or more. And now that it handles antennas, too, your creativity will know no bounds. For the most accurate EM results in minutes rather than hours, go with AXIEM. Grab a test copy today at awrcorp.com/AXIEM.

Stop waiting and start designing™

AXIEM®
3D PLANAR EM

Microwave Journal

TECHNICAL FEATURES

74 **Comparing Microstrip and CPW Performance**

John Coonrod, Rogers Corp. and Brian Rautio, Sonnet Software Inc.

In-depth look at building a better EM simulation model that includes the effects of a PCB's metal surface roughness, microstrip and coplanar waveguide circuits while closely comparing to find the best fit for different applications

88 **PA Termination Impedance Selection Utilizing Temperature Contours**

Alan Victor and Walter Nagy, Nitronex Corp.

Presents a power amplifier technique that focuses on control of device temperature rise by careful selection of the termination impedance

PRODUCT FEATURES

100 **Highly Integrated 60 GHz Radio Transceiver Chipset**

Hittite Microwave Corp.

Introduction to a highly integrated silicon chipset solution in recognition of important developments taking place in the 57 to 64 GHz band

108 **1 to 650 MHz Ultra Low Noise OCXOs**

Wenzel Associates Inc.

Introduction to the Citrine Series crystal oscillators developed to provide a broad product offering for demanding applications requiring low phase noise performance in both static and dynamic conditions

114 **New Thermal Solver for RF Applications**

IMST GmbH

Introduction to the latest release, the EMPIRE XCcel 3D EM solver featuring a thermal solver for the simulation of the temperature distribution of power electronics, RF circuits and ICs, as well as EM heating in the human body

Departments

17.... Mark Your Calendar
18.... Coming Events
41.... Defense News
45.... International Report
49.... Commercial Market
52.... Around the Circuit
118.... Catalog Update
122.... New Products
126.... The Book End
128.... Ad Index
128.... Sales Reps
130.... MWJ Puzzler

Executive Editorial Office:
685 Canton Street, Norwood, MA 02062
Tel: (781) 769-9750
FAX: (781) 769-5037
e-mail: mwj@mwjournal.com

European Editorial Office:
16 Sussex Street, London SW1V 4RW, England
Tel: Editorial: +44 207 596 8730 Sales: +44 207 596 8740
FAX: +44 207 596 8749

www.mwjournal.com

Printed in the USA

Microwave Journal Online

Visit us @ mwjournal.com

Free Webinars

Innovations in Signal Analysis
by: Agilent Technologies
Wireless Site Survey Using a Handheld Spectrum Analyzer — 7/11/12 at 1:00 PM ET

Agilent in Aerospace/Defense
Phase Noise Measurement Methods and Techniques — 7/19/12 at 1:00 PM ET

Agilent in LTE
Wideband Digital Pre-Distortion Modeling for LTE-Advanced — 7/26/12 at 1:00 PM ET

Web Survey

Your most productive month is...

Look for our multiple choice survey online at mwjournal.com

May Survey

"What do you like best about IMS?"

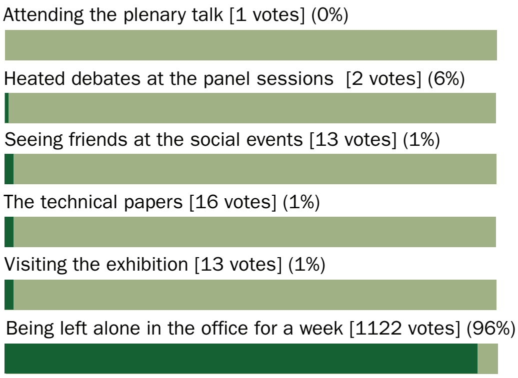

Executive Interview

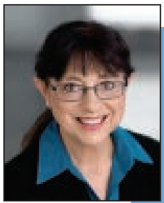

Liz Ronchetti, owner of **Wenzel Associates,** talks about the joys of engineering and finding opportunities for a company willing to take on the most challenging custom design requirements in high precision frequency control.

White Papers

Measurement of Group Delay Using the 6840 Series Microwave System Analyzer
White Paper, Aeroflex

IMS Architecture: The LTE User Equipment Perspective
White Paper, Spirent Communications

Intermodulation Distortion in RF Connectors
White Paper, RF Industries

Impact of Materials on Microwave Cable Performance
White Paper, W. L. Gore & Associates

Harmonic Mixer Primer: The Gateway to the Millimeter Wave Frontier is Harmonic Mixer Technology
David Vondran, OML Inc.

RF & Microwave Community Watch

in

Over **12,360** Members

Recent Discussions:

Francisco is looking to simulate a dual-shaped antenna

Wayne has found a nano-tube that operates at 0.46 THz

Michal wants to share a phase noise & VCO Biasing video

COM

29

More Q. Less Cu

Copper
63.546

These tiny new air core inductors have the highest Q and current handling in the smallest footprint.

Coilcraft's new SQ air core inductors have unmatched Q factors: most are above 200 in the 1-2 GHz range! That's 3 times higher than comparably sized 0805 chip coils.

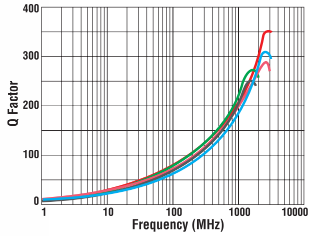

Q factors are 3X higher than standard chip inductors

And with their extremely low DCR, they can handle 4 to 8 times more current: up to 4.4 Arms.

SQ air core inductors are perfect for your LC filter and RF impedance matching applications. They come in 15 values ranging from 6 to 27.3 nH, all with 5% tolerance.

These coils are significantly smaller than existing air core inductors. We reduced the footprint by using close-wound construction and keeping the leads close to the body. The square shape cuts the height to as low as 1.5 mm and creates flat top and bottom surfaces for easy automated handling and stable mounting.

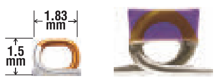

The square shape and narrow footprint reduce board space by 60-75% over conventional air core inductors.

See how the ultra-high Q and current handling of Coilcraft's new SQ air core inductors can maximize the performance of your next design. For complete specifications and free evaluation samples, visit **www.coilcraft.com/sq**

Coilcraft®

www.coilcraft.com 800/322-2645

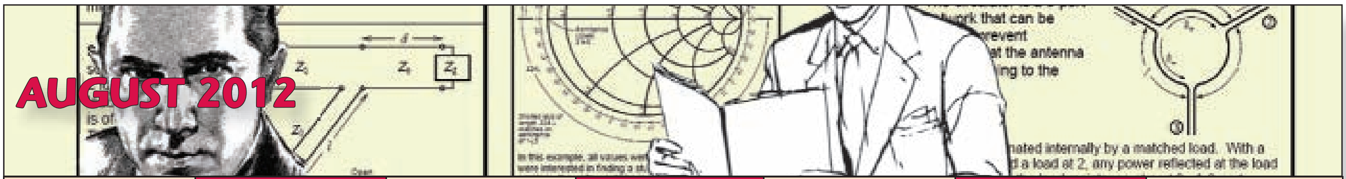

SUNDAY	MONDAY	TUESDAY	WEDNESDAY	THURSDAY	FRIDAY	SATURDAY
29	30	31	1 ediconchina.com EDI CON **Call for Papers Deadline** **Webinar: Innovations in EDA** Sponsored by Agilent Technologies	2	3	4
5 **EMC 2012** Pittsburgh, PA	6 AUVSI'S 2012 Las Vegas, NV; NATIONAL INSTRUMENTS **NI WEEK 2012** Austin, TX	7	8	9 **Webinar: Agilent in Wireless Communications** Sponsored by Agilent Technologies	10	11
12	13	14	15	16 **Webinar: Agilent in Aerospace/Defense** Sponsored by Agilent Technologies	17	18
19	20	21	22	23 **Webinar: Agilent in LTE** Sponsored by Agilent Technologies	24	25
26	27	28	29	30	31	1

Go to: mwjournal.com/events

Coming Events

CALL FOR PAPERS

EDI CON 2013
Deadline: August 1, 2012

IEEE International Symposium on RF Integration Technology
Deadline: August 6, 2012

Microwave Update 2012
Deadline: August 18, 2012

mwjournal.com

AUGUST

IEEE EMC 2012
August 5–10, 2012 • Pittsburgh, PA
http://2012emc.org

AUVSI Unmanned Systems N. America 2012
August 6–9, 2012 • Las Vegas, NV
www.auvsishow.org

NI Week 2012
August 6–9, 2012 • Austin, TX
www.ni.com/niweek

SEPTEMBER

MMS 2012
12th Mediterranean Microwave Symposium
September 2–5, 2012 • Istanbul, Turkey
www.mms2102.org

MWP 2012
IEEE International Topical Meeting on Microwave Photonics
September 11–14, 2012
Noordwijk, The Netherlands
www.congrexprojects.com/12A11

ICUWB 2012
IEEE International Conference on Ultra-Wideband
September 17–20, 2012 • Syracuse, NY
www.icuwb2012.org

ION GNSS 2012
September 17–21, 2012 • Nashville, TN
www.ion.org/meetings/?conf=gnss

PT/Expo Comm China 2012
September 18–22, 2012 • Beijing, China
www.expocommcn.com

AOC 2012
49th Annual AOC International Symposium and Convention
September 23–26, 2012 • Phoenix, AZ
www.crows.org/conventions/conventions.html

OCTOBER

COMSOL Conference 2012
8th Annual Multiphysics Conference
October 3–5, 2012 • Boston, MA
www.comsol.com/conference2012/usa

MUD 2012
Microwave Update
October 18–21, 2012 • Santa Clara, CA
www.microwaveupdate.org

AMTA 2012
34th Annual Symposium of the Antenna Measurement Techniques Association
October 21–26, 2012 • Bellevue, WA
www.amta.org

RADAR 2012
International Conference on Radar
October 22–25, 2012 • Glasgow, UK
www.radar2012.org

EuMW 2012
European Microwave Week
October 28–November 2, 2012
Amsterdam, The Netherlands
www.eumweek.com

MILCOM 2012
Military Communications Conference
October 29–November 1, 2012 • Orlando, FL
www.milcom.org

4G World 2012
October 29–November 1, 2012 • Chicago, IL
www.4gworld.com

NOVEMBER

IME 2012
7th International Conference and Exhibition on Microwave and Antenna
November 5–7, 2012 • Shanghai, China
www.imwexpo.com

electronica 2012
November 13–16, 2012 • Munich, Germany
www.electronica.de

DECEMBER

APMC 2012
Asia Pacific Microwave Conference
December 4–7, 2012 • Kaohsiung, Taiwan
www.apmc2012.com

JANUARY

IEEE RWS 2013
Radio and Wireless Symposium
January 20–23, 2013 • Austin, TX
www.radiowirelessweek.org

IEEE MEMS 2013
26th IEEE International Conference on Micro Electro Mechanical Systems
January 20–24, 2013 • Taipei, Taiwan
www.mems2013.org

FEBRUARY

NATE 2013
18th Annual Conference & Exposition for the National Association of Tower Erectors
February 18–21, 2013 • Fort Worth, TX
http://natehome.com/annual-conference

MARCH

EDI CON 2013
Electronic Design Innovation Conference
March 12–14, 2013 • Beijing, China
www.ediconchina.com

EDI CON Electronic Design Innovation Conference 电子设计创新会议 2013

Eye on EDI CON

EDI CON, the new conference/exhibition being organized by Microwave Journal and Horizon House for next March in Beijing, reflects the industry trend to broaden its scope on multiple fronts – technology, geography and opportunity.

With regard to technology, EDI CON is an acknowledgment that today's electronics are developed through multiple disciplines, targeting diverse platforms. Highly specialized engineering skills must integrate with other knowledge centers. As physical component-level design goes hand in hand with system integration, the component designer must be cognizant of system requirements and vice versa. Supported by new technologies (i.e., semiconductors, materials, passives, interconnect, etc.) and new solutions in simulation and testing, the designer is both empowered and perhaps overwhelmed. Meanwhile, the challenges facing physical design at RF and microwave frequencies are virtually equivalent to those of high speed multi-gigabit design. Much of the difference is in terminology. Knowledge of system-level and high-speed design along with newly available technologies at the individual engineering level leads to professional advancement and allows our industry as a whole to grow.

Regarding geography, technology's steady march forward is driven by need and opportunity, both of which are in abundance in the world's largest emerging markets. The correlation between a country's access to information technology and its wealth has the governments of India and China looking to develop infrastructure on par with leading economies. As a result, they are heavily investing in technology and the training to either buy it or build it. Responding to Beijing policies, Chinese universities have produced a large population of engineers and the country is now home to many leading, multi-national technology companies as well as home-grown telecommunication giants such as Huawei and ZTE. Keeping in step with the global aspirations of our industry, EDI CON will join these companies in China to provide a forum for face-to-face interaction.

As for opportunity, the "I" in EDI CON stands for innovation – the act of introducing new things and methods through innovative thinking. In 2006, the Chinese government introduced an "indigenous innovation" policy to help steer its economy from low wage manufacturing to higher wage design. The initial policy, which gave preferential treatment to Chinese companies over multi-nationals, has since been modified to encourage innovation regardless of the company's origins. This is appropriate as many of these North American - and European - based companies operating in China are being staffed by Chinese engineers with a wide range of skills, working closely with their respective companies' global engineering teams. EDI CON will be that opportunity for all parties to exchange knowledge, understand new challenges and discover opportunities for growth. Innovation brought on by the confluence of technologists from all over the world for the benefit of the entire microwave community, regardless of location.

With this in mind, we now are accepting papers for presentation in Beijing, March 2013.

David Vye
Microwave Journal Editor

Microwave Journal invited the following contributors to share their tips, tricks and techniques in this month's cover feature. Call them Gigahertz Gurus or Microwave Merlins, each contributor was asked to offer up some useful advice covering areas such as testing, tweaking and troubleshooting in approximately 500 words or less.

COVER FEATURE
INVITED PAPERS

HOW LOW CAN YOU GO

Optimizing Phase Noise

Communication systems rely on a low-phase-noise VCO for reliable voice communications and to ensure transmitted data integrity. As data requirements increase beyond 2 Gb/s, the phase noise of the VCO becomes critical for achieving acceptable bit-error-rate (BER) performance. For low phase noise signal source (VCO) applications, simple tips can cut the design time and be useful for oscillator design engineers.

The frequency tuning feature is realized in an LC resonator VCO by varying the capacitance of the tuning diodes (Varactors). Select low loss resistance varactors and implement back-to-back in the tuning circuit for the minimization of tuning network noise. Care must be taken to avoid breakdown, saturation, or overheating effects in the varactor at the cost of reduced loaded-Q.

Maximize the resonator loaded Q-factor (high group delay); in the series LC-resonant circuits preferably use a large inductor, and in parallel LC-resonant circuits a large capacitor. Care must be taken to suppress the undesired modes in a high Q-factor resonator (especially quartz crystal, ceramic and acoustic resonators) by optimizing the drive-level across the resonator for a given dominant mode.

Use an active device (Bipolar/FET) with low 1/f noise and noise figure at operating frequencies. The trade-off is to use a high frequency transistor that has a small junction capacitance and operate it at moderately high bias voltage to reduce phase modulation due to junction capacitance noise modulation. Care must be taken to prevent modulation of the input and output dynamic capacitances of the transistor, otherwise it leads to amplitude-to-phase conversion and therefore introduces noise.

Since all noise sources, except thermal noise, are generally proportional to the average current flow through the active device, it is logical that reducing the current flow through the device will lead to lower noise levels. The 1/f noise depends on the current density in the transistor, therefore transistors with high I_{cmax} used at low currents will exhibit low flicker noise contribution. In BJTs, as VCE increases, the flicker corner increases as the white noise increases, but the magnitude of the 1/f noise is constant. As base current increases, the flicker corner frequency increases with the magnitude of the 1/f noise and the increased shot noise current. The effect of flicker noise can be reduced through RF feedback. An un-bypassed emitter resistor of a few ohms in a BJT circuit can improve the flicker noise significantly.

Passive components in the oscillator circuit also exhibit short-term instability. Passive components (resistors, capacitors, inductors, reverse-biased, varactor diodes) exhibit varying levels of flicker-of-impedance instability whose effects can be comparable to or higher than to that of the sustaining stage amplifier 1/f AM and PM noise in the oscillator circuit.

Maximize the output RF power carefully; otherwise severe phase noise degradation can occur due to active device noise elevation at compression. For low phase noise, tap the output signal through the resonator to the output load, thereby using the resonator transmission response selectivity to filter the carrier noise spectrum.

The VCO ground plane must be the same as that of the printed circuit board, including adequate decoupling capacitors between the DC supply and ground. Noisy power supplies may cause additional noise. Power supply induced noise may be seen at offsets from 20 Hz to 1 MHZ from the carrier. If the VCO is powered from a regulated power supply, the regulator noise will increase depending on the external load current drawn from the regulator. The phase noise performance of the VCO may degrade depending on the type of regulator used, and also upon the load current drawn from the regulator. To improve the phase noise performance of the VCO under external load conditions, it is always a good design philosophy to provide RF bypassing of power and DC control lines to the VCO.

For ultra low phase noise, use noise reduction techniques: DC noise-feedback, mode-coupling, injection-locking, degenerative noise filtering, feed-forward and other noise reduction techniques. Narrowing the current pulse width in the active device will decrease the time that noise is present in the circuit and therefore, decrease the effective noise factor for a given drive-level and minimize the phase noise.

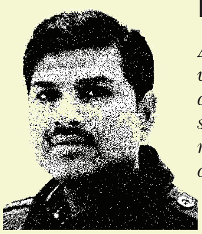

Dr. Ajay Poddar, Chief Scientist

Ajay is Chief Scientist at Synergy Microwave where he is responsible for design and development of state-of-the-art RF modules such as oscillators, synthesizers, antennas, mixers, amplifiers, filters, and MEMS based RF components.

SHOWING BIAS

GaN HEMT PA Gate Currents

GaN HEMT based power amplifiers (PA) can have somewhat different compression characteristics compared to other RF semiconductor based PAs. Depending on the setting of the quiescent drain current they often will have soft compression characteristics. Very often a conventional P1dB metric is not valid for a GaN HEMT PA since the real criteria are peak output power, two-tone nonlinearity and spectral re-growth which may depend more on Psat than P1dB. Of course, AM-PM characteristics will matter in the nonlinear performance of the PA but, again, GaN HEMT transistors tend to have rather different AM-PM characteristics versus output power than, say, Si LDMOS FETs or GaAs MESFETs. As Psat is approached, the AM-PM curve versus output power will often "turnover" (i.e., a negative going phase change will become positive going).

In unison with such behavior the gate current of the GaN HEMT transistor as a function of RF input power will also undergo a change so it is worth monitoring the magnitude and "sign" of the gate current. This monitoring will allow the designer (particularly at the prototyping stage) to know when the PA is getting close to its Psat condition. The gate bias supply must be able to source and sink current (i.e., reverse and forward current). Cree has an application note on its website called "GaN HEMT Biasing Circuit with Temperature Compensation"[1] that indicates the desirable features of a typical biasing arrangement. In most cases (e.g., Class A/B), the gate current will have a negative value at RF output power levels that are less than Psat. As Psat is approached the negative gate current will reach its maximum value and then reverse and go positive. This is due to the HEMT Schottky diode starting to be overdriven by input RF swings. The data sheets on all Cree GaN HEMT devices provide a maximum forward gate current that the designer needs to be aware of. In the case of one of our 25 W transistors,[2] this value is 7 mA. Although no damage will be done to the transistor for short periods of time if this forward gate current limit is somewhat exceeded, it is always considered that the limit be respected and is an excellent indicator that the device has reached its Psat output power. Incidentally, the RF input power level at which the gate current "flips" its direction is almost coincident with the AM-PM phase characteristic reversal. Clearly, there are other nonlinearities taking place in the device such as gate-to-source capacitance and source resistance that also effect the AM-PM characteristics.

Ray Pengelly,
Strategic Bus. Dev. Manager

Ray is responsible for wide bandgap technologies for RF and microwave applications among Cree RF and microwave products.

1. www.cree.com/~/media/Files/Cree/RF/Application%20Notes/Appnote%2011.pdf
2. www.cree.com/~/media/Files/Cree/RF/Data%20Sheets/CGH40025.pdf

In memory of my father, Aharon Hershtig (1927-2012), a Holocaust survivor, a strong and sensitive person, who inspired me.

FILTER THIS

Calculating Coupling

Extracting coupling values (known by technicians as "loading bandwidths") from filter networks is essential for tuning filters and troubleshooting. In the early 90s, wireless communication called for bandpass filters in basestations to exhibit elliptic responses with sharply skewed rejection skirts, exemplified by the Tx/Rx duplexer. Following the filter design recipe book, the first step was to find the lowpass prototype network and use its g-values to calculate external and internal coupling values. While the desired bandpass was asymmetric and sharply skewed to one side, the transformation from lowpass to bandpass is symmetric. As a last resort, many filter designers started with an all-pole network, introduced and refined cross couplings via optimization with a linear simulation tool, and extracted coupling values from the network very much as they would do on the bench when prototyping filters. A select few companies, such as those that had supplied filters to the satellite communication market in the 70s and 80s and those with university professors on staff, had access to skills and computer programs for directly synthesizing elliptical bandpass filters and easily extracting coupling values using matrix manipulations. For those outside that group, it was essential to develop generalized formulas for calculating coupling values for arbitrary elliptic response networks.

Since coupling values could be easily computed from g-values for all-pole networks, it seemed reasonable that practical formulas might exist in analogous form for asymmetrical networks. Further, most of the sophisticated direct synthesis programs could deal with just one doubly-terminated channel and couldn't take into account multiple filters connected to a junction. When real estate doesn't permit the "phasing" of filters, as with most basestation filters, external couplings and some internal couplings have to be adjusted. Deviation from the doubly-terminated condition depends on rejection at the crossover frequencies. If two filters are duplexed together and brought as close as 3 dB at crossover, coupling values will change dramatically from the doubly-terminated to singly-terminated case.

Generalized Coupling Formula – Inductor

External and internal coupling values for inductive coupled parallel LC resonators:

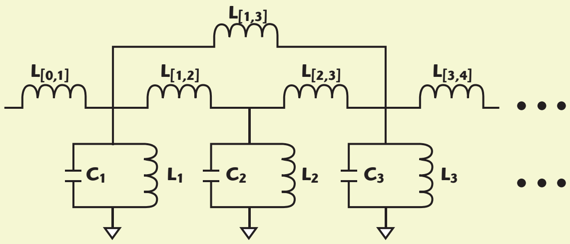

$$\frac{1}{L_i'} = \sum_{\text{all } k} \frac{1}{L_{[i,k]}} + \frac{1}{L_i} + \sum_{\text{all } k} \frac{1}{L_{[k,i]}}$$

$$J = \frac{1}{\omega_0 L_{[0,1]}} \left(\frac{1}{\sqrt{1+\left(1/\omega_0^2 L_{[0,1]}^2 G_a^2\right)}} \right)$$

$$Q_e = \frac{G_a}{\omega_0 L_1' J^2}$$

$$Q_{BWL} = f_0 / Q_e$$

$$k_{ij} = \sqrt{L_i' L_j'} / L_{[i,j]} \qquad K_{ij} = f_0 k_{ij}$$

$$\left.\begin{array}{l} G_a = \dfrac{1}{Z_0} \\ \omega_0 = 2\pi f_0 \\ Z_0 = 50\Omega \end{array}\right\} \text{for both cases}$$

Generalized Coupling Formula – Capacitor

External and internal coupling values for capacitive coupled parallel LC resonators:

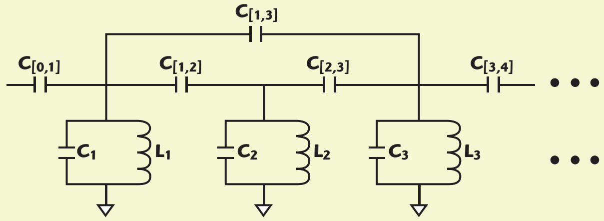

$$C_i' = \sum_{\text{all } k} C_{[i,k]} + C_i + \sum_{\text{all } k} C_{[k,i]}$$

$$J = \omega_0 C_{[0,1]} \left(\frac{1}{\sqrt{1+\left(\omega_0^2 C_{[0,1]}^2 / G_a^2\right)}} \right)$$

$$Q_{ec} = \frac{\omega_0 G_a C_1'}{J^2}$$

$$Q_{BWC} = f_0 / Q_{ec}$$

$$k_{ij} = \frac{C_{[i,j]}}{\sqrt{C_i' C_j'}} \qquad K_{ij} = f_0 k_{ij}$$

Once filters are simulated using lumped elements, coupling values can be calculated for any scenario for implementation with any technology, including TEM, TE, etc. In the mid 90s, Kevin Asplen and I wrote a program at K&L Microwave to extract coupling values from directly synthesized networks produced by S/Filsyn and other design tools and duplexed and optimized with various linear simulators. The "black magic" was gone. Tuning and troubleshooting filters became much easier.

Rafi Hershtig, VP of Advanced Engineering and R&D

Rafi continues to evolve the state of the art in filter design at K&L Microwave through innovations that lead to improving performance, shrinking the footprint and integrating capabilities.


26 years ago, National Instruments redefined instrumentation with LabVIEW.
PXI
This summer, we're doing it again.
Visit RFredefined.com for a sneak peek at the next big thing in instrumentation.

GIMME MORE

Amplifier Bandwidth

Published literature and conference sessions are booming with techniques for maximizing efficiency, improving linearity, reducing size, etc. of amplifiers, but often these techniques come at the sacrifice of bandwidth. An ideal solution could realize these performance enhancements without reducing the frequency response. Designing for the widest bandwidth possible requires subtlety.

Start with good active models. Although foundry transistor models have become much better in recent years, they are made to appeal to the widest audience possible. This "one model fits all" approach works for narrowband applications (i.e., add a few tunable components for the bench test and you're golden). For wideband applications, you need transistor models that provide accuracy over the entire frequency range of interest. Creating a scalable, wideband behavior model that represents thermal effects (resistive and capacitive), process variation (i.e., supports Monte Carlo), and bias dependency is non-trivial. Before starting a wideband design, always compare the model against measured data. If the model is not accurate over the entire range of interest (with some margin), extract a custom model.

Start with good passive models. Similarly, passive models have become much better in recent years. Component-level parasitic effects are the most limiting factor in achieving wide bandwidth. Substrate permittivity, mounting orientation, proximity to ground plane, and self-resonance are some of the parasitic effects often overlooked. If models with this level of detail are not available, mount the component in a representative fixture (i.e., use the same substrate as the final product), measure S-parameters, de-embed the fixture, and use the measured results in simulation. For a more versatile solution, have a custom model made (I use the Modelithics scalable model).

Create your own N-section transformer. A common way of achieving wide bandwidth matching networks is with N-section transformers, where N is usually 2, 3 or 4. The three most popular algorithms are exponential, equal ripple, and maximally flat (listed from widest bandwidth with most ripple to narrowest bandwidth with least ripple). Using these three configurations as a starting point, the Smith Chart Utility in Agilent ADS is a powerful tool for tweaking the section impedances to find the right balance of bandwidth and ripple that works for the application (seek the Microwaves101.com free Excel calculator to get started). To minimize size, meander the RF traces and/or replace transmission lines with lumped components.

Know the system need. Fact: Amplifiers have less gain, power, and efficiency at higher frequency than lower frequency. To achieve equal performance across a wide frequency band, low-end performance is worsened to match the high end. When designing for extremely wide bandwidths (i.e., multiple octaves or decades), this can amount to a significant degradation at the low end (i.e., -6 dB gain per octave adds up quickly). Is a flat response really necessary? Somewhere in the front-end is an antenna with positive gain per octave. Negative amplifier gain slope over frequency could be a benefit!

Know the limiting factor. In every system, there is a bandwidth-limiting element. Always know what it is. Often, packaging is the culprit. Watch for practical limitations from feedback circuits and reactive matches. Passive components, like couplers and splitters, usually have well-defined band edges (especially when wideband). In general, any technique using a phase shifter is going to be bandwidth limited. When exploring the widest bandwidth possible, knowing the limiting factor will allow the designer to focus on the greatest area of constraint.

Dr. Nickolas Kingsley, Director of Engineering

Nick manages the engineering team at Auriga Microwave. His research interests include the design, miniaturization, fabrication, packaging and testing of RF MEMS multilayer front ends.


AMPLIFIERS
HIGH PERFORMANCE
100 kHz to 50 GHz
• To Your Specification
• Reasonable Prices
Most can be delivered in one week!
+15V
IN B&Z SN: 3837 OUT
+15V
IN B&Z SN: 1966 OUT
Visit our Web Site at www.bnztech.com
Fill Out the Custom Specification form
Receive a Quotation within 24 hours!
B&Z TECHNOLOGIES
INNOVATING TO EXCEL
Ph: +1 (631) 444-8827
Fax: +1 (631) 444-8825
E-Mail: info@bnztech.com
Web: www.bnztech.com
Made in USA
Year 3 Warranty

Cover Feature

DISTORTED TONES

Measurement Fidelity

Third order distortion measurements such as intermodulation distortion (IMD) and third order intercept (IP3) at high power levels (think IP3 at +40 dBm and higher) are often some of the most difficult RF measurements to make. Often, these measurements require careful attention to minimizing the IMD products of both the source signal and the RF signal analyzer. Here are a few important tips for creating the best possible source signal and for squeezing the last few dB out of your signal analyzer.

Let's start with the source, typically consisting of two RF signal generators and a combiner network. Here, one of our primary concerns to isolate the sources to prevent RF energy from leaking between them – a problem that could ultimately produce IMD products in the test signal. While choosing a combiner with excellent port-to-port isolation (like a Wilkinson power combiner) is a good start, getting the best source isolation requires a little more effort.

There are several methods to improve source isolation – each with varying degrees of effectiveness and difficulty. Couplers and isolators are the simplest technique to get an additional 30 to 40 dB of isolation – but are generally only effective within one frequency octave. When setting up a broadband test bench, an amplifier (with high reverse isolation) or attenuator (or both) placed between each signal source and the power combiner can be a highly effective technique to isolate each source to produce the best two-tone signal.

Once you've set up a clean two-tone source, the next step is to analyze the IMD products of both the stimulus signal and the RF signal analyzer. Here, squeezing out the last few dB of dynamic range requires a basic understanding of the receiver's architecture. Generally, you'll first want to control the analyzer's front-end attenuation either manually or by setting the reference level. An easy way to determine if your RF signal analyzer is contributing its own distortion is to slowly increase the front-end attenuation while observing IMD products. If the IMD products decrease in power as attenuation increases, you can quickly deduce that your instrument is contributing to the measurement error. However, if IMD products remain constant with an increase in attenuation, you can be certain that these intermodulation products are inherent to the signal source. Eventually, too much attenuation will begin to raise the noise floor of the instrument and you'll need to either reduce resolution bandwidth or apply averaging to continue to observe IMD products.

If you determine that IMD products are the result of the RF signal analyzer's linearity, a second technique to further improve the analyzer's linearity is to condition the signal at the intermediate frequency (IF). Often, the linearity of the IF digitizer of the instrument is a major contributor to distortion products. Thus, one can improve the linearity of the instrument by setting a narrow IF bandwidth and ensuring that the frequency spacing of the two-tone signal exceeds the bandwidth of the IF filter.

Once you've verified that both the source and receiver have IMD levels that are low enough to make your measurement, it's time to connect your DUT. Of course, remember that you'll want to increase the reference level or attenuation of the RF signal analyzer by the expected gain of the DUT to ensure that you're operating the receiver at the same power level you've optimized it for already. Finally, you're ready to measure the power of both the 1st and 3rd order distortion products to determine IP3 or IMD performance of your DUT.

David Hall, Senior Product Manager

At National Instruments, David applies his expertise in digital signal processing and communications systems to develop product demos, provide user feedback, and write application notes.

Cover Feature

STABLE AS A ROCK

Spurious Oscillations

Amplifier instability can show as spurious (unwanted) signals in the frequency domain, sometimes only visible when there is a (wanted) output signal, at other times they can appear as noise 'humps' or unexpected decreases in output power or gain – appearing like a 'bite' out of the frequency response. Although in a system context they may be tolerable (low enough or in a non-interfering part of the spectrum) they are indicative of a design that could be better controlled. We are not considering switching frequency sidebands, which may appear on the output signal through the bias circuits, but frequencies produced within the devices themselves. If it looks like ohms law isn't working – search for oscillations.

The normal approach to stable amplifier design is to consider the 'k' factor. However, this will only address a group of oscillations referred to as even mode, and to comprehensively account for these, one should consider the behaviour of the device during switch on and at all the input drive levels. This is because the calculations for k depend on device transconductance and parasitic elements, many of which are input power level and bias dependant. Odd mode oscillations occur within the combining loops of parallel transistors that make up power devices and MMICs. They may not even directly appear at the device output.

Essentially to prevent oscillations, gain must be reduced at the frequency(s) concerned, which tends to oppose one of the key design aims, hence it must be applied in a frequency selective manner. On the input, some series resistance can be tolerated and may make matching easier, but this is rarely acceptable at the output. Series negative feedback is commonly applied in low noise amplifiers where it can have the added benefit of bringing into line the input match and optimum noise figure impedance, but is impractical for power designs. Shunt feedback can be employed to flatten gain and used with bias line de-coupling to produce highly stable amplifiers. Care must be taken with the bias line connections, particularly coupling between stages, where positive feedback is possible; hence, it is important to analyze such structures over the full bandwidth from DC to the maximum operating frequency of the device. To this end the bias decoupling should include resistive loss and a sufficient range of capacitor values. Although the main RF decoupling capacitor should be low loss, higher loss dielectrics can usefully be employed for the lower frequencies. Do not share via holes to ground on decoupling capacitors; good solid grounding, although going against some standard design rules (thermal breaks), reduces inductance.

Signals don't always flow the way you want them, and physical constraints mean that the cavity is often larger than we would like. In this case, we need to reduce the risk of modes being started (launched) and ensure they are attenuated as quickly and as much as possible. High impedance lines should be realized in coplanar waveguide, if possible, containing the radiated fields. Pillars grounded at both ends can be erected within the cavity to break up box modes. The judicious use of Radar Absorbent Material (RAM) is not 'applying bandages' as some would see it, but a valid technique.

Testing needs to be carried out across the range of input power and load impedances, and also the full temperature range, especially cold where gain is highest and spurs are likely to be encountered. Low temperature oscillations may be removed by powering up the amplifier in advance of use, raising the temperature sufficiently.

Dominic FitzPatrick, Principal Consultant

Dominic is a specialist in RF and microwave solid state amplifiers. As Technical Director of two British microwave amplifier companies, he was responsible for technological innovation and new product development, serving customers worldwide.


Anaren
H100N
A30X4

Cover Feature

MAKING CENTS

E-Band Modules

At frequencies up to around 40 GHz, the vast majority of RF components are supplied in Surface Mount Technology (SMT) packages. Components operating in the un-licensed 60 GHz band and at E-Band will ultimately also be available in SMT packages, but this requires advances in both chip-scale packaging technology and PCB technology. Current commercially available components addressing these bands are normally supplied as bare die and one of the first challenges to the user is routing RF signals to and from the die without suffering serious performance degradation.

A 1 mm length of bondwire has an inductive reactance of around 340 Ω at 60 GHz and 486 Ω at the top of E-Band (71 to 76 GHz and 81 to 86 GHz). At these frequencies, bond interface parasitics can seriously degrade the performance of a die and must be minimized. The first step is to ensure that the surface of the interface substrate is at the same level as the surface of the ICs. There are essentially two practical approaches; both require the use of a substrate material of similar thickness to the die. The first approach is to use a hard substrate (such as quartz or alumina). In this case, the substrate and die can be butted up to minimize bonding distances but multiple substrates may be required resulting in a more complex assembly. The second approach is to use a soft substrate (such as LCP or RT Duroid) with holes cut into the substrate into which the die can sit. This allows a single interface substrate but tolerances on hole dimensions can increase bonding distances.

The inductance of the bond itself can be reduced by using multiple parallel wires or tape bonds instead of wire. Direct die to die bonding offers the ultimate in minimizing bonding distances and parasitics. Bonding of the ground pads as well as the signal pads can improve the performance of the transition. If tape bonding is not available, two parallel wire bonds can provide acceptable performance. When bonding from the die to a microstrip track on the interface substrate, the wider substrate track allows the formation of a "v" bond, which will reduce the mutual inductance.

Many of the datasheets for mm-wave die recommend the use of Single Layer Capacitors (SLC) for de-coupling. These are much more expensive than SMT capacitors and require wire-bond assembly. In fact, this approach is often a hang-over to the days of microwave chip and wire assembly. SLCs do offer high capacitance with low parasitics but a well designed mm-wave IC will have adequate on-chip de-coupling for the microwave and mm-wave frequency range. At RF frequencies and below, for which the higher value de-coupling capacitors are actually required, inexpensive SMT capacitors are often perfectly adequate. The effectiveness of this approach should be confirmed with appropriate trials but it can reduce cost and complexity without sacrificing performance.

For E-Band and 60 GHz assemblies aimed at volume production, the largest potential cost saving can obtained by developing custom MMICs. E-Band LNAs fabricated on 0.1 μm gate length PHEMT processes cost over $100 in 1000-off quantities. Parts of the same die area can be produced on commercially available foundry processes for around $5. This excludes the NRE development costs but for a high volume application this is soon amortized with production.

Liam Devlin, Director of RF Integration

Liam has led the design and development of over 70 custom ICs on a range of GaAs and Si processes at frequencies up to 90 GHz for Plextek Ltd., a UK design consultancy.

Cover Feature

TRICKY TRADE-OFFS

Doherty Power Amplifiers

Doherty power amplifiers (PA) use main and auxiliary (peaking) amplifiers, connected in parallel, to attain relatively high efficiency over a range of output powers. Designing one can be a tricky proposition since there are many different parameters to be adjusted and multiple responses to look at, most of which are specified versus the output power, which unlike the input power is also a response from the simulation. In order to make the trade-offs necessary to meet specifications over a wide range of output powers, the engineer must determine which parameters have a dominant effect on performance.

A number of techniques can be employed to improve Doherty PA performance. Sweeping one parameter at a time allows the engineer to sweep an arbitrary parameter in the design and see how the performance varies. This provides quick insight into whether or not a specific parameter has any effect on performance, this technique is a reasonable first step to take when trying to understand and improve Doherty PA performance. Sweeping two parameters at a time extends the single parameter sweep to provide an effective means of understanding the interaction between two parameters. Results can be viewed on contour (and other) plots.

Design of Experiments (DOE) varies many different parameters simultaneously, while keeping track of the results. It quickly lets the engineer know which parameters most strongly influence performance. Examining one parameter at a time to gain such information would be too tedious and time consuming. On the downside, some time and effort is required to set up this technique's methodical simulations and DOE is not supported by all CAD tool vendors.

Optimization is a common approach to improving amplifier performance. Somewhat simpler to set up than DOE, it is automated and can run for an indefinite length of time. However, it must combine all goals together to create a single error function. Although it may produce reasonable results, it doesn't provide insight into what trade-offs are being made to reduce error. Additionally, optimizers can get stuck while systematically searching through the design space. Some engineers find value in using both DOE and optimization.

Monte Carlo (MC) analysis is much like running a multi-dimensional parameter sweep, this novel technique investigates the sensitivity of the amplifier's performance to as many parameters as the engineer desires. Two types of parameters can be simulated: design variables, which the engineer can control, and random variables (e.g., foundry statistical variables), which the engineer cannot control. Because this technique samples a lot of points at random, a more thorough or complete sampling of the solution space can be achieved. The computing cost is independent of the number of random variables. On the downside, it requires some post processing and additional effort to obtain correlations. Advanced Design System (ADS) from Agilent, for example, has example data display files set up to show these results. Most tools support the technique itself, but may not offer added post processing or correlation capabilities. MC will not necessarily provide better results than DOE.

While each of these techniques has some value, the general rule of thumb is to first run a single and/or double parameter sweep. If doing so provides feedback that a design can satisfy all of its specifications, then the job is done. If not, the next step is to employ DOE or MC, or perhaps even run both in that order. At the end of the day, if the Doherty PA is unable to meet all of its specifications, then the data obtained from either of these techniques can be used as the basis of further discussion with the system designer regarding trade-offs in the specifications.

Andy Howard, Senior Applications Engineer

Andy currently focuses on power amplifier simulation techniques for Agilent Technologies, working with many different applications of Agilent's ADS, RFDE and GoldenGate simulators.

1. www.rf-design-tips.com/doherty-power-amplifier-performance-investigation/.

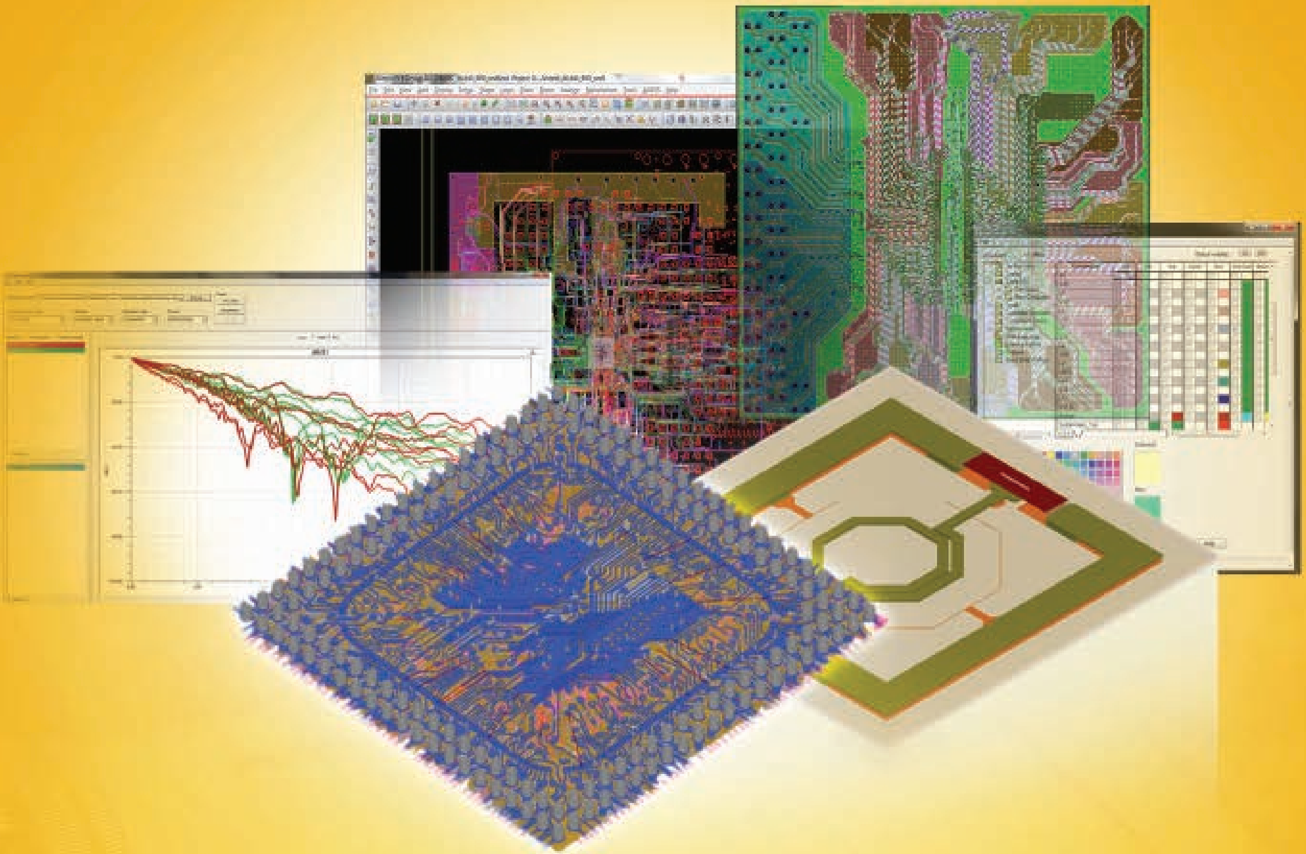

YER DONE SON

When to Stop Engineering

The key to achieving expedient first pass design success with filters is to use both software and test and measurement tools as efficiently as possible. In most cases, "efficiency" is nothing more than cutting out unnecessary design steps, automating tedious steps, and ultimately knowing when to "stop engineering." Below are tips to avoid getting caught in infinite design iterations.

Overdesign for return loss and ignore insertion loss. Return loss is always worse in real life due to discontinuities. By leaving at least 5 dB of margin, the real life design will be acceptable. Conversely, ignore insertion loss because accurately modeling such physics is computationally intensive. As for insertion loss, "it is what it is." Don't fight it in the first pass. If insertion loss matters, use low surface roughness options like rolled copper, it makes a huge difference.

Learn your fabrication technology's tendencies. Learning tendencies of the fab house requires experience, so pay attention to every design iteration and record the trends. We find that when we send our filter designs out, the center frequency tends to be about 100 to 200 MHz off and the bandwidth is reduced a little (say from 7 to 5%). Compensating for the fab drift allows us to do custom filter work in a matter of days, instead of months.

Above a few, GHz lumped elements don't act like lumped elements. Inductors are the worst, followed by capacitors and resistors. We limit the use of chip inductors to designs below 6 GHz but use capacitors and resistors beyond 40 GHz. For lumped elements, the smaller the better. If you insist on simulating Rs, Ls and Cs above a few GHz, consider including the parasitic reactance, and pray the models are correct.

When debugging, blame yourself first, and blame the vendors last. When you build your prototype and it doesn't work, first assume you made a mistake. In RF, the two most common mistakes are connector transitions and grounding issues. Another potential error source is forgetting to simulate something. Issues like connector transitions and metal lids can wreak havoc on your delicate circuitry, and circuit solvers typically ignore these effects. Debugging should be systematic, and assuming the vendor made a mistake is a last resort option rife with peril. Vendor mistakes happen occasionally, design mistakes happen daily.

When to stop engineering. The biggest waste of time is fighting for a few tenths of a dB in software. Time is money, and sometimes it is cheaper to release the design, build a prototype, take measurements, and then go back to the software only after you get your sanity check. Don't fall in love with your CAD software, sometimes it lies! Real life testing will keep your software honest.

Chris Marki, Director of Research

Chris is responsible for the design and commercialization of many of Marki's fastest growing product lines.

If You Can't Find The Power You Need Here, It Doesn't Exist.

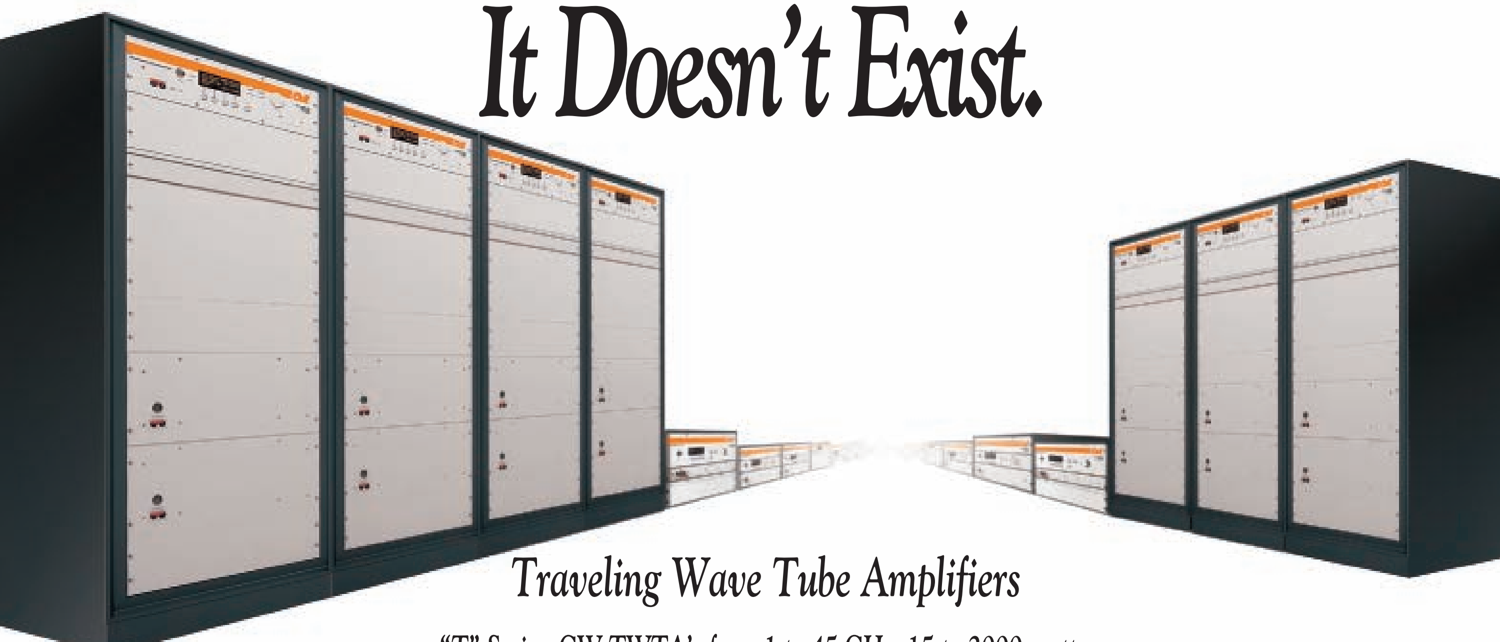

Traveling Wave Tube Amplifiers

"T" Series–CW TWTA's from 1 to 45 GHz. 15 to 2000 watts.
"TP" Series–Pulsed TWTA's from 1 to 18 GHz. 1000 to 10,000 watts.

When it comes to the largest selection of Traveling Wave Tube (TWT) Amplifiers, AR has no equal. We cover a wider range of high-power, broadband amplifiers for your specific test application than any other brand.

CW models also have the capability to faithfully reproduce AM, FM, and pulse modulation input signals. Features that are included at no extra cost are our "Sleep mode" which prolongs the tube life, rugged construction for the rigorous treatment in test labs, modular supplies to reduce repair turn-around, and well thought out digital displays to help you monitor essential amplifier conditions.

So before you choose a look-alike traveling wave tube amplifier, examine all the features and benefits that come along at no extra charge with an AR amplifier. If you want a TWTA that will take you farther, you'll choose the one with the AR logo on it ... the company that stands behind our products with the global service and support that you demand.

To learn more, visit www.arworld.us or call us at 215-723-8181.

www.arworld.us/twta

ISO 9001:2008
Certified

rf/microwave instrumentation

Other ar divisions: modular rf • receiver systems • ar europe

USA 215-723-8181. For an applications engineer, call 800-933-8181.
In Europe, call ar United Kingdom 441-908-282766 • ar France 33-1-47-91-75-30 • emv GmbH 89-614-1710 • ar Benelux 31-172-423-000

www.arworld.us

RF Amplifiers and Sub-Assemblies for Every Application

Delivery from Stock to 2 Weeks ARO from the catalog or built to your specifications!

- Competitive Pricing & Fast Delivery
- Military Reliability & Qualification
- Various Options: Temperature Compensation, Input Limiter Protection, Detectors/TTL & More
- Unconditionally Stable (100% tested)

ISO 9001:2000 and AS9100B CERTIFIED

OCTAVE BAND LOW NOISE AMPLIFIERS

Model No.	Freq (GHz)	Gain (dB) MIN	Noise Figure (dB)	Power-out @ P1-dB	3rd Order ICP	VSWR
CA01-2110	0.5-1.0	28	1.0 MAX, 0.7 TYP	+10 MIN	+20 dBm	2.0:1
CA12-2110	1.0-2.0	30	1.0 MAX, 0.7 TYP	+10 MIN	+20 dBm	2.0:1
CA24-2111	2.0-4.0	29	1.1 MAX, 0.95 TYP	+10 MIN	+20 dBm	2.0:1
CA48-2111	4.0-8.0	29	1.3 MAX, 1.0 TYP	+10 MIN	+20 dBm	2.0:1
CA812-3111	8.0-12.0	27	1.6 MAX, 1.4 TYP	+10 MIN	+20 dBm	2.0:1
CA1218-4111	12.0-18.0	25	1.9 MAX, 1.7 TYP	+10 MIN	+20 dBm	2.0:1
CA1826-2110	18.0-26.5	32	3.0 MAX, 2.5 TYP	+10 MIN	+20 dBm	2.0:1

NARROW BAND LOW NOISE AND MEDIUM POWER AMPLIFIERS

Model No.	Freq (GHz)	Gain (dB) MIN	Noise Figure (dB)	Power-out @ P1-dB	3rd Order ICP	VSWR
CA01-2111	0.4 - 0.5	28	0.6 MAX, 0.4 TYP	+10 MIN	+20 dBm	2.0:1
CA01-2113	0.8 - 1.0	28	0.6 MAX, 0.4 TYP	+10 MIN	+20 dBm	2.0:1
CA12-3117	1.2 - 1.6	25	0.6 MAX, 0.4 TYP	+10 MIN	+20 dBm	2.0:1
CA23-3111	2.2 - 2.4	30	0.6 MAX, 0.45 TYP	+10 MIN	+20 dBm	2.0:1
CA23-3116	2.7 - 2.9	29	0.7 MAX, 0.5 TYP	+10 MIN	+20 dBm	2.0:1
CA34-2110	3.7 - 4.2	28	1.0 MAX, 0.5 TYP	+10 MIN	+20 dBm	2.0:1
CA56-3110	5.4 - 5.9	40	1.0 MAX, 0.5 TYP	+10 MIN	+20 dBm	2.0:1
CA78-4110	7.25 - 7.75	32	1.2 MAX, 1.0 TYP	+10 MIN	+20 dBm	2.0:1
CA910-3110	9.0 - 10.6	25	1.4 MAX, 1.2 TYP	+10 MIN	+20 dBm	2.0:1
CA1315-3110	13.75 - 15.4	25	1.6 MAX, 1.4 TYP	+10 MIN	+20 dBm	2.0:1
CA12-3114	1.35 - 1.85	30	4.0 MAX, 3.0 TYP	+33 MIN	+41 dBm	2.0:1
CA34-6116	3.1 - 3.5	40	4.5 MAX, 3.5 TYP	+35 MIN	+43 dBm	2.0:1
CA56-5114	5.9 - 6.4	30	5.0 MAX, 4.0 TYP	+30 MIN	+40 dBm	2.0:1
CA812-6115	8.0 - 12.0	30	4.5 MAX, 3.5 TYP	+30 MIN	+40 dBm	2.0:1
CA812-6116	8.0 - 12.0	30	5.0 MAX, 4.0 TYP	+33 MIN	+41 dBm	2.0:1
CA1213-7110	12.2 - 13.25	28	6.0 MAX, 5.5 TYP	+33 MIN	+42 dBm	2.0:1
CA1415-7110	14.0 - 15.0	30	5.0 MAX, 4.0 TYP	+30 MIN	+40 dBm	2.0:1
CA1722-4110	17.0 - 22.0	25	3.5 MAX, 2.8 TYP	+21 MIN	+31 dBm	2.0:1

ULTRA-BROADBAND & MULTI-OCTAVE BAND AMPLIFIERS

Model No.	Freq (GHz)	Gain (dB) MIN	Noise Figure (dB)	Power-out @ P1-dB	3rd Order ICP	VSWR
CA0102-3111	0.1-2.0	28	1.6 Max, 1.2 TYP	+10 MIN	+20 dBm	2.0:1
CA0106-3111	0.1-6.0	28	1.9 Max, 1.5 TYP	+10 MIN	+20 dBm	2.0:1
CA0108-3110	0.1-8.0	26	2.2 Max, 1.8 TYP	+10 MIN	+20 dBm	2.0:1
CA0108-4112	0.1-8.0	32	3.0 MAX, 1.8 TYP	+22 MIN	+32 dBm	2.0:1
CA02-3112	0.5-2.0	36	4.5 MAX, 2.5 TYP	+30 MIN	+40 dBm	2.0:1
CA26-3110	2.0-6.0	26	2.0 MAX, 1.5 TYP	+10 MIN	+20 dBm	2.0:1
CA26-4114	2.0-6.0	22	5.0 MAX, 3.5 TYP	+30 MIN	+40 dBm	2.0:1
CA618-4112	6.0-18.0	25	5.0 MAX, 3.5 TYP	+23 MIN	+33 dBm	2.0:1
CA618-6114	6.0-18.0	35	5.0 MAX, 3.5 TYP	+30 MIN	+40 dBm	2.0:1
CA218-4116	2.0-18.0	30	3.5 MAX, 2.8 TYP	+10 MIN	+20 dBm	2.0:1
CA218-4110	2.0-18.0	30	5.0 MAX, 3.5 TYP	+20 MIN	+30 dBm	2.0:1
CA218-4112	2.0-18.0	29	5.0 MAX, 3.5 TYP	+24 MIN	+34 dBm	2.0:1

LIMITING AMPLIFIERS

Model No.	Freq (GHz)	Input Dynamic Range	Output Power Range Psat	Power Flatness dB	VSWR
CLA24-4001	2.0 - 4.0	-28 to +10 dBm	+7 to +11 dBm	+/- 1.5 MAX	2.0:1
CLA26-8001	2.0 - 6.0	-50 to +20 dBm	+14 to +18 dBm	+/- 1.5 MAX	2.0:1
CLA712-5001	7.0 - 12.4	-21 to +10 dBm	+14 to +19 dBm	+/- 1.5 MAX	2.0:1
CLA618-1201	6.0 - 18.0	-50 to +20 dBm	+14 to +19 dBm	+/- 1.5 MAX	2.0:1

AMPLIFIERS WITH INTEGRATED GAIN ATTENUATION

Model No.	Freq (GHz)	Gain (dB) MIN	Noise Figure (dB)	Power-out @ P1-dB	Gain Attenuation Range	VSWR
CA001-2511A	0.025-0.150	21	5.0 MAX, 3.5 TYP	+12 MIN	30 dB MIN	2.0:1
CA05-3110A	0.5-5.5	23	2.5 MAX, 1.5 TYP	+18 MIN	20 dB MIN	2.0:1
CA56-3110A	5.85-6.425	28	2.5 MAX, 1.5 TYP	+16 MIN	22 dB MIN	1.8:1
CA612-4110A	6.0-12.0	24	2.5 MAX, 1.5 TYP	+12 MIN	15 dB MIN	1.9:1
CA1315-4110A	13.75-15.4	25	2.2 MAX, 1.6 TYP	+16 MIN	20 dB MIN	1.8:1
CA1518-4110A	15.0-18.0	30	3.0 MAX, 2.0 TYP	+18 MIN	20 dB MIN	1.85:1

LOW FREQUENCY AMPLIFIERS

Model No.	Freq (GHz)	Gain (dB) MIN	Noise Figure dB	Power-out @ P1-dB	3rd Order ICP	VSWR
CA001-2110	0.01-0.10	18	4.0 MAX, 2.2 TYP	+10 MIN	+20 dBm	2.0:1
CA001-2211	0.04-0.15	24	3.5 MAX, 2.2 TYP	+13 MIN	+23 dBm	2.0:1
CA001-2215	0.04-0.15	23	4.0 MAX, 2.2 TYP	+23 MIN	+33 dBm	2.0:1
CA001-3113	0.01-1.0	28	4.0 MAX, 2.8 TYP	+17 MIN	+27 dBm	2.0:1
CA002-3114	0.01-2.0	27	4.0 MAX, 2.8 TYP	+20 MIN	+30 dBm	2.0:1
CA003-3116	0.01-3.0	18	4.0 MAX, 2.8 TYP	+25 MIN	+35 dBm	2.0:1
CA004-3112	0.01-4.0	32	4.0 MAX, 2.8 TYP	+15 MIN	+25 dBm	2.0:1

CIAO Wireless can easily modify any of its standard models to meet your "exact" requirements at the Catalog Pricing.

Visit our web site at **www.ciaowireless.com** for our complete product offering.

Ciao wireless

Ciao Wireless, Inc. 4000 Via Pescador, Camarillo, CA 93012

Tel (805) 389-3224 Fax (805) 389-3629 sales@ciaowireless.com

Lockheed Martin Submits Bid for Medium-Range Ballistic Missile Targets

Lockheed Martin announced that it has submitted its bid for the Medium-range Ballistic Missile Targets contract to the U.S. Missile Defense Agency (MDA). The Lockheed Martin-led industry team completed delivery of the proposal to the MDA's Targets and Countermeasures Directorate in Huntsville, Ala.

The contract will provide Medium-range Ballistic Missile (MRBM) Targets to support Ballistic Missile Defense System element and system flight tests. Requirements include development and manufacturing of MRBMs, integrated logistics support to include inventory storage and maintenance, pre- and post-mission analysis, launch preparation and execution and engineering services. The MDA issued the final request for proposal April 18 and anticipates contract award in 2012.

"Target missiles are important to our nation's missile defense mission," said John W. Holly, vice president of Missile Defense Systems for Lockheed Martin Space Systems Co. "Our targets provide threat-relevant scenarios to the system under test, creating tough and stressing engagements. Our team's proposal for Medium-range Ballistic Missile Targets delivers the reliability, threat relevance and cost effectiveness needed to best support the mission. Lockheed Martin is applying our unmatched mission success record and demonstrated cost efficiencies to the nation.

Lockheed Martin has named Brian Kelly program manager. Under the proposal, Lockheed Martin will perform engineering and program management in Huntsville and production in Courtland, Ala. The Lockheed Martin-led team includes: Cummings Aerospace, Huntsville; Davidson Technologies Inc., Huntsville; IERUS Technologies Inc., Huntsville; and Orbital Sciences Corp., Chandler, Ariz.

To meet the government's requirements, Lockheed Martin will apply more than 15 years of experience as a leading provider of target missiles for missile defense testing. Lockheed Martin has achieved an unmatched 98-percent success rate in 42 out of 43 target missions since 1996, including legacy and next-generation ballistic missile targets. Target reliability contributes to the overall affordability of a flight test, due to the costs associated with the weapon system and sensors.

Lockheed Martin has implemented innovations in next-generation target production and operations that focus on cost effectiveness without sacrifices in reliability. Modular hardware components reduce costs and maximize mission flexibility. A central production facility streamlines fabrication, integration, testing, storage and shipment. The ship-and-shoot approach delivers an integrated target ready to launch, reducing time at the test range. Lockheed Martin's proven experience in relevantly representing the characteristics of real-world threats includes: unitary and separating; short-, medium- and intermediate-range; and ground-, sea- and air-launched targets. The next-generation target systems developed by the company significantly increase threat-relevant capabilities while improving mission flexibility.

U.S. Navy Awards Raytheon $338 M for Tomahawk

The U.S. Navy awarded Raytheon Co. a $338 million contract for the Tomahawk Block IV tactical cruise missile. The contract includes replenishment of weapons used during Operation ODYSSEY DAWN and procurement for the government's fiscal year 2012.

"Tomahawk Block IV is important for U.S. national security because it enables commanders to precisely engage heavily-defended and high-value targets from extremely long distances," said Capt. Joseph Mauser, the U.S. Navy's Tomahawk program manager. "With more than 2,000 combat uses and 500 successful tests, Tomahawk has proven highly reliable and effective." The contract calls for Raytheon to build and deliver the Tomahawk Block IV cruise missiles and provide warranties, flight test and life-cycle support. Production is scheduled to begin this year.

"Tomahawk has a record of reliability, effectiveness and accuracy that no other tactical cruise missile in the world can come close to matching."

"Tomahawk has a record of reliability, effectiveness and accuracy that no other tactical cruise missile in the world can come close to matching," said Harry Schulte, vice president of Raytheon Missile Systems' Air Warfare Systems. "This is made possible by more than 250 Raytheon employees building Tomahawk and supporting its

Go to mwjournal.com for more defense news items

depot, and by our suppliers across the country. They are critical to our success and the security of our country and our allies."

With a range of more than 1000 nautical miles (1150 statute miles), the Tomahawk Block IV is a surface- and submarine-launched, precision-strike, stand-off weapon. Tomahawk is designed for long-range precision-strike missions against high-value and heavily defended targets, such as integrated air defense systems.

Tomahawk Block IV employs a two-way satellite data link that enables a strike controller to flex the missile in flight to preprogrammed alternate targets or redirect it to a new target. This targeting flexibility includes the capability to loiter over the battlefield and await a more critical target.

Northrop Grumman Completes Critical Design Review for U.S. Army

Northrop Grumman Corp. has successfully completed the Critical Design Review (CDR) for the U.S. Army's Integrated Air and Missile Defense (IAMD) Battle Command System (IBCS). The CDR provided an in-depth assessment by a government team of experts and managers, that the IBCS design is programmatically and technically realistic and attainable. The successful review determined the IBCS detailed design satisfies cost, schedule and performance requirements and demonstrates the maturity for proceeding with full-scale fabrication, assembly, integration and test.

In addition to the Integrated Air and Missile Defense Project Office, the IAMD community of interest organizations participating in the CDR included: Office of the Secretary of Defense, U.S. Missile Defense Agency, Army Program Executive Office Missiles and Space, Army Fires Center of Excellence, Training and Doctrine Command Capability Manager for Army Air and Missile Defense, Army Lower Tier Project Office, Army Counter-Rocket, Artillery and Mortar Project Office, and Army Cruise Missile Defense System Project Office.

"The Army and Northrop Grumman IBCS team has made substantial progress on this important program that will bring innovative, affordable and life-saving capabilities to the warfighter," said Kelley Zelickson, vice president of air and missile defense systems for Northrop Grumman Information Systems. "With this significant milestone achieved, we look forward to an early demonstration of IBCS combat capability during the IAMD exercise planned for 2013."

Richard Mumford, International Editor

Wireless Communication: EARTH Project Takes Green Approach

With the carbon footprint of the mobile communications sector set to triple by 2020, making the way we communicate greener is a key priority of the European Commission's Digital Agenda strategy. The EU-funded Energy Aware Radio and Network Technologies (EARTH) project, which set out to do just that, was completed in June 2012, with the products developed expected to be available on the market in 2014.

The project's researchers successfully optimised the energy use of 4G LTE-based stations, which account for the highest energy consumption in the mobile network. The project's industrial and small- and medium-sized enterprises (SME) partners have already started to transfer the project results into real products for the multi-billion Euro global 4G product market.

The European Commission vice president, Neelie Kroes, commented, "The ICT sector is growing, but its carbon footprint should not follow. I congratulate the partners of the EARTH project who have found ways to deliver the services we need while reducing CO_2 emissions and cutting down on energy bills."

> *"The ICT sector is growing, but its carbon footprint should not follow."*

Since it began in January 2010, EARTH, which received almost €9.5 million of funding under the Information and Communication Technology (ICT) theme of the EU's Seventh Framework Programme (FP7), has brought together researchers from 15 partner institutions across 10 European countries: Belgium, Germany, Spain, France, Italy, Hungary, Portugal, Finland, Sweden and the United Kingdom. The project partners that make up the consortium hail from both industry and academia.

The team contests that by optimising the network's energy use, electricity bills for operators will gradually fall, making it more affordable to use a mobile phone, with the added benefit of also reducing pollution and carbon emissions. By reducing the power required to operate each mobile base station, it is also expected that in the future these stations could be operated reliably by renewable energy, further reducing emissions.

UK Government Invests £20 M to Stimulate Technology Innovation

Innovation in a broad range of growth-creating technology areas, from nanotechnology to electronics and ICT and from biosciences to advanced materials, is to benefit from over £20 million of new UK government investment. Grant funding totalling over £18 million, from the Technology Strategy Board, Scottish Enterprise and the Biotechnology and Biological Sciences Research Council (BBSRC) will be invested in over 40 major business-led collaborative research and development projects that will lead to the creation of new products and processes to be used across a variety of different application areas.

> *"...new technologies can be a significant driver of economic growth."*

Over 120 UK businesses and institutions and 20 universities will share this funding and take part in the R&D projects. In addition, over 80 small and micro businesses from across the country are to receive grants of up to £25,000 each from the Technology Strategy Board to carry out smaller-scale feasibility studies to test out new ideas.

The research and development projects and feasibility studies fall within five key enabling technology areas – advanced materials; biosciences; electronics, photonics and electrical systems; information and communications technology; and nanoscale technologies.

UK universities and science minister David Willetts said, "Developing and adopting new technologies can be a significant driver of economic growth and create new jobs. These exciting research and development projects will translate technically feasible ideas into more developed and advanced innovations that could be applied across a range of areas, such as in healthcare, transport, food, environmental sustainability and construction, stimulating growth, keeping the UK at the forefront of modern technology and providing solutions to significant technical challenges.

Iain Gray, chief executive of the Technology Strategy Board, added: "The aim of these funding competitions is to stimulate projects inspired by new discoveries and breakthroughs, including ideas that are yet to find specific applications in a recognised market or business sector. We were delighted with the quality of proposals, are excited about the research work that lies ahead and look forward to seeing the development of some valuable new technology products and processes."

VTT Seeks Solutions to Autonomic Service Networks

The amount of network-connected devices capable of M2M communication is increasing rapidly. Connecting these devices to a network and services is challenging even for experts and almost impossible for consumers. Therefore, VTT Technical Research Centre of Finland is coordinating a European ICT project that focuses on services offered through M2M networks consisting of a variety of electronic devices, such as mobile phones, sensors, actuators and machines.

The project, which will run until spring 2014, aims to apply autonomic computing and communication paradigms in a way that permits problems caused by increasing

Go to mwjournal.com for more international news items

complexity in M2M networks to be solved. The Autonomic Services in the M2M networks (A2Nets) project approaches the problem from a horizontal viewpoint, aiming to fulfil the requirements of several domains. The horizontal architecture, standards and enabling solutions of M2M systems are being developed to boost the technology usage in several vertical solutions. The results of the project are being evaluated in test environments related to telematics, energy and well-being.

Made up of 24 partners, the international Eureka/ITEA2 A2Nets consortium has received €23.5 million of funding for its M2M research. In addition to VTT, the project consortium includes, among others, Atos, Bull, Gemalto, Innova, Polar, Rücker Lypsa and Thales. The project will run until spring 2014.

ITU Declaration Calls for Lifecycle Approach

Participants at the 7th International Telecommunication Union (ITU) Symposium on ICTs, the Environment and Climate Change have issued a declaration that encourages ICT manufacturers to make their products more easily upgradable without need for replacing the entire device.

The call to promote a lifecycle approach in the design of ICTs also means taking into account how components in a device can be recycled. Reducing e-waste and providing incentives and encouragement for e-waste take back schemes were just some of the issues included in the declaration.

"…engagement in the design of technology solutions and standards is essential."

The declaration, adopted by the approximately 150 participants at the event, also called for enabling policies to encourage investment in smart technologies and ICT-based clean technologies as a way of promoting green growth and sustainable development. In addition, the support of ITU methodologies to measure the impact of ICT and a recommendation to ramp up research and development on the use of ICTs for monitoring, mitigating and adapting to the effects of climate change are mentioned.

Malcolm Johnson, director of ITU's Telecommunication Standardization Bureau (TSB) commented, "We very much hope that Technology Transfer mechanism agreed in Durban at COP17 for implementation this year will encourage ICT projects that help adapt to and mitigate the effects of climate change. The key components for a successful strategy are a combination of policies and regulatory incentives and standards that encourage the use of ICTs to combat climate change at the international, regional and national levels. Active participation in international climate change discussions and engagement in the design of technology solutions and standards is essential."

photo courtesy of the
U.S. Military & NASA


Mini-Circuits
LAVI

90 Million Homes Worldwide Will Employ Home Automation Systems by 2017

New subscription-based home automation offerings are rapidly transforming the way consumers will monitor, secure and control their homes. Long the preserve of more expensive, custom-installed technology, home automation is moving into the mainstream, with companies such as ADT, Comcast, Verizon, Lowe's, and many others all adding home automation to their customer services.

ABI Research's "Home Automation, Security, and Monitoring" report examines the evolving marketplace for home automation systems and how the rise of managed subscriptions will impact existing luxury, DIY and mainstream home automation markets.

Annual Home Automation System Shipments by Region
World Market: 2012 – 2017

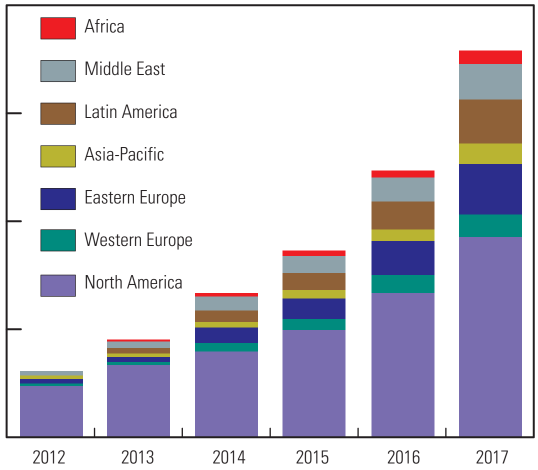

Source: ABI Research

The Market for Tower Mounted Amplifiers Nears $500 Million

Tower mounted amplifiers have now become a common addition to most macro base station systems. They increase overall system performance and are now easily mounted and monitored. Tower mounted amplifiers can provide significant BTS performance improvement for a moderate investment. Lance Wilson, research director, mobile networks, notes, "The use of tower mounted amplifiers in wireless infrastructure base station systems represents one of the most cost effective ways of improving overall system performance."

A tower mounted amplifier is a low-noise RF amplifier that is inserted in the receive path of a macro mobile wireless infrastructure base station. They are generally placed in the coaxial transmission line that goes from a ground mounted base station to the antenna array. Tower mounted amplifiers are normally located as close to the antenna as possible.

The tower mounted amplifier holds an almost unique spot in the base station RF hardware chain. It can be a portion of a complete system from the outset of an installation or they can be added later as needed. There are new hardware technologies, however, namely remote radio heads and active antennas, which will represent a threat to TMA market growth. "Although tower mounted amplifiers still represent healthy business, that market position will be threatened by the increasing use of remote radio heads and active antennas, both of which include the tower mounted antenna functionality," adds Wilson.

"The use of tower mounted amplifiers in wireless infrastructure base station systems represents one of the most cost effective ways of improving overall system performance."

Standalone Vs. Integrated Dilemma is Major Theme of $37 B Mobile Handset Semiconductor Market

Revenues for core semiconductor components used in mobile handsets, including platform ICs and wireless connectivity ICs, are expected to reach almost $37 billion per annum in 2012. The market has seen strong growth from 2009 as the smartphone market has increased significantly, driving growth for many components, including applications processors and Wi-Fi ICs.

"The smartphone has offered many opportunities to semiconductor vendors as it has largely been dominated by standalone IC solutions," comments practice director Peter Cooney. "However, the market is transitioning to one of more integrated solutions, particularly in the high growth, low- and mid-end tiers of the market. This will mean less available sockets and therefore much stronger competition for these in the future."

Qualcomm dominates the overall market with over one-quarter of total market revenues in 2011. It is also the best-placed company to take advantage of the growing integrated solutions market, as demonstrated by the success of its Snapdragon portfolio of products. There are many other suppliers, such as Broadcom and ST-Ericsson, who are racing to compete in this section of the market, e.g., ST-Ericsson's NovaThor and its recent success with a number of handsets suppliers, including Samsung.

"Based on current market conditions and product portfolios, it seems Qualcomm is the clear favorite to continue its dominance of the handset IC market. I'd expect that

Go to mwjournal.com for more commercial market news items

Qualcomm will increase its market share of the overall platform IC market over the next five years," says Cooney. "This doesn't mean it will be a closed shop, however, and there is certainly room for two or three other suppliers to have a long-term position in the market. Currently there are a number of contenders that have an eye on second or third place, including Broadcom, Intel, ST-Ericsson, NVIDIA, MediaTek and Marvell."

The overall market for handset ICs is forecast to peak in 2014, reaching almost $40 billion. It is then expected to fall, as handset shipment growth starts to stall and IC average selling prices continue to fall. Expect even more fierce competition for sockets in the future.

Smartphone Accessory Revenues Valued at $20 B in 2012

Smartphones will drive $20 billion in aftermarket accessory revenues in 2012, accounting for more than half of the $36 billion that all aftermarket handset accessories will produce. By 2017, smartphone accessories will grow to $38 billion in revenues, while feature phone accessory revenues decline to $12 billion.

"The increasing penetration of smartphones is driving a shift in accessory design toward smart accessories that drive higher levels of consumer interaction, product value and brand recognition," says Michael Morgan, senior analyst, devices, applications and content. "For new market entrants, developing brand recognition is paramount in capturing market share from the incumbents. This is best accomplished by the development of engaging, innovative accessories that extend the value proposition of today's mass market accessories."

Feature phone consumers will spend an average of $28.17 on accessories per device, while smartphone owners will spend $56.18 on accessories per device. The difference in spending is driven by a combination of consumers spending more per accessory and purchasing more accessories for smartphones as compared to feature phone owners.

"As smartphones continue to expand the value of mobile handsets, accessories will need to equally deliver higher levels of product engagement, customization, and predict consumers' shifting mobility use cases," adds Jeff Orr, practice director, devices, applications and content.

ABI Research's report, "Mobile Handset Accessories," focuses on key handset accessories and the market for these products, including in-depth analysis for both in-box as well as aftermarket handset accessories. It also examines key market drivers and barriers to growth, acquisition channels, technological trends, and future market potential for handset accessories.

Around the Circuit

Laura Glazer, Staff Editor

INDUSTRY NEWS

Teledyne Technologies Inc. and **LeCroy Corp.** have entered into a definitive agreement that provides for the merger of LeCroy Corp. with a wholly-owned subsidiary of Teledyne. Pursuant to the transaction, Teledyne will acquire all of the outstanding common shares of LeCroy for $14.30 per share payable in cash. The aggregate value for the transaction is approximately $291 million, taking into account LeCroy's stock options, stock appreciation rights and net debt as of March 31, 2012. The transaction was unanimously approved by the Boards of Directors of Teledyne and LeCroy.

Silicon Laboratories Inc. has signed a definitive agreement to acquire **Ember Corp.** for an initial consideration of $72 million. Ember is a late-stage private company offering silicon, software and development tools for 2.4 GHz wireless mesh networking solutions being deployed in monitoring and control applications. The boards of each company have approved the acquisition, which awaits the satisfaction of regulatory requirements and other customary closing conditions.

ANSYS Inc. and **Esterel Technologies S.A.** signed a definitive agreement whereby ANSYS will acquire Esterel Technologies for a cash purchase price of approximately euro 42 million (or approximately US$53 million), subject to certain working capital adjustments at close. The agreement also includes retention provisions for key members of management and employees. The transaction, currently anticipated to close in the third calendar quarter of 2012, is subject to customary closing conditions and regulatory approvals.

CPI International Holding Corp. and its wholly owned subsidiary **CPI International Inc.** announced they have entered into a definitive agreement to acquire the **Codan Satcom** business from **Codan Ltd.** Codan Satcom is a supplier of solid-state RF subsystems for satellite communications services to commercial and government end users. Under the terms of the agreement, CPI will acquire Codan Satcom for $9 million in cash, subject to certain adjustments, to be funded entirely from cash on hand.

DragonWave Inc. announced the closing of the acquisition of **Nokia Siemens Networks**' microwave transport business including its associated operational support system and related support functions. The acquisition was effected pursuant to the Amended and Restated Master Acquisition Agreement between DragonWave Inc., its wholly-owned subsidiary **DragonWave S.à r.l.** and Nokia Siemens Networks dated May 3, 2012. Nokia Siemens Networks retains responsibility for its existing solution sales and associated services for microwave transport, while DragonWave is responsible for the microwave transport product line, including R&D, product management and operations functions.

Teseq Holding AG intends to acquire New York-based **Instruments for Industry** (IFI), a designer and manufacturer of solid state and traveling wave tube (TWT) amplifiers. IFI's New York location will be integrated into the Teseq Group as its fourth competency center joining Luterbach, Switzerland; Berlin, Germany and Ryde, Isle of Wight, UK. Moving forward, the new business unit will focus primarily on TWTs, class AB technology and customer specific models for the general amplifier and military markets.

EDI CON Electronic Design Innovation Conference 电子设计创新会议 2013

Horizon House has announced plans to launch the inaugural Electronic Design Innovation Conference (**EDI CON 2013**) in Beijing, China in March 2013. EDI CON will be an annual event dedicated to providing design engineers and system integrators with the opportunity to learn about the latest RF, microwave and high speed digital products and technologies for today's communications, computing, RFID, industrial wireless monitoring, navigation, aerospace and related markets. The conference program is being developed in partnership with industry and local academia. For more information, visit www.ediconchina.com.

CONTRACTS

Harris Corp. has been awarded a two-year, $19 million contract by the **U.S. Department of Veterans Affairs Office of Information and Technology** to create a wireless network infrastructure for medical centers nationwide. Harris will design, install, validate and provide training for a secure wireless infrastructure to accommodate the voice, video, and real-time-location-services necessary for mobility. With all options exercised, Harris will deploy this infrastructure to 26 customer sites as part of one of the largest healthcare mobility infrastructure deployments.

Raytheon BBN Technologies has been awarded $1.9 million by the **U.S. Air Force Research Laboratory** under the Force Protection program. BBN is a wholly owned subsidiary of Raytheon Co. Networks of sensors, commonly called force protection kits, are used to alert troops to potential dangers in perilous environments before they become immediate threats. BBN will develop a platform to extend the reach of such force protection kits.

Applied Radar Inc. has received two new contracts: a new Phase 1 SBIR ($150,000) on Passive Airborne Radar Using Opportunistic Signals (PASAROS) with the **U.S. Air Force Research Lab** at WPAFB, OH, and a Phase 2 Enhancement ($500,000) on Adaptive Distributed

For up-to-date news briefs, visit www.mwjournal.com

Aperture Radar Mainlobe Jammer Suppression with the **U.S. Missile Defense Agency** (MDA) in Huntsville, AL.

Polaris Wireless announced a significant customer contract for a multi-million dollar deployment of the Polaris Wireless Altus and OmniLocate location surveillance product suite in the Europe-Middle East-Africa (EMEA) region. This is the 14th deployment of the Polaris Wireless high-accuracy wireless location surveillance solution outside the U.S., and 38th globally. Polaris Wireless high-accuracy location solutions have been extensively deployed since 2003 for public safety applications in the U.S. market.

PERSONNEL

Laird Technologies Inc. announced the appointment of **David Lockwood** OBE as its chief executive officer. Lockwood brings experience from a variety of market and technology sectors relevant to Laird Technologies' business, particularly in wireless communication. He has experience in international operations gained from his roles at GPT (Marconi), BAE Systems, Intense Ltd., a phototonics high-tech start-up and Thales Corp.

ANADIGICS Inc. announced that **Tim Laverick** has joined the company as vice president, infrastructure products, and **Robert Bayruns** has been appointed vice president and chief technology officer. Laverick is a business and engineering leader with over 20 years of experience in the RF and microwave semiconductor industry and Bayruns has over 30 years of leadership and engineering experience.

Cree Inc. announced that **John Kurtzweil** has resigned as executive vice president-finance and chief financial officer, effective May 21, 2012, to pursue other opportunities, and that **Michael McDevitt** has been appointed CFO on an interim basis. Cree has commissioned a search for a replacement through Russell Reynolds Associates.

Analog Devices Inc. (ADI) has appointed **Somshubhro (Som) Pal Choudhury** as managing director for operations in India. Pal Choudhury will manage Analog Devices' presence in the country specifically defining and executing strategies to expand business by further developing and strengthening ADI's relationships with strategic customers, the government and local universities. Based in Bangalore, Choudhury will be responsible for operational, statutory and compliance accountabilities.

▲ *Neil Sparling*

Linwave Technology announced the appointment of **Neil Sparling** to the role of technical director. Qualified as a BEng in electrical and electronic engineering, Sparling brings a wealth of project management and microwave technology innovation to the business. He has spent significant time on the design of components and systems for microwave applications in defence radar, EW and sensing, Marine and commercial applications most recently as programes director at a world leading EW specialist.

▲ *Ian Hunter*

The **Royal Academy of Engineering**, **Radio Design Ltd.** and the **University of Leeds,** UK, announced the establishment of a new Research Chair focused on original research in the field of microwave signal processing. Professor **Ian Hunter** of the School of Electronic and Electrical Engineering has been appointed to this position and will head up a Centre of Microwave Signal Processing Processing at Leeds University.

REP APPOINTMENTS

CST has announced that **Delcross Technologies**' Electromagnetic Interference Toolkit (EMIT) is now available through the CST of America sales channel. The software will be fully supported by CST's team of electromagnetic specialists.

LadyBug Technologies announced it has selected **Partner Electronic** of İzmir, Turkey as its authorized distributor in Turkey for LadyBug's range of USB power sensors covering average power, peak and pulse power, and pulse profile measurements. Additionally, **Sea-Port Technical Sales** of Bellevue, WA, has been named as authorized distributor for the Pacific Northwest for LadyBug's entire range of USB Power Sensors.

Modelithics Inc. signed with **Medeos SRL** for support of sales and services in Italy. Larry Dunleavy, Modelithics' president and CEO, and Giuseppe Fabiano, president of Medeos, signed a comprehensive representative and reseller agreement authorizing Medeos to sell Modelithics products and services throughout Italy.

G.T. Microwave Inc., of Randolph, NJ, announced the appointment of domestic representative, **GTEK LLC**, to cover CT, ME, MA, NH, RI and VT. Aldo Guarino, president of GTEK LLC, and his sales team were allotted the task of supporting prospective customers in the northeastern region of the U.S. GTEK LLC is a regional manufacturer's representative organization focused on providing hardware solutions and engineering services to electronic component engineers and manufacturers in the military, aerospace, wireless and industrial markets.

WEBSITE

New pages have been added to **Intelliconnect (Europe) Ltd.**'s website showing stock levels of its standard products. If the required connecter is not in stock, most connector, adapter, cable assembly solutions are available within a maximum of six to eight weeks with quotations and drawings confirmed within 24 hours of enquiry. The new stock index pages will be available at www.intelliconnect.co.uk/products/stock-index as well as from all product pages.

2 W, 5 W, and 20 W

PRECISION ATTENUATORS

NOW up to 26 GHz from $29.95 ea. (1-49)

RoHS compliant

For rugged, reliable, and repeatable attenuation when accuracy is key, our customers have come to rely on Mini-Circuits Fixed Precision Attenuators, rated at 2W or 5W for DC-18 GHz signals. And now we've gone even further, with a new series of **2 W models up to 26 GHz,** and a new series of **20 W models from DC-18 GHz!** They feature stainless steel construction, precision attenuation from 1 to 50 dB, and SMA or N-type connectors for 50 Ω systems.

Inherent accuracy, and finely-graded attenuation levels, make our "BW" family invaluable on the bench or in the field. They're a ready solution for extending the range of test instrumentation or meeting circuit- and system-level requirements, such as better matching for high-VSWR components, reducing power to maximize sensitive applications, or protecting valuable circuitry. Just go to minicircuits.com—they're on the shelf and ready to ship today, at the low prices you've come to expect!

See minicircuits.com for specifications, performance data, and surprisingly low prices!
Mini-Circuits...we're redefining what VALUE is all about!

Mini-Circuits®
ISO 9001 ISO 14001 AS 9100

P.O. Box 350166, Brooklyn, New York 11235-0003 (718) 934-4500 Fax (718) 332-4661

Yoni2® ***The Design Engineers Search Engine*** *finds the model you need, Instantly* • For detailed performance specs & shopping online see **minicircuits.com**

U.S. Patents
7739260, 7761442

IF/RF MICROWAVE COMPONENTS

331 rev S

Testing Radar and EW Systems for the Real-World

OPERATING IN A COMPLEX ENVIRONMENT

The latest generations of radar and EW systems operate in a variety of frequency bands and use wideband or UWB signals that carry highly complex modulation schemes. These systems also use advanced DSP techniques to mask or disguise their operation and thereby avoid jamming.

Within the operating environment, the complexities may include multiple targets, ground clutter, sea clutter, jamming, interference, wireless communication signals and other forms of electromagnetic noise. Depending on the type of radar or EW system, the test platform must be capable of producing a variety of signals: pulse Doppler, wideband, UW and beyond.

In the field, radar and electronic warfare (EW) systems face an environment filled with known and unknown signals: target returns, clutter, jamming, interference and electromagnetic noise. During design and development it has been difficult and costly to simulate realistic scenarios that thoroughly exercise system performance.

Today, a combination of COTS instrumentation and electronic design automation (EDA) software is making it easier to create scenarios such as multi-target returns in a complex electromagnetic environment. The software provides an environment for electronic system-level (ESL) design and includes a library of radar models. The key instruments are arbitrary waveform generators (AWG) and vector signal generators (VSG).

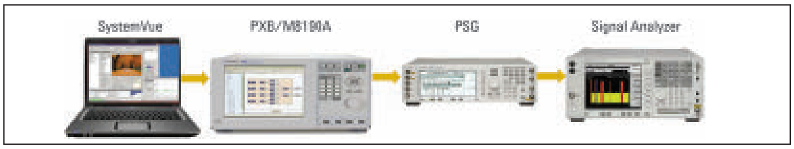

▲ *Fig. 1 System configuration for the radar target generator.*

Complex baseband signals or sequences are created in the ESL environment and downloaded into the memory of an AWG capable of producing modulated carrier signals. If a wideband AWG is used, it can drive the I/Q inputs of a VSG to produce wideband or ultra-wideband (UWB) scenarios.

This synergistic combination of hardware and software provides a platform that can be used for component testing and scenario simulation for system test. The addition of a signal analyzer or wideband oscilloscope running vector signal analysis (VSA) software provides measurement and analysis capabilities that are

Dingqing Lu
Agilent Technologies, Santa Clara, CA

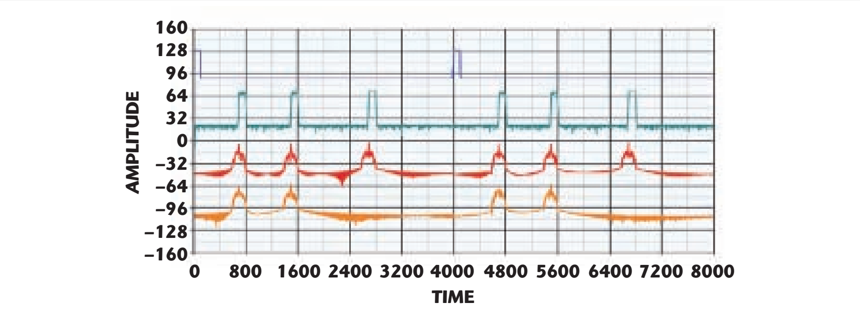

▲ *Fig. 2 Simulation results for transmission signal (blue), three received target returns (green), received returns with clutter (red), and the return signal after MTI processing (orange).*

useful in the development of transmitters, receivers, amplifiers and other subsystems.

MODELING SYSTEMS AND CREATING SIGNALS

To meet these requirements, two solutions have been developed: a radar target generator and a test platform for radar and EW testing. The chosen combination of software and hardware elements makes it possible to create realistic and dynamic scenarios for component and system testing. The software environment can be used for modeling, simulation, verification and testing during system design and implementation. It also has the flexibility to incorporate models created using tools such as C++, MATLAB and HDL.

Specific to radar, the ESL software provides four key capabilities: the generation of custom waveforms; support for advanced measurements; control of hardware and software instruments; and emulation of "golden" transmitters, detectors or receivers. The first step is to assemble the desired radar system within the software environment. To simulate multiple types of systems, the software lets the user specify individual components within the block diagram: signal sources, transmitter and receiver modules, antennas, RF and IF modules and signal-processing techniques. Further, measurements and the surrounding radar environment can be defined as part of the model. The software also includes links to enable the downloading of simulated waveforms to AWGs, which can play back the simulated waveforms for the testing of transmitters and receivers.

GENERATING RADAR TARGET SIMULATIONS

The major attributes of a radar target generator include RF details such as carrier frequency and modulation bandwidth as well as scenario parameters: number of target returns, duration of target returns, range, speed, azimuth, radar cross-section (RCS), types of clutter, jamming, interference and more. Within the ESL software, these are entered as details within the system model described above.

The configuration is shown in ***Figure 1***. Starting on the left side, the

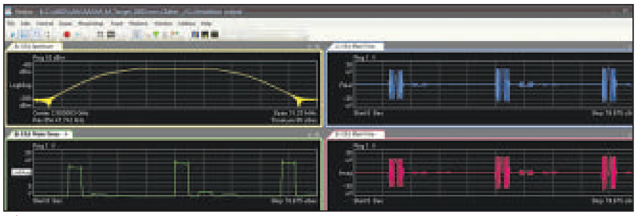

▲ *Fig. 3 Generated radar test signals: received spectrum (yellow); and radar target returns with clutter, displayed as amplitude (green), real part (blue) and imaginary part (red).*

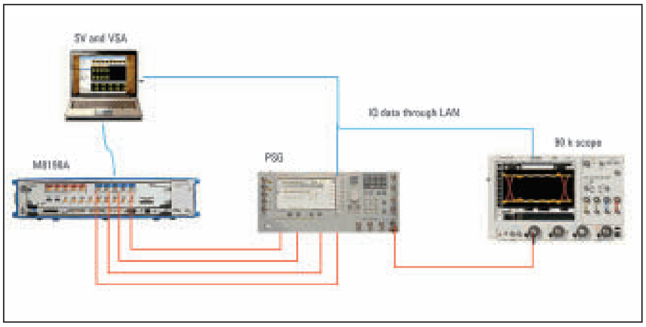

▲ *Fig. 4 System configuration for the UWB radar test platform.*

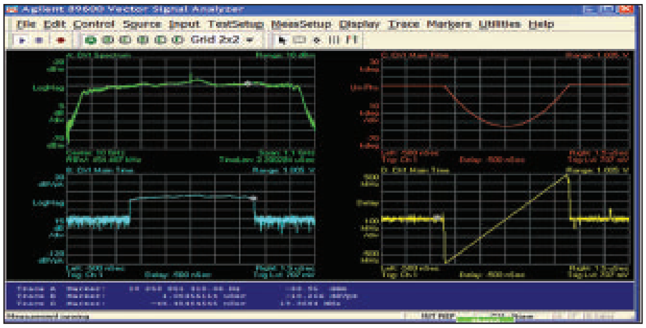

▲ *Fig. 5 Spectrum, time waveform, phase and group delay measurements of an LFM UWB radar signal.*

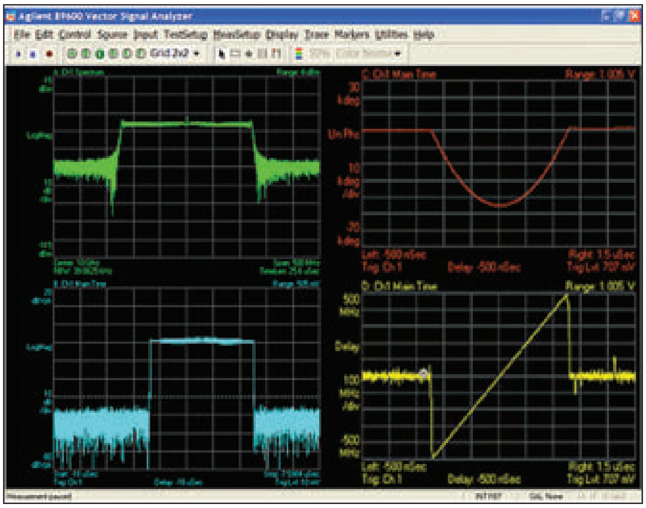

▲ *Fig. 6 Spectrum, time waveform, phase and group delay measurements of a pulsed UWB radar signal.*

first three elements are used to generate the signals necessary for transmitter and receiver testing. The signal analyzer is used to verify the test signals. Signal simulation also proceeds from left to right, starting with the creation of a block diagram-based radar design within the ESL software. In this case, the model used a transmitter waveform generator to produce a baseband waveform that was then modulated. Next, three target signals were created, combined with each other, combined with clutter signals and output to an antenna model. The resulting signal was analyzed within the ESL environment and, when the scenario was finalized, downloaded to the AWG.

Figure 2 shows the results from a three-target simulation with individual range values of 500, 1500 and 2500 m and velocity values of 100, 200 and 0 m/s. As shown, moving target indication (MTI) processing removed the stationary (0 m/s) target from the bottom (orange) trace.

Figure 3 shows the simulation signal created in software and subsequently downloaded to a vector signal generator with AWG capability. The

Trust the Leader: RFMD® Custom Foundry Services

The RFMD Foundry globally manufactures outstanding compound semiconductor technologies and offers customers access to our industry-leading services for the fabrication of custom parts to specifications. Our unmatched manufacturing scale, supported by two of the largest III-V factories in the world, enables best-in-class cycle times backed by our on-time shipment pledge.

Our Custom Foundry Services

- **GaN Process Technologies**
  GaN1 high power
  GaN2 high linearity
  rGaN-HV™
  IPC3 integrated passive components for high power

- **GaAs Process Technologies**
  FD25 low noise pHEMT
  FD30 high power pHEMT
  FET1H switching pHEMT
  FET2 E/D pHEMT
  HBT8 rugged InGaP

Industry-Leading Cycle Time from RFMD

- **Our best-in-class cycle time is backed by our on-time pledge**
- **Prototype and shuttle lot cycle time = 6 weeks**
- **Production lot cycle time = 6 weeks**

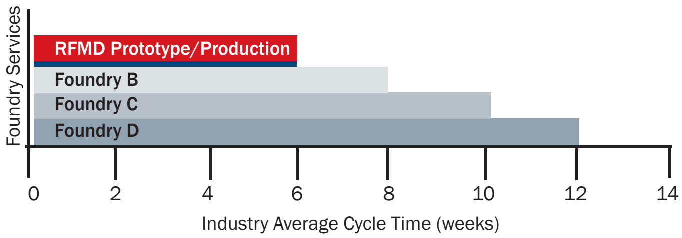

Our Global Presence

Greensboro, NC Fabrication Facility

Newton Aycliffe, UK Fabrication Facility

For more information contact the RFMD Foundry at (336) 678-5555.

four traces provide different views of the RF test signal, which is emulating radar returns from three targets.

CREATING A TEST PLATFORM FOR UWB RADAR

The configuration shown in ***Figure 4*** is a component test system in which different UWB signals can be generated in software, downloaded to a wideband AWG, upconverted by the vector signal generator and applied to the hardware component as a stimulus. The real-time oscilloscope provides waveform analysis and also supports signal analysis through the VSA software running on the PC.

This system was used to create the signal shown in ***Figure 5***, which is an LFM UWB radar with a 1 GHz bandwidth and 1 µs pulse repetition interval (PRI). The same configuration was used to produce the pulsed UWB transmission signals shown in ***Figure 6***. The example signal has a 250 MHz bandwidth and 1 µs PRI, as measured with Agilent's PXI-based vector signal analyzer.

ENHANCING TEAM PRODUCTIVITY

The solutions described above do more than address a wide range of present and future radar systems: They also help overcome organizational hurdles. For example, the development of complex radar or EW systems typically requires the involvement of multiple people working in teams that may be physically or geographically separated. System integration can be especially difficult without a consistent, shared set of tools for simulation and testing. The software environment described here supports team collaboration across the radar block diagram and between team members working in different locations. ■

Dingqing Lu *has been with Agilent Technologies/Hewlett Packard Co. since 1989 and is a scientist with Agilent EEsof EDA, working on modeling, simulation, testing and implementation of Military and Satellite Communications and Radar EW systems. From 1981 to 1986, he was with University of Sichuan as Lecturer and Assistant Professor. He was a Research Associate in the Department of Electrical Engineering at University of California (UCLA) from 1986 to 1989. He is IEEE senior member and has published 20 papers on* IEEE Transactions, Journals and Conference Proceedings*. He also holds a U.S. patent on fast DSP search algorithm. His research interests include system modeling, simulation and measurement techniques.*

Advance Your System With Our Affordable & Smart GaN Solutions

- PHASED ARRAY RADAR
- MARINE RADAR
- AIR TRAFFIC CONTROL RADAR
- IFF RADAR
- TACTICAL RADIOS
- WEATHER RADAR

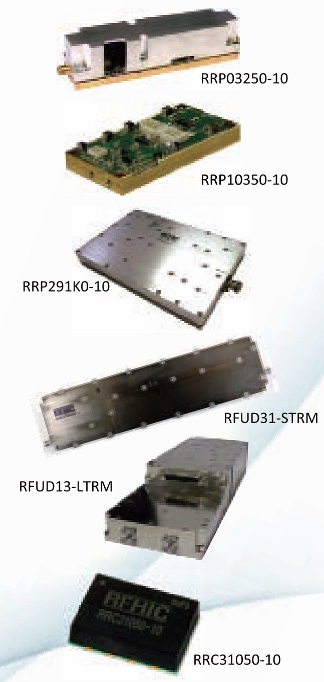

Pallet Amplifier

Part Number	Frequency (MHz)	Gain (dB)	Pout (W)	Eff. (%)	Pulse Droop (dB)	Duty (%)	Pulse Width (µs)	VDD (V)	Dimension (mm)
RRP03250-10	135 ~ 460	31	300	45	0.5	20	500	50	114.3 x 25.4 x 28
RRP10350-10	1030 ~ 1090	28	350	50	0.5	5	200	50	53.2 x 28 x 8
RRP13330-10	1200 ~ 1400	14	330	65	0.5	20	500	50	85 x 40 x 10
RRP29280-10	2700 ~ 3100	9	280	50	0.5	20	500	50	86 x 39 x 10

kW SSPA

Part Number	Frequency (MHz)	Gain (dB)	Pout (W)	Eff. (%)	Pulse Droop (dB)	Duty (%)	Pulse Width (µs)	VDD (V)	Dimension (mm)
RRP131K0-10	1200 ~ 1400	53	1000	45	0.5	20	500	50	250 x 150 x 28
RRP291K0-10	2700 ~ 3100	60	1000	32	0.5	20	500	50	220 x 145 x 27

T/R Module

Part Number	Frequency (GHz)	Tx Pout (W)	Rx NF (dB)	Rx Gain (dB)	Tx Gain (dB)	Duty Cycle (%)	Pulse Width (µs)	Attenuator	Phase Shifter
RFUD95-X15-200	9.3 ~ 9.5	15	3.5	30	32	10	100	6 Bit, 31.5dB	N/A
RFUD31-STRM	2.7 ~ 3.5	200	3.5	25	53	20	500	6 Bit, 31.5dB	6 Bit, 360deg
RFUD13-LTRM	1.2 ~ 1.4	250	3.5	35	54	20	500	6 Bit, 31.5dB	6 Bit, 360deg

GaN Hybrid Amplifier

Part Number	Frequency (MHz)	Gain (dB)	Pout (W)	Eff. (%)	Pulse Droop (dB)	Duty (%)	Pulse Width (µs)	VDD (V)	Dimension (mm)
RRC13050-10	1200 ~ 1400	36	50	60	0.5	10	100	50	20.5 x 15 x 4.8
RRC29050-10	2700 ~ 3100	26	50	55	0.5	10	100	50	20.5 x 15 x 4.8
RRC31050-10	2700 ~ 3500	25	50	50	0.5	10	100	50	20.5 x 15 x 4.8
RRY56025-10	5400 ~ 5900	20	25	42	0.5	10	100	50	20.5 x 15 x 4.8
RRC94030-10	9300 ~ 9500	17	25	40	0.5	10	100	50	20.5 x 15 x 4.8
RNP04006-A1	400 ~ 450	33	4	72	0.5	10	100	24	20.5 x 15 x 4.8

√ Please contact us for your customized solution.

Radar LNA

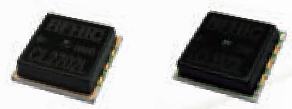

CL2702-L
package : CP-16A

LCL3322-L
package : CP-16B

5W-2kW GaN High Power Amplifier Pallet & Module

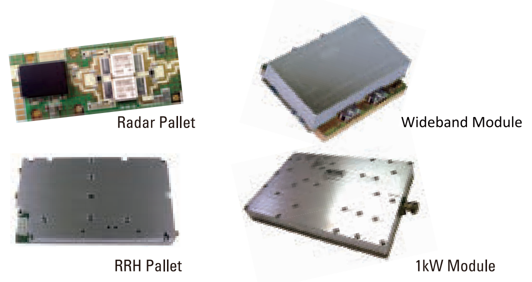

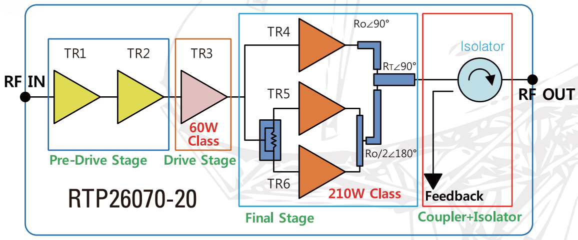

Application

- Telecom
- Radar
- Medical
- Industrial

Frequency & Mode

VHF > L-Band > S-Band > C-Band > X-Band

C.W, Pulse, LTE/WCDMA/GSM

RF & MW is our business & passion

USA Facilities
Tel : 919-677-8780 / E-mail : sales@rfhicusa.com

Korea Facilities
Tel : 82-31-250-5078 / E-mail : rfsales@rfhic.com

RFHIC
www.rfhicusa.com

The 3D Smith Chart and Its Practical Applications

The mathematical theory of the 3D Smith chart[1] unifies active and passive microwave circuit design on the surface of a Riemann sphere. The reflection coefficient plane is mapped stereographically through the South Pole on the surface of a unit sphere. As a result, the classical 2D Smith chart including the passive loads[2] is mapped stereographically into the North hemisphere, while the circuits with negative resistance (that are outside the classical planar Smith chart) are mapped into the South one. The East hemisphere is the place of inductive circuits, whereas the West hemisphere hosts the capacitive circuits. Meantime, the Greenwich meridian is the locus of pure resistive circuits (see ***Figure 1***, where the constant resistance r and reactance x circles are drawn in blue and red, respectively).

The 3D Smith chart differs from previous attempts[4] to generalize the planar 2D Smith chart in a fundamental way: the way in which infinity is treated. The preceding theories fail to merge the active and passive worlds in a simple and rigorous manner, since they propose an empirical solution to map an infinite region into a finite surface. These approaches turned into complicated transforming equations, making the visual and intuitive interpretation of microwave problems very difficult.

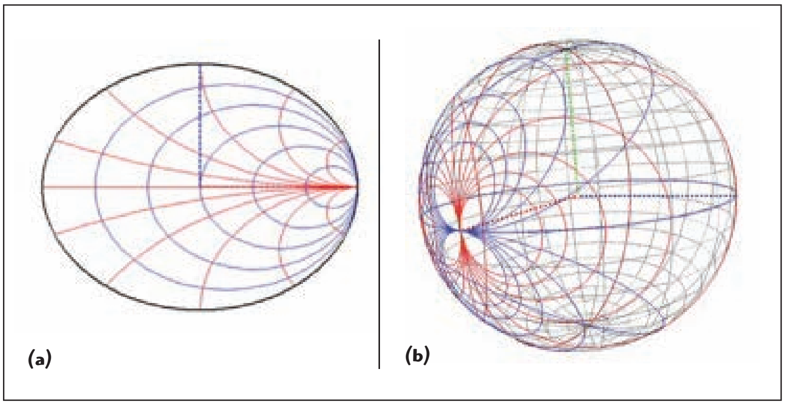

Fig. 1 Representation of the 2D (a) and 3D (b) Smith charts.[3]

In this article, how the 2D and 3D Smith charts deal with the infinite regions are first described. Next, the advantages of using the 3D Smith chart to represent both active and passive loads are illustrated with two examples: the stability circles of an amplifier and the impedance of a microwave oscillator.

TREATMENT OF INFINITY IN SMITH CHARTS

The infinite region of the normalized impedance or z-plane is due to the open circuit, because the magnitude of the input impedance grows to infinity as the load tends to an open circuit. Since in practical applications, impedances can be found close to the open circuit, it is rather uncommon to use the z-plane to perform a visual representation of loads.

For the reflection coefficient plane (ρ-plane), the infinite region corresponds to the load with the same magnitude and opposite sign to the characteristic impedance of the line (that is the infinite mismatch or $z = -1$ in normalized impedance terms). Although it denotes a particular active load, this input impedance is important in some practical applications such as oscillator design. To be able to represent the infinite mismatch, practitioners can use a planar Smith chart plotted in the $1/\rho$-plane called negative Smith chart.[5] This graphical representation gives an important role to the infinite mismatch, which is placed in its center, but moves the matched load ($\rho = 0$) to infinity. Analogously, the open circuit is

Andrei Müller, Dan C. Dascalu
IMT-Bucharest, Romania
Pablo Soto, Vicente E. Boria
Univ. Politécnica de Valencia, Spain

placed in the center of the normalized admittance or y-plane, where another important load, the short circuit, is thrown to infinity.

It can be concluded that all the usual 2D planar representations are unable to keep these four key impedances (open circuit, short circuit, matched load and infinite mismatch) in a bounded region. In fact, all these planes extend to infinity, where one of the aforementioned key loads is located.

The 2D Smith chart is a graphic representation of the ρ-plane, including the constant resistance and reactance lines in the z-plane transformed by means of the Möbius transformation

$$\rho(z) = \frac{z-1}{z+1} \qquad (3)$$

Since Equation 3 is an inversive transformation, it maps infinite lines in the z-plane in generalized circles in the ρ-plane. All the lines in the z-plane extend to infinity and, therefore, all its transformed circles pass through $\rho = 1$ (the reflection coefficient of the open-circuit). An infinite region of the z-plane is compressed around this point (that is an accumulation point), as also reveals the singular behavior of the transformation between the ρ-plane and the z-plane (that is the reciprocal transformation to Equation 3) in this particular point. On the other hand, the region around the short circuit ($\rho = 1$) is expanded by the Möbius transformation.

The 2D Smith chart successfully compiles in a bounded region the unit circle and all of the passive loads with the matched load in its center. Although the passive loads are the more common ones, certain applications involve the use of active devices, whose impedances can be very far from the unit circle (for instance in oscillators or negative resistance amplifiers, to cite a few). Moreover, in other applications, it can be interesting to represent both active and passive loads simultaneously (for example, stability circles in amplifiers, representation of the impedance of devices whose input resistance can be positive or negative depending on the bias point or frequency, or mixed problems involving both active and passive devices). The 2D Smith chart has limitations in these applications, mainly because the Möbius transformation expands the region occupied by the active loads to infinity.

These limitations are successfully addressed by the 3D Smith chart. To build this graphical representation, one must first place the ρ-plane in the

Maxime Bocher, born in 1867 in Boston, professor at Harvard University and president of the American Mathematical Society (1908-1910), was the one that finalized the theory of inversive geometry. The Bocher Memorial Prize is awarded for outstanding achievements in Mathematics appearing in an American journal,[6] and was awarded in 1933 to Norbert Wiener, who played a major role in Information Theory.

Bocher established the theory of the direct inversive and indirect inversive transformations,[7] respectively,

$$t(z) = \frac{az+b}{cz+d} \qquad (1)$$

$$t'(z) = \frac{a\bar{z}+b}{c\bar{z}+d} \qquad (2)$$

where a, b, c and d are arbitrary complex numbers satisfying $ad - bc \neq 0$ and $\bar{z}$ is the extended complex conjugate of the complex variable z. These two transformations map generalized circles (that is circles and infinite lines) into generalized circles, keep the magnitude of the angles and maintain or reverse their orientation. There was a problem with these transformations concerning the points that were thrown at infinity. In his article,[8] Bocher maintained his well-known attitude of seeking for the simplest solution to solve and clarify each problem and argued that points thrown to infinity by inversive transformations should form a single point on the Riemann sphere. In fact, he showed that Equations 1 and 2 were always mapping lines and circles into circles on the Riemann sphere and forming a group under the composition of functions.

He proposed a practical conception of infinite regions and his theory of inversive geometry was used by famous mathematicians such as Klein, Caratheodory and Mandelbrot, and in the arts by Escher.

equatorial plane and next perform its stereographical projection from the South Pole in a Riemann sphere of unit radius.[1] Proceeding in this way, the passive loads will be placed in the North hemisphere of the sphere and the active loads are located in the South hemisphere, packaging all loads in a bounded sphere of unit radius without resorting to infinity. Moreover, the four key loads occupy especially important points of the sphere: the matched and infinite mismatch loads are placed in the North and South Pole, respectively, whereas the West Pole contains the open circuit and the East Pole is the short circuit (the West and East Pole are the poles of the sphere with respect to the Greenwich meridian plane, or in other words, the points of the sphere with maximum and minimum x-coordinate, respectively).

It can also be proven that the same representation can be obtained, if the impedance plane is placed in the Greenwich meridian plane and the stereographic projection to the unit sphere is performed from the West Pole. This property proves the completeness of the 3D Smith chart, since both the ρ-plane and the z-plane will be obtained after performing the inverse stereographic projection in the two main planes cutting the Riemann sphere.

The 3D Smith chart has a wide number of properties that can be helpful to solve microwave problems graphically.[1] In fact, it has more properties than the planar Smith chart due to its completeness. The stereographic projection is also a conformal mapping, thus transforming circles in the 2D Smith chart into circles in the surface of the 3D Smith chart. In addition, infinite lines in the planar Smith chart are mapped into circles in the Riemann sphere passing through the South Pole (the locus of the infinite mismatch load), whereas finite lines are transformed into circle arc sections. The same can be stated for circles and lines drawn in the impedance and admittance planes. As a result, and similarly to the 2D Smith chart, a wide variety of microwave problems can be solved graphically in this new tool by drawing and intersecting circles.

APPLICATION EXAMPLES

In order to work with negative impedances, engineers have to either use different tricks or face scaling problems, which causes problems with the task of handling both active and passive microwave on the same chart. These problems disappear on the 3D Smith chart, where infinity becomes a handy issue.

Amplifier Stability Circles

One of the applications that reveal the limitations of the planar Smith chart and the advantages of the 3D Smith chart is the stability analysis of microwave amplifiers. To guarantee the stability of the amplifier and prevent unexpected oscillations, this analysis must be performed over a very wide frequency range. At each frequency, a stability factor is first computed to determine whether the amplifier is conditionally or unconditionally stable.[9,10] If the amplifier is conditionally stable, it is required to plot both the source and load instability regions, which define the loads at the input and the output of the amplifier that should be avoided to prevent a potential oscillation at this particular frequency.

In the ρ-plane, and therefore in the 2D Smith chart, the boundary between stability and instability regions are circles. The center and radius of the source and load stability circles can be easily computed from the S-parameters of the transistor (or, in general, the active circuit providing the amplification).[9,10] In most cases, however, one or both circles include active loads, thus being placed partially outside of the 2D Smith chart. In a wide frequency range, this problem generates visualization problems in 2D, due to the scaling required to be able to plot the entire stability circles, identify the problematic regions and look for a possible solution.

The 3D Smith chart does not require any type of scaling, since all the active and passive loads are successfully represented in a bounded surface. Moreover, and due to properties of the stereographic projection, the stability circles in the planar Smith chart transform into circles in the Riemann sphere.

To illustrate these concepts, the stability of a Motorola transistor, with S-parameters given in ***Table 1***, has been analyzed at 100 MHz. ***Figure 2*** depicts the source (in green) and load (in magenta) stability circles of this conditionally stable transistor in both the 2D and 3D Smith charts. To visualize the complete circles, the ρ-

TINY

Wideband Transformers

0.15-6200 MHz as low as 99¢ each (qty. 1000) RoHS compliant.

Rugged, repeatable performance.
At Mini-Circuits, we're passionate about transformers. We even make own transmission line wire under tight manufacturing control, and utilize all-welded connections to maximize performance, reliability, and repeatability. And for signals up to 6 GHz, our rugged LTCC ceramic models feature wrap-around terminations for your visual solder inspection, and they are even offered in packages as small as 0805!

Continued innovation: Top Hat.
A Mini-Circuits exclusive, this new feature is now available on every open-core transformer we sell. Top Hat speeds customer pick-and-place throughput in four distinct ways: (1) faster set-up times, (2) fewer missed components, (3) better placement accuracy and consistency, and (4) high-visibility markings for quicker visual identification and inspection.

More models, to meet more needs
Mini-Circuits has over 200 different SMT models in stock. So for RF or microwave baluns and transformers, with or without center taps or DC isolation, you can probably find what you need at minicircuits.com. Enter your requirements, and Yoni2, our patented search engine, can identify a match in seconds. And new custom designs are just a phone call away, with surprisingly quick turnaround times gained from over 40 years of manufacturing and design experience!

See minicircuits.com for technical specifications, performance data, pricing, and real-time, in-stock availability!
Mini-Circuits...we're redefining what Value is all about!

Mini-Circuits®
ISO 9001 ISO 14001 AS9100

P.O. Box 350166, Brooklyn, New York 11235-0003 (718) 934-4500 Fax (718) 332-4661

Yoni2® **The Design Engineers Search Engine** *finds the model you need, Instantly* • For detailed performance specs & shopping online see **minicircuits.com**

U.S. Patents
7739260, 7761442

IF/RF MICROWAVE COMPONENTS

377 rev Y

TABLE I

S-PARAMETERS OF A MOTOROLA 2N667A BIPOLAR TRANSISTOR (BIAS POINT: V_{CE}=15 V, I_C=25 MA)

Frequency (GHz)	S_{11} |-|	S_{11} ∠	S_{21} |-|	S_{21} ∠	S_{12} |-|	S_{12} ∠	S_{22} |-|	S_{22} ∠
0.1	0.60	–76	38.6	141	0.01	55	0.83	–20
0.5	0.67	–158	12.7	95	0.02	40	0.50	–27
1	0.68	–178	6.6	77	0.03	53	0.46	–32
2	0.69	162	3.4	54	0.05	54	0.47	–50
3	0.69	146	1.3	31	0.07	55	0.53	–70
4	0.69	131	1.7	11	0.09	51	0.57	–89
5	0.69	114	1.4	–9	0.12	44	0.62	–106
6	0.69	98	1.1	–28	0.15	33	0.68	–122

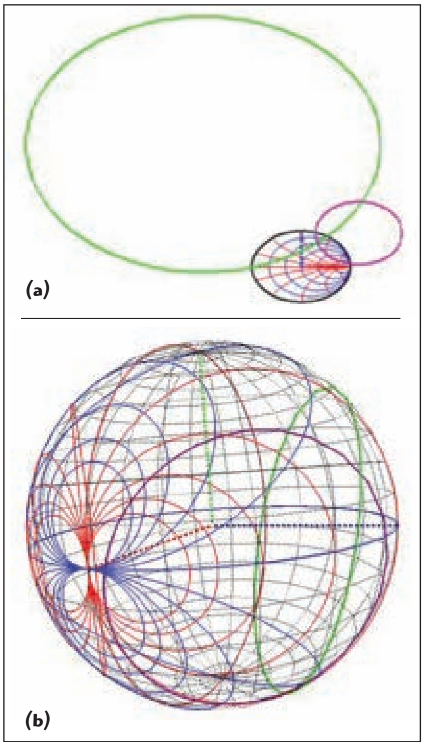

▲ *Fig. 2 Representation in the 2D (a) and 3D (b) Smith charts of the stability circles of a Motorola 2N667A bipolar transistor at 100 MHz.*

plane must be scaled in the 2D representation. This scaling reduces the 2D Smith chart, thus making it more difficult to get a visual insight of the problem even for a single frequency.

The instability regions in the 3D Smith chart correspond to the loads in the surface of the sphere delimited by the stability circles and not containing the North Pole. It can be easily seen that the output instability is due to sources with low and moderate impedance magnitude, and inductive or slightly capacitive character. The input or load instability, on the other hand, can be caused by inductive passive loads with a high quality factor Q. Using this information, the engineer can add elements into the amplifier circuit to move the source and load instability circles to the South hemisphere.

Oscillator Design

To obtain an oscillator at a specified frequency, the microwave active circuit must be designed to provide an infinite reflection coefficient at such a frequency. This requires moving to infinity in the reflection plane, thus being useless in a planar Smith chart representation. To solve this type of problem graphically, two solutions are normally considered: (i) using a 1/ρ-plane or negative Smith chart representation[5] or (ii) plot the conjugate impedance of some circuits[10] in the 2D Smith chart. Both solutions require combining two different types of planar representations to plot the loads.

The 3D Smith chart allows solving this type of problem graphically using a unique visual representation, since the infinite mismatch point is placed in a bounded and finite position: the South Pole of the unit sphere. The engineer's task therefore consists of designing the circuit to put the impedance in the South Pole at the oscillation frequency.

Figure 3 shows the 2D and 3D Smith chart representation of the input impedance (in black) of a microwave oscillator at 1 GHz based on an Infineon BFP 640 bipolar transistor designed in the literature.[10] The 2D Smith chart is incapable of plotting the impedance of the oscillator close to the resonant frequency, whereas it can be successfully plotted in the 3D Smith chart without using a different type of representation. These examples show the practical use of the 3D Smith chart. ■

POWER AMPLIFIERS

Efficient Solutions for Point-to-Point & Point-to-Multi-Point Radios!

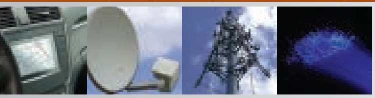

Analog, Digital & Mixed-Signal
ICs, Modules, Subsystems & Instrumentation

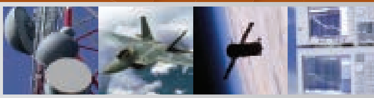

HMC1029
2W Power Amplifier, 29 - 37 GHz

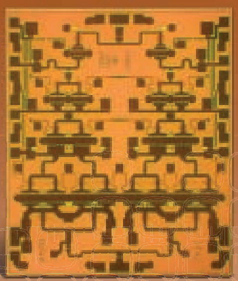

- ***High Saturated Output Power: +35 dBm @ 25% PAE***
- ***Output IP3 to +42 dBm***
- ***High Gain: 24 dB***
- ***DC Supply: +6V @ 1400 mA***

Delivers Over 3 Watts of Saturated Output Power in a Chip Area of <7 mm^2!

A SELECTION OF OUR LINEAR & POWER AMPLIFIERS

	Part Number	Frequency (GHz)	Function	Gain (dB)	OIP3 (dBm)	P1dB (dBm)	Bias Supply	Package
NEW!	**HMC994**	DC - 30	Power Amplifier, 1/2 Watt	14	36	28	+10V @ 250mA	Chip
NEW!	**HMC952**	9 - 14	Power Amplifier with Power Detector, 2 Watt	36	42	34.5	+6V @ 1400mA	Chip
NEW!	**HMC952LP5GE**	9 - 14	Power Amplifier with Power Detector, 2 Watt	33	43	34	+6V @ 1400mA	LP5G
	HMC995LP5E	12 - 16	PA with Power Detector, 3 Watt	27	41	34.5	+7V @ 1200mA	LP5
	HMC965LP5E	12.5 - 15.5	Power Amplifier, 2 Watt	27	40	32	+6V @ 1200mA	LP5
	HMC757LP4E	16 - 24	Power Amplifier, 1/2 Watt	20.5	34.5	26.5	+5V @ 400mA	LP4
	HMC863LP4E	22 - 26.5	Power Amplifier, 1/2 Watt	21.5	33	26.5	+6V @ 350mA	LP4
	HMC943LP5E	24 - 31.5	Power Amplifier, 1.5 Watt	21	41	34	+5.5V @ 1200mA	LP5
NEW!	**HMC1040LP3CE**	24 - 43.5	Low Noise Amplifier	22	22	12	+2.5V @ 70mA	LP3C
	HMC906	27.3 - 33.5	Power Amplifier, 2 Watt	23	43	33	+6V @ 1200mA	Chip
NEW!	**HMC1024**	27.5 - 33.5	Power Amplifier, 1 Watt	24	40	29	+6V @ 600mA	Chip
NEW!	**HMC1029**	29 - 37	Power Amplifier, 2 Watt	22	42	32	+6V @ 1200mA	Chip
NEW!	**HMC1014**	33.5 - 46.5	Power Amplifier, 1/2 Watt	21	35	24.5	+6V @ 500mA	Chip
	HMC968	37 - 40	Power Amplifier, 1 Watt	21	38	30.5	+6V @ 900mA	Chip
	HMC969	40 - 43.5	Power Amplifier, 1 Watt	22	38	29	+6V @ 900mA	Chip
	HMC1022	DC - 48	Wideband Power Amplifier	12	32	22	+10V @ 150mA	Chip

Contact Us With Your Custom Power Amplifier Requirements!

Hittite
MICROWAVE CORPORATION

2 Elizabeth Drive • Chelmsford, MA 01824
978-250-3343 tel • 978-250-3373 fax • timing@hittite.com

Visit Us: www.hittite.com
Receive the latest product releases - click on "My Subscription"

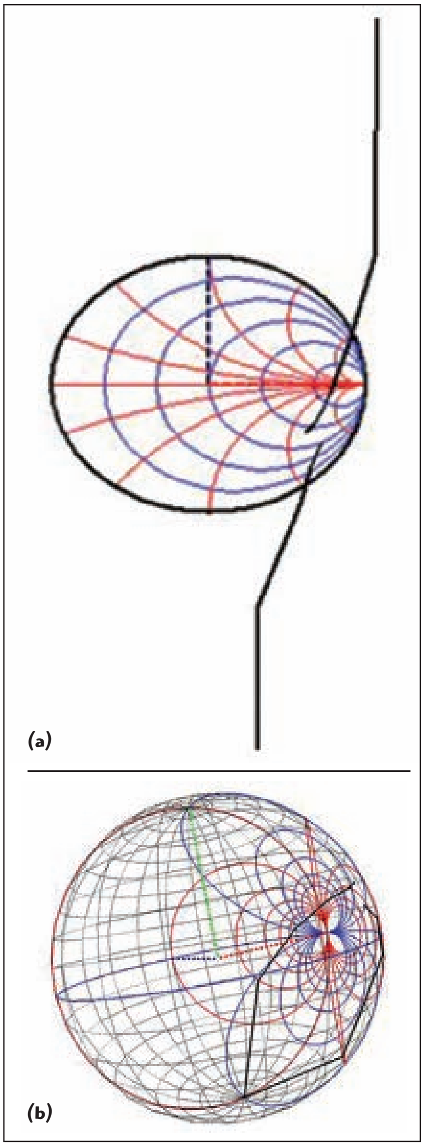

▲ *Fig. 3 Input impedance (in black) of a microwave oscillator at 1 GHz in both the 2D (a) and 3D (b) Smith charts.*

References

1. A.A. Müller, P. Soto, D. Dascalu, D. Neculoiu and V.E. Boria, "A 3D Smith Chart Based on the Riemann Sphere for Active and Passive Microwave Circuits," *IEEE Microwave and Wireless Components Letters*, Vol. 21, No. 6, June 2011, pp. 286-288.
2. P. H. Smith, "Transmission-line Calculator," Electronics, Vol. 12, No. 1, January 1939, pp. 29-31.
3. 3D Smith Chart Application available at www.3dsmithchart.com/, last accessed in November 2011.
4. Y. Wu, Y. Zhang, Y. Liu and H. Huang, "Theory of the Spherical Smith Chart," *Microwave and Optical Technology Letters*, Vol. 51, No. 1, January 2009, pp. 95-97.
5. H.F. Lenzing and C. D'Elio, "Transmission Line Parameters with Negative Conductance Loads and the "Negative" Smith Chart," *Proceedings of the IEEE*, Vol. 51, No. 3, March 1963, pp. 481-482.
6. W.F. Osgood, "Maxime Bocher- A Biographical Memoir," National Academy Press, *Biographical Memoirs*, Vol. 82, WA, 2002.
7. D.A. Brannan, M.F. Esplen and J.J. Gray, "Geometry," Cambridge University Press Cambridge, UK, 2007.
8. M. Bocher, "Infinite Regions of Various Geometries," *Bulletin of the American Mathematical Society*, Vol. 20, No. 4, 1913, pp. 185-200.
9. J.F. White, "High Frequency Techniques: An Introduction to RF and Microwave Engineering," John Wiley & Sons, Hoboken, NJ, 2004.
10. R. Gilmore and L. Besser, "Practical RF Circuit Design For Modern Wireless Systems, Vol. II: Active Circuits and Systems," Artech House, Norwood, MA, 2003.

Andrei Müller *obtained an MSC in Telecommunications Engineering in 2005, a second MSC in Microsystems in 2007 and a PhD degree in Telecom Engineering from UPB-Bucharest in 2011. He performed microwave related research stages at HFT-Munich-Germany (2007-2008) and at CEFIM-Pretoria-South Africa (2009). During his PHD, Andrei chose to use a fellowship in order to complete a seven month stage in pure mathematics at IUMPA, Valencia, Spain, 2010. His current interests are the extensions of the 3D Smith chart tool (www.3dsmithchart.com) and applications of projective, inversive and non-euclidian geometry in EM design.*

Dan C. Dascalu *is the founder and the first Director General of IMT (1993-2011), today the National Institute for R&D in Microtechnologies (IMT-Bucharest). He graduated from the Electronics Department of the University "Politechnica" of Bucharest, Romania (1965) and obtained his Ph.D. from the same university (1971). His particular interest was related to transit-time effects. He is a full Member of the Romanian Academy (of Sciences). Prof. Dascalu is now the Coordinator of Center for Nanotechnologies from IMT and President of the Coordinating board of IMT centre for Micro- and NANOFABrication (IMT-MINAFAB). IMT is a hub of micro- and nanotechnologies in Romania (scientific networking, innovation, education) and hosts a European Centre of excellence in RF MEMS and MOEMS.*

Pablo Soto *received his M.S. degree in Telecommunication Engineering from the Universidad Politécnica de Valencia in 1999, where he is currently working toward the Ph.D. degree. In 2000 he joined the Departamento de Comunicaciones, Universidad Politécnica de Valencia, where he has been a Lecturer since 2002. In 2000, he was a fellow with the European Space Research and Technology Centre (ESTEC-ESA), Noordwijk, the Netherlands. His research interests include numerical methods for the analysis, synthesis, and automated design of passive waveguide components.*

Vicente E. Boria *received his M.S degree (with first-class honors) and his Ph.D. degree in Telecommunications Engineering from the Universidad Politécnica de Valencia, Spain, in 1993 and 1997, respectively. In 1993, he joined the Departamento de Comunicaciones, Universidad Politécnica de Valencia, where he has been full Professor since 2003. In 1995-1996, he held a Spanish Trainee position with the European Space Research and Technology Centre (ESTEC-ESA), Noordwijk, The Netherlands, where he was involved in the area of EM analysis and design of passive waveguide devices. His current research interests include numerical methods for the analysis of waveguide and scattering structures, automated design of waveguide components, radiating systems, measurement techniques, and power effects (multipactor and corona) in waveguide systems.*

Comparing Microstrip and CPW Performance

By building a better electromagnetic (EM) simulation model, which includes the effects of a PCB's metal surface roughness, microstrip and coplanar waveguide, circuits can be closely compared to find the best fit for different applications.

Matching a microwave transmission-line technology to an application requires careful consideration of more than a few factors. Depending on the requirements of an application, high-frequency circuit designers may be concerned with loss budgets, propagation mode issues, radiation losses and electromagnetic interference (EMI), and even the printed-circuit-board (PCB) assembly logistics and the relative difficulty of adding components to a PCB. Microstrip has been one of the most popular microwave transmission-line formats for decades and is well characterized. Coplanar waveguide (CPW) transmission lines have also been used extensively in microwave PCB applications, although they are not as well understood as microstrip lines. Typically, conductor-backed coplanar waveguide (CBCPW) circuits are often used in conjunction with microstrip in microwave circuit designs. A common approach is the use of CBCPW in the circuit's signal launch area, transitioning to microstrip for the remainder of the circuit to enable simple component placement and PCB assembly.

To help designers understand differences between microstrip and CPW transmission-line approaches, measurement data from different test circuits fabricated with the same, well-known commercial substrate material will be compared. Further analysis will be performed with the aid of electromagnetic (EM) models and EM simulation software. The software modeling will help validate the measured results and also show how effective software modeling can alleviate concerns, when using new transmission-line approaches and/or circuit topologies.

Microstrip and CPW formats are often selected over other high-frequency transmission-line options, such as stripline, due to their simplicity. Stripline can deliver excellent high-frequency performance, with good noise immunity and isolation between adjacent circuit traces. But it is also more difficult and expensive to fabricate than microstrip or CPW. Stripline is essentially a flat metal transmission line between two ground planes, with the ground planes separated by a dielectric substrate material. The width of the transmission line, the thickness of the substrate, and the relative dielectric constant of the substrate material determine the characteristic impedance of the transmission line. Difficulties with stripline

John Coonrod
Rogers Corp., Chandler, AZ
Brian Rautio
Sonnet Software Inc., North Syracuse, NY

Efficient High Power Solid State Switches

- Amplifiers
- Attenuators - Variable
- DLVA & ERDLVA & SDLVA's
- DTO's
- Filters
- Form, Fit & Function Products
- Hybrids, Dividers & Couplers
- IFM's & Frequency Discriminators
- Integrated MIC/MMIC Modules
- I/Q Vector Modulators
- Limiters & Detectors
- Log Amplifiers
- Pulse & Bi-Phase Modulators
- Phase Shifters
- Rack & Chassis Mount Products
- Receiver Front Ends
- Single Sideband Modulators
- SMT & QFN Products
- Solid-State Switches
- Switch Matrices
- Switch Filter Banks
- Threshold Detectors
- USB Products

PIN Diode & FET High Efficiency Designs

- SPST thru SP16T
- Reflective and Absorptive
- Input Power up to 2kW Peak, 200W Average
- Custom Packages and Designs
- Form, Fit & Function Replacements

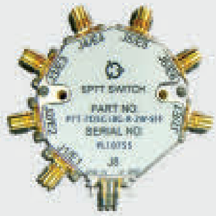

Model Number	Style	Frequency Range (GHz)	Insertion Loss (dB)	Isolation (dB)	Reflective / Absorptive	Switching Speed (nSec)	Operating Input Power	DC Voltage & Current
P1T-0R310R0G-60-R-SFF-20W	SPST	0.3 – 18.0	2.5	60	Reflective	250	20 Watt Peak 7 Watt Average	+5vdc@100mA -12vdc@50mA
P1T-1R0G18R0G-80-R-SFF-75W	SPST	1.0 – 18.0	2.5	80	Reflective	25	75 Watt Peak 2 Watt Average	+5vdc@65mA -12vdc@20mA
P1T-0R5G2R0G-80-R-SFF-LVT-10W	SPST	0.5 – 2.0	1.0	80	Reflective	25	10 Watt Peak 2 Watt CW	+5vdc@50mA -5vdc@5mA
P1T-0R6G1R3G-70-SFF-4W	SPST	0.6 – 1.3	1.5	70	Absorptive	30	4 Watts	+5vdc@100mA -5vdc@100mA
P2T-335M535M-30-R-SFF-20W	SPDT	0.335 – 0.535	0.9	45	Reflective	100	20 Watts	+5vdc@31mA
P2T-1G18G-10-R-528-SFF-HIP10W	SPDT	1.0 – 18.0	3.0	25	Reflective	40	10 Watts	+5vdc@5mA -28vdc@5mA
P2T-0R1G2R0G-40-SFF-100W	SPDT	1.0 – 2.0	1.5	40	Reflective	<1µSec	100 Watts CW	+5vdc@150mA -15vdc@70mA
PEC-9R510R7-100W-SFF-120W	SPDT	9.5 – 10.7	1.5	40	Reflective	400	120 Watts	+5vdc@160mA -28vdc@15mA
P2T-0R5G18G-60-SFF-10W	SPDT	0.5 – 18.0	1.5	60	Reflective	150	10 Watts	+5vdc@100mA -15vdc@75mA
P2T-14D415D4-15-SMT-20W Surface Mount, Driverless	SPDT	14.4 – 15.4	0.5	15	Reflective	50	20 Watts	Bias 50mA
P3T-0R1G2R0G-40-SFF-100W	SP3T	0.1 – 2.0	1.5	40	Reflective	<1µSec	100 Watts CW	+5vdc@150mA -15vdc@70mA
P3T-0R5G18G-70-SFF-200W	SP3T	0.5 – 18.0	3.75	70	Absorptive	100	200 Watts Peak 12 Watts CW	+5vdc@150mA -15vdc@100mA
P4T-2G18G-45-TFF-100W	SP4T	2.0 - 18.0	3.1	45	Reflective	200	100 Watts Peak 1 Watt CW	+5vdc@105mA -15vdc@70mA
P4T-0R1G2R0G-40-SFF-100W	SP4T	0.1 – 2.0	1.5	40	Reflective	<1µSec	100 Watts CW	+5vdc@150mA -15vdc@70mA
P4T-0R1G18G-65-SFF-75W	SP4T	0.1 – 18.0	2.6	65	Reflective	50	75 Watts Peak 1 Watt CW	+5vdc@150mA -15vdc@50mA
P4T-900M1300M-35-SFF-50W	SP4T	0.9 – 1.3	2.0	35	Absorptive	<5µSec	50 Watts	28vdc
P8T-2R37G2R39G-60-SFF-10W	SP8T	2.37 – 2.39	2.5	60	Reflective	<2µSec	10 Watts	+5vdc@500mA -27vdc@10mA
P8T-8G18G-50-SFF-10W	SP8T	8.0 – 18.0	4.0	50	Reflective	75	10 Watts Peak 4 Watts CW	+5vdc@450mA -15vdc@150mA

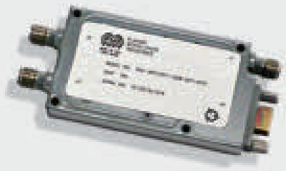

14.4 to 15.4 GHz
20 Watt, SPDT, SMT,
PIN DIODE SWITCH

PMI

PLANAR MONOLITHICS INDUSTRIES, INC.

7311-F Grove Road, Frederick, Maryland 21704 USA
Tel: 301-662-5019 | Fax: 301-662-1731
Email: sales@pmi-rf.com | www.pmi-rf.com

ISO9001:2008 Certified

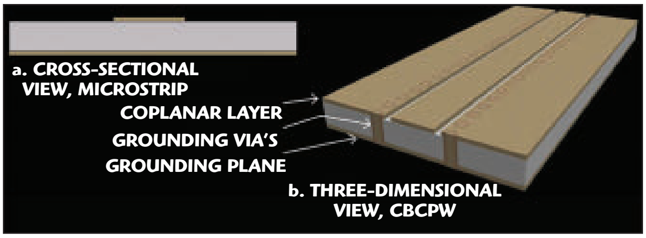

▲ *Fig. 1 Cross-sectional view of a microstrip line (a) and three-dimensional view of a CBCPW line (b).*

include ground planes that must be shorted together, requiring electrical via connections between the two metal ground planes and the lack of direct access to the signal layer for component mounting. Stripline's second ground plane also results in narrower transmission-line widths, for a given substrate thickness and characteristics impedance, than for microstrip.

In contrast, microstrip and CPW circuits feature an exposed signal layer, greatly simplifying component assembly on the PCB. ***Figure 1*** shows simple drawings of microstrip and CBCPW transmission lines. The microstrip circuit has a signal conductor on the top of the dielectric substrate and a ground plane on the bottom. In a CBCPW circuit, a coplanar layer with ground-signal-ground (GSG) configuration replaces the signal layer of microstrip. The CBCPW circuit's top ground planes are tied to the bottom ground plane by means of vias. CBCPW is sometimes known as grounded coplanar waveguide.

In terms of wave propagation, microstrip transmission-line circuits generally operate in a quasi transverse-electromagnetic (TEM) mode. Hybrid transverse-electric (TE) and hybrid transverse-magnetic modes are also possible with microstrip, but these modes are sometimes the result of undesired spurious wave propagation. In general, CBCPW circuits offer propagation behavior similar to that of microstrip circuits.

For both microstrip and CBCPW circuits, spurious parasitic wave propagation can be a problem. As a general rule, the circuit geometry (that is its cross-sectional features) for either transmission-line approach should be less than 45° long at the highest operating frequency of interest. For microstrip, the circuit parameters of concern include the thickness of the substrate (that is the distance between the signal and ground planes) and the width of the signal conductor (transmission line width). For CBCPW, attention must be paid to those two parameters, as well as to the distance between the GSG spacing on the coplanar layer.

For proper grounding, CBCPW circuits employ vias to connect the top-layer coplanar ground planes and the bottom-layer ground plane. The placement of these vias can be critical for achieving the desired impedance and loss characteristics, as well as for suppressing parasitic wave modes. When grounding vias are effectively positioned in a CBCPW circuit, a much thicker dielectric substrate can be used at higher frequencies than would be possible for a microstrip circuit at the same frequencies. A review of the practical tradeoffs of via placement for CBCPW circuits is available in the literature.[1] ***Figure 2*** offers an overview of signal loss (S_{21}) performance for microstrip, coplanar-launched microstrip, and CBCPW circuits fabricated on 30-mil-thick RO4350B™ circuit-board material from Rogers Corp.

GCPWG refers to a grounded coplanar waveguide and is actually the same configuration as CBCPW. The top ground microstrip configuration is essentially a coplanar-launched microstrip circuit – a microstrip circuit with a CBCPW configuration in the connector signal launch area. The curve-fit data for microstrip and coplanar-launched microstrip are taken from the literature.[1] The traces reveal some interesting traits to consider for the different transmission lines. For example, CBCPW typically suffers higher loss than microstrip or coplanar-launched microstrip. The GSG configuration of the CBCPW coplanar layer exhibits higher conductor loss than microstrip-based circuits. Still, the loss for CBCPW follows a constant slope, while the loss curves for microstrip and coplanar-launched microstrip undergo slope transitions at approximately 27 and 30 GHz, respectively. These loss transitions are associated with radiation losses. With proper spacing and via spacing, CBCPW can be fabricated with minimal radiation loss.

In wideband applications, dispersion can be important. Microstrip transmission lines are dispersive by nature: the phase velocity for EM waves is different in the air above the signal conductor than through the dielectric material of the substrate. CBCPW circuits can achieve much less dispersion when there is tight coupling at the GSG interfaces on the coplanar layer, since more of the E-field occurs in air to reduce the effective inhomogeneity of wave travel through different media.

Using proper design techniques, CBCPW circuits can achieve a much wider range of impedances than microstrip circuits. In addition, applications where crosstalk may be a concern, circuit performance can benefit from the coplanar ground plane separation of CBCPW's neighboring signal conductors. Due to their significantly

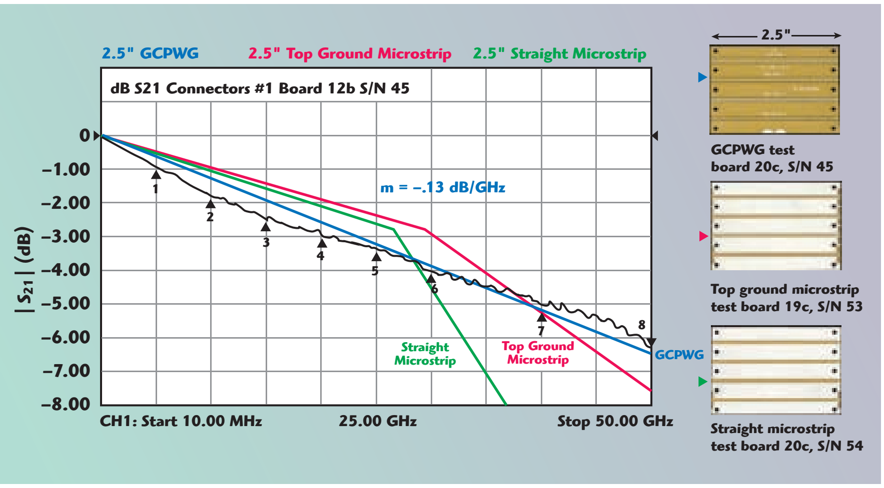

▲ *Fig. 2 Comparison of test data for 2½" GCPWG, 2½" top ground microstrip and 2½" straight microstrip test boards.*

TABLE I

DIFFERENT CIRCUITS DIMENSIONS AND MEASURED CHARACTERISTIC IMPEDANCES

	Measures Characteristic Impedance (Ohm)			Nominal Circuit Dimensions	
	RMS = 0.4 μm	RMS = 1.8 μm	RMS = 2.8 μm	Conductor Width (μm, mils)	Signal-Ground Space (μm, mils)
Microstrip	51.2	47.5	47.2	762 (30)	
CPW Launch Microstrip	50.2	47.8	47.7	762 (30)	
CBCPW Tightly Coupled	47.1	44.8	44.0	609.6 (24)	127 (5)
CBCPW Moderate Coupled	50.6	49.2	46.2	660.4 (26)	203.2 (8)
CBCPW Loosely Coupled	50.8	48.1	46.2	711.2 (28)	304.8 (12)

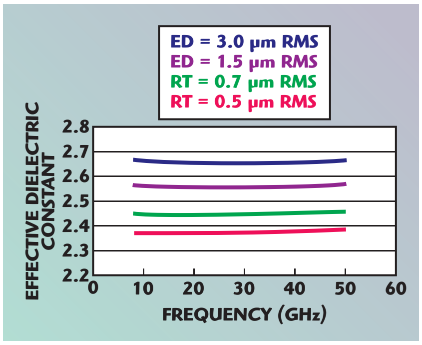

▲ *Fig. 3 Effective dielectric constant of a 4 mil LCP laminate with a 50 Ω microstrip line with different surface roughness.*

reduced radiation losses, dispersion and parasitic wave mode propagation, CBCPW circuits are often used at much higher frequencies than microstrip circuits. At millimeter-wave frequencies, for example, it is often that a simple wire-bonded air bridge will be used to connect the ground planes on both sides of the CBCPW signal conductor. The air bridge approach serves as a "trap" for specific frequencies of concern when spurious wave mode propagation is an issue.[2]

COPPER SURFACE ROUGHNESS

The copper surface roughness of PCB substrates has been known to affect conductor losses as well as the propagation constant of the transmission line.[3] The effect on a transmission-line's propagation constant causes a circuit to have a different "apparent dielectric constant" than expected. Of course, the material parameter is unchanged by the roughness of the material's metal layer. Rather, the amount of metal surface roughness causes the observed effects by influencing electric field and current flow. As ***Figure 3*** shows,[3] the effective dielectric constant can vary widely for the same dielectric substrate when the copper surface roughness is different. The effective dielectric constant increases as the surface roughness of the copper increases, as indicated by copper surfaces with higher root-mean-square (RMS) roughness values.

In addition to observed dielectric constant effects, the surface roughness of a microstrip is known to impact insertion loss performance.[3-7] The topology of the circuit may be more or less prone to such copper surface roughness effects, simply due to current and E-field distribution within the circuit. For example, the copper surface roughness has less effect on a tightly coupled CBCPW transmission line than on a microstrip. In a CBCPW circuit, the current and E-field are tightly maintained within the GSG on the coplanar layer. For a microstrip circuit, the field and current move more toward the bottom of the metal, where the roughness lies.

MEASURING DIFFERENCES

All of the circuits evaluated in this article were fabricated on a 254 μm (10-mil) thick RT/duroid® 5880 laminate from Rogers Corp. The same dielectric material was used in all cases, although with different copper types: rolled copper with surface roughness of 0.4 μm RMS, electrodeposited (ED) copper with surface roughness of 1.8 μm RMS, and high-profile ED copper with surface roughness of 2.8 μm RMS. ***Table 1*** provides details on the dimensions of the different circuits, along with their measured characteristic impedances. The nominal circuit dimensions noted in the table are per the circuit design; however, typical PCB fabrication tolerances apply. On the actual circuits, the signal-to-ground spacing for the coplanar layer of the CBCPW and the copper thickness had appreciable circuit-to-circuit variation.

There is also a real-life issue affecting most PCB circuits and especially CBCPW, which can cause more variation in circuit performance due to standard fabrication effects. This is the conductor trapezoidal effect, or "edge profile," where the PCB conductors are ideally rectangular in a cross-sectional view but the actual circuits are trapezoidal in shape. This can cause the current density in the coplanar GSG area to vary; an ideal rectangular conductor structure will have more current density up the sidewalls of the adjacent conductors in this region, whereas the trapezoidal structure will have more current density at the base (copper-substrate interface). When there is more current density at the base due to the trapezoidal effect, the copper surface roughness will have more influence on losses and the propagation constant. The trapezoidal concerns for CBCPW PCBs are shown in ***Figure 4***.

Figure 5 compares the effective dielectric constants for two different coplanar circuit types and how they are affected by two extreme cases of copper surface roughness. The phase response measurements that were made for one data set of circuits employed a differential phase length method.[8] Circuits were made in very close proximity on the same processing panel and the only difference for the two circuits being measured was the physical length of the transmission lines.

The figure shows that the difference at 10 GHz for the microstrip (cpw micro), for smooth vs. rough copper, RMS = 0.4 vs. RMS = 2.8, respectively, is approximately 0.09 in terms of the effective dielectric constant. The same consideration for the tightly coupled CBCPW is approximately 0.06. Even though trapezoidal

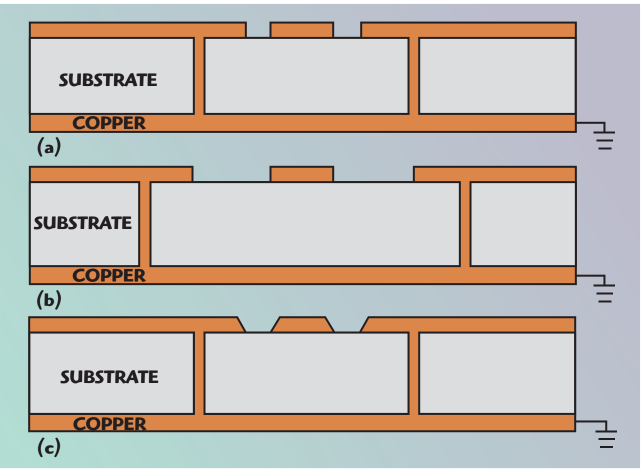

▲ *Fig. 4 Cross-sectional views of ideal tightly coupled CBCPW (a), ideal loosely coupled CBCPW (b) and tightly coupled CBCPW with trapezoidal effects (c).*

effects will cause more variation on the results of CBCPW than for microstrip, the plot shows that the effect of copper surface roughness on propagation constant is much less for CBCPW than for microstrip. The figure also shows a difference in dispersion, where the effective dielectric constant will vary more with frequency for microstrip than for CBCPW. Trapezoidal effects are not considered in the data shown; however, CBCPW circuits could have slightly more dispersion than normal if trapezoidal effects are greater.

Figure 6 shows the insertion loss associated with the two different circuit types and with different copper surface roughnesses. At 10 GHz, the difference in loss for microstrip on rough copper versus smooth copper is approximately 0.250 dB/in. to 0.121 dB/in. For CBCPW, the difference is about 0.280 dB/in. to 0.167 dB/in. The insertion loss performance of CBCPW is less affected by copper surface roughness than the insertion loss performance of microstrip. Trapezoidal effects will have more influence on insertion loss performance for CBCPW than for microstrip.

SIMULATIONS AND MEASUREMENTS

To better understand the performance of the circuits studied in this article, models were constructed and analyzed with the help of Sonnet Suite Professional V13.54, a three-dimensional (3D) planar EM simulation software from Sonnet Software. Based on microsectional data from the circuits tested, the simulation geometries, such as substrate thickness and metal surface profile, were entered into the software. An optical coordinate measuring machine (CMM) was used to determine the circuit length accurately. ***Figure 7*** shows an image of one of the CBCPW circuits as it appears in

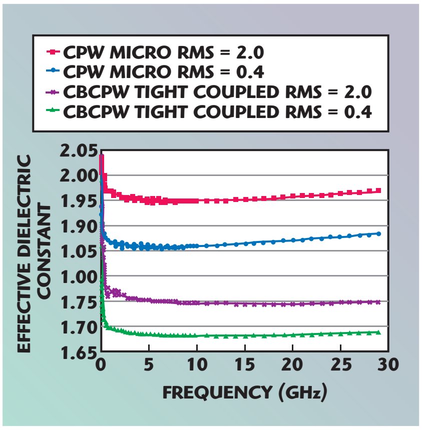

▲ *Fig. 5 Effective dielectric constant for two circuit types and two levels of copper surface roughness.*

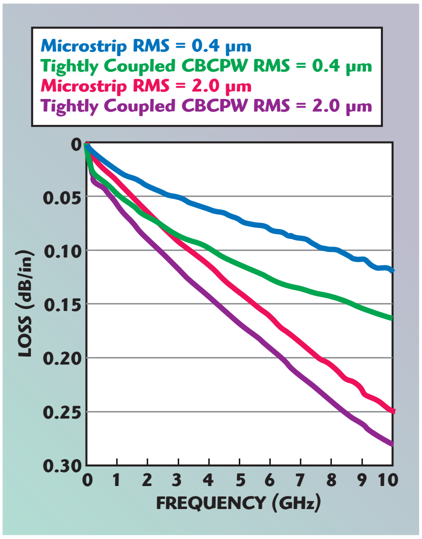

▲ *Fig. 6 Comparison of loss between microstrip and tightly coupled CBCPW circuits with different copper surface roughness.*

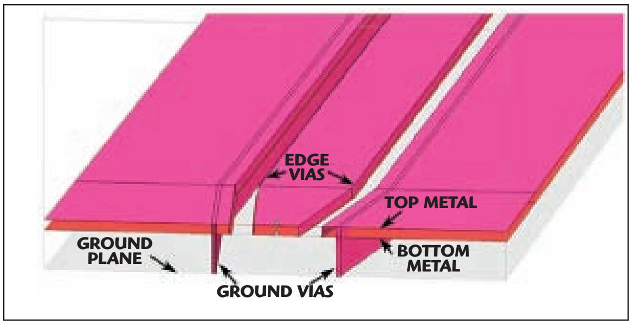

▲ *Fig. 7 Isometric view of a CBCPW cross-section in Sonnet.*

the Sonnet software, while ***Figure 8*** shows a microphotograph of the corresponding cross-section of the circuit.

While Sonnet contains a native support for modeling thick metal, Figure 7 shows a thick metal approximation drawn manually using the software. Two infinitely thin metals were used in this model, separated by the physical thickness of the metal. The top-layer metal has a width equivalent to the top of the physical metal, and the bottom-layer metal has a width equivalent to the bottom. The layers are then connected with edge vias. This serves to effectively model the thickness of the metal as well as the CBCPW trapezoidal effects — the bottom metal can be seen protruding slightly past the edge via, providing the "sharpness" of the physical profile.

A key to achieving success in the simulation of these types of microstrip and CBCPW circuits is a recently introduced surface-roughness model to V13 of the Sonnet software. The model, which was developed by Sonnet Software's software engineers in collaboration with Rogers' material developers, represents a significant advance in metal profile modeling, accounting for the effects on surface inductance of current following partial "loops" in a metal conductor's profile.[9] While it is possible to use the new surface roughness model on the top and bottom of a PCB, it is only applied to the bottom surface of the bottom metal. Roughness is intentionally added only to this physical surface, to aid adhesion to the PCB dielectric material.

Figure 9 offers a comparison between a simulated model and the measured data for microstrip transmission

▲ *Fig. 8 Microphotograph of a cross-section of a CBCPW circuit.*

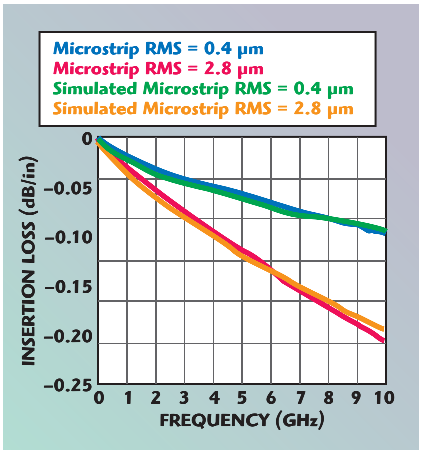

▲ *Fig. 9 Simulated and measured microstrip insertion loss.*

lines. The simulation shows insertion loss for 1". of microstrip transmission line without the connector launch, in order to be a valid comparison with a differential length measurement. Despite working in a scale of only hundredths of decibels, good agreement was achieved between the simulated and measured results for both smooth (0.4 µm RMS) and rough (2.8 µm RMS) metal surfaces. This close agreement provides reassurance of the test setup, the measurement procedure and the validity of the new Sonnet/Rogers surface roughness model.

Figure 10 shows similar agreement between simulations and measurements for CBCPW structures. While the agreement for the CBCPW circuits is not as close as that for the microstrip geometries, it is well within the limits of experimental error, confirming the accuracy of the model and the measurements made in this article.

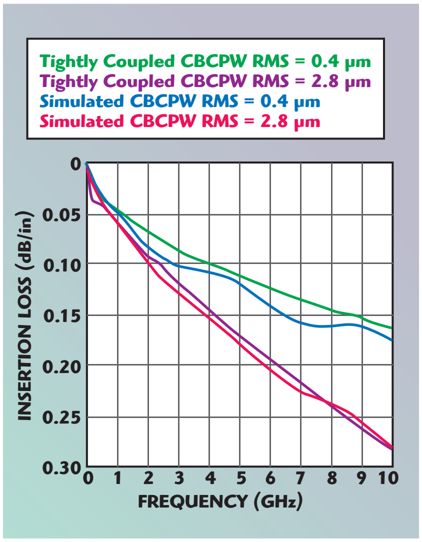

▲ *Fig. 10 Simulated and measured CBCPW insertion loss.*

Having established the validity of the surface roughness simulations, it might be beneficial to see how they can be further used in high-frequency circuit design. For example, a common issue with circuit topologies like CBCPW is finding the desired impedance. While many textbook formulas are available for this purpose for conventional microstrip circuits, it is less true for CBCPW circuits. Fortunately, EM simulators are suitable for finding CBCPW geometries for the desired impedance for nearly any reasonable circuit topology. The impedance of a CBCPW design for any PCB material can be broken down to three main parameters: conductor width, material thickness and ground plane separation. As ***Figure 11*** shows, the effects of each of these parameters on CBCPW transmission-line impedance can then be readily analyzed within the EM simulator environment.

Once parameterization is complete, a simulation can be run, which automatically "sweeps" all combinations of the three parameters within a desired range. It is then convenient to plot all impedances on the same graph, allowing a designer to choose the best geometry and impedance from the results. ***Figure 12*** shows an example of such an impedance plot.

CONCLUSION

The performance levels of microstrip, CBCPW launched microstrip and CBCPW transmission lines were evaluated under controlled conditions. Both measurements and

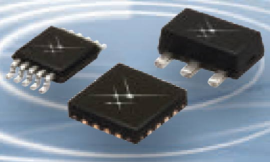

SKYWORKS®

High Performance RF Solutions

Handsets and Mobile Devices

Part Number	Description	Frequency (GHz)	Package (mm)
SKY65534	WLAN / Bluetooth® Front-End Module with Integrated PA, Filter, LNA, and T/R Switch	2.4	QFN 20L 2.5 x 2.5 x 0.45
SKY65535	WLAN Front-End Module with Integrated PA with Filter, LNA, and SPDT Switch	5.0	QFN 16L 2.5 x 2.5 x 0.45
SKY77701-16	High PAE Power Amplifier Module for CDMA / WCDMA / HSPA+ / LTE – Band I	1.92–1.98	10-pin MCM 3 x 3 x 0.9

WiFi Connectivity

SE5516A	802.11ac Dual-Band Front-End Module with PA, LNA, and SP2T Switch	2.4, 5.0	LGA 4 x 4 x 1
SE5003L1	802.11ac Matched Power Amplifier with Harmonic Filter	5.0	QFN 20L 4 x 4 x 0.9
SKY13317-373LF	pHEMT GaAs IC SP3T Switch	0.02–6.0	MLP 8L 1.5 x 1.5 x 0.45
SKY13351-375LF	GaAs SPDT Switch	0.2–6.0	QFN 6L 1 x 1 x 0.45
TT20P6-0709P0-1825E	High Power Infrastructure Filter can be Configured in a Pass Band Design	0.7–2.1	5" x 1.9" x 1"

Wireless Infrastructure

SKY12210-478LF	High Power (100 W) T/R SPDT Switch, 44 dB Isolation @ 2.6 GHz	0.9–4.0	QFN 16L 4 x 4 x 1.5
SKY13419-365LF	CMOS DBS Switch Matrix with Tone/Voltage Detector High Isolation 40 dB @ 900 MHz	0.25–2.15	QFN 20L 4 x 4 x 0.9
SKY65185	Dual-Channel Variable Gain Amplifier Front-End Module with 31.5 dB Control Range	1.7–2.7	32-pin MCM 7 x 7 x 1.35
SKY65373-11	Variable Gain Low Noise Amplifier with High Linearity @ 35 dB and Low NF @ 1 dB	1.7	16-pin MCM 8 x 8 x 1.3
SKY67001-396LF, SKY67002-396LF, SKY67003-396LF	High Linearity, Active Bias Low Noise Amplifiers	0.6–1.2 1.6–2.1 2.0–3.0	DFN 6L 1.5 x 1.5 x 0.45
SKY67130-396LF	High Linearity Amplifier Driver with +16 dBm $OP_{1\,dB}$ and 39.5 dBm OIP3 @ 22 mA	0.7–2.7	DFN 8L 2 x 2 x 0.75
SKY73208	Wideband Rx Mixer with Integrated Integer-N PLL and VCO	0.35–5.0	36-pin MCM 6 x 6 x 1.35
SKYFR-000782	Single Junction Circulator with Very Low Insertion Loss of 0.08 dB Typical	2.11–2.17	Drop-in 19 mm
SKYFR-000827	Single Junction Circulator with Very Low Insertion Loss of 0.10 dB Typical	2.3–2.4	SMT – Robust Lead, 23 mm

Smart Energy—Connected Home and Automation 802.15.4, ISM, and ZigBee®

SE2435L	High Power RF Front-End Module, 1 W High Efficiency with Integrated PA, LNA, and Diversity Switch	0.86–0.93	QFN 24L 4 x 4 x 0.9
SE2436L	High Power 0.5 W Front-End Module for ISM Band Applications, with PA, LNA, Bypass and Antenna Diversity	2.4	QFN 24L 4 x 4 x 0.9
SE2438T	Ultra Low Power ZigBee® Front-End IC with PA, LNA, Tx/Rx Bypass	2.4	QFN 20L 3 x 3 x 0.5
SKY13370-374LF	SPDT Switch, 50 Ohm Terminated	0.5–6.0	DFN 6L 1.5 x 1.5 x 0.45
SKY65367-11	High Power / High Efficiency Tx/Rx Front-End Module with Integrated PA and Bypass	0.17	16-pin MCM 4 x 4 x 0.9
SKY67012-396LF	Low Noise Amplifier with < 0.85 dB NF and < 5 mA Current @ 3.3 V	0.3–0.6	DFN 8L 2 x 2 x 0.75

Receive Skyworks Product News

New products (indicated in **blue, bold**). Join our customer email program today to start receiving information on new product releases, literature, upcoming tradeshow events, and more!

Skyworks Green™ products are compliant to all applicable materials legislation and are halogen-free. For additional information, refer to Skyworks Definition of Green™, document number SQ04-0074.

For more information, please visit our Web site at www.skyworksinc.com.

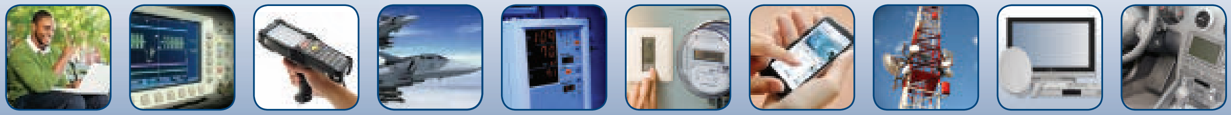

USA: 781-376-3000 • Asia: 886-2-2735 0399 • Europe: 33 (0)1 43548540 • Email: sales@skyworksinc.com
www.skyworksinc.com • NASDAQ: SWKS

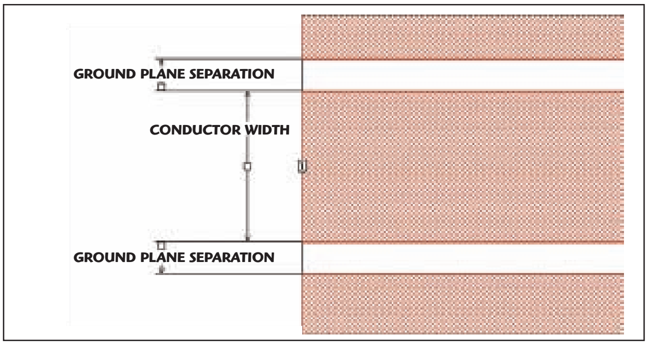

▲ *Fig. 11 CBCPW geometry can be broken into three key parameters.*

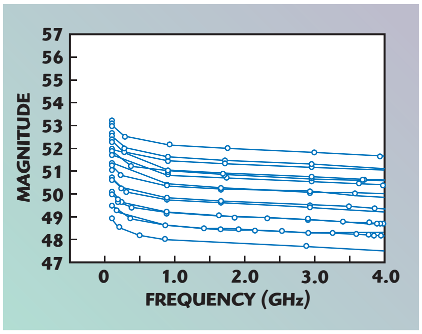

▲ *Fig. 12 Example of a "parameter sweep" simulation.*

computer simulations were performed using a commercial, low-loss microwave substrate material with different copper types, including different values of copper conductor surface roughness. The effects of copper surface roughness were evaluated and compared, showing that greater roughness typically means greater loss. Different circuit topologies were compared through both measurements and simulations and, by properly applying computer simulation software, it is possible to reduce the difficulties often encountered with lesser-known circuit topologies. ■

References

1. B.Rosas, "*Optimizing Test Boards for 50 GHz End Launch Connectors: Grounded Coplanar Launches and Through Lines on 30-mil Rogers RO4350B with Comparison to Microstrip*," Southwest Microwave Inc., Tempe, AZ, 2007, www.southwestmicrowave.com.
2. R.N. Simons, "*Coplanar Waveguide Circuits, Components and Systems*," John Wiley & Sons, New York, NY, 2001.
3. J.W. Reynolds, P.A. LaFrance, J.C. Rautio and A.F. Horn III, "*Effect of Conductor Profile on the Insertion loss, Propagation Constant and Dispersion in Thin High Frequency Transmission Lines*," DesignCon, 2010.
4. S.P. Morgan, "Effect of Surface Roughness on Eddy Current Losses at Microwave Frequencies," *Journal of Applied Physics*, Vol. 20, No. 4, 1949, pp. 352-362.
5. S. Groisse, I. Bardi, O. Biro, K. Preis and K.R. Richter, "Parameters of Lossy Cavity Resonators Calculated by Finite Element Method," *IEEE Transactions on Magnetics*, Vol. 32, Part 1, No. 3, May 1996, pp. 1509-1512.
6. G. Brist, S. Hall, S. Clouser and T. Liang, "Non-classical Conductor Losses Due to Copper Foil Roughness and Treatment," *2005 IPC Electronic Circuits World Convention Digest*, Vol. 2, S19, pp. 898-908.
7. T. Liang, S. Hall, H. Heck and G. Brist, "A Practical Method for Modeling PCB Transmission Lines with Conductor Roughness and Wideband Dielectric Properties," *2006 IEEE MTT-S International Microwave Symposium Digest*, pp. 1780-1783.
8. N.K. Das, S.M. Voda and D.M. Pozar, "Two Methods for the Measurement of Substrate Dielectric Constant," *IEEE Transactions on Microwave Theory and Techniques*, Vol. MTT-35, No. 7, July 1987, pp. 636-642.
9. A.F. Horn, J.W. Reynolds and J.C. Rautio, "Conductor Profile Effects on the Propagation Constant of Microstrip Transmission Lines," *2010 IEEE MTT-S International Microwave Symposium Digest*, pp. 868-871.

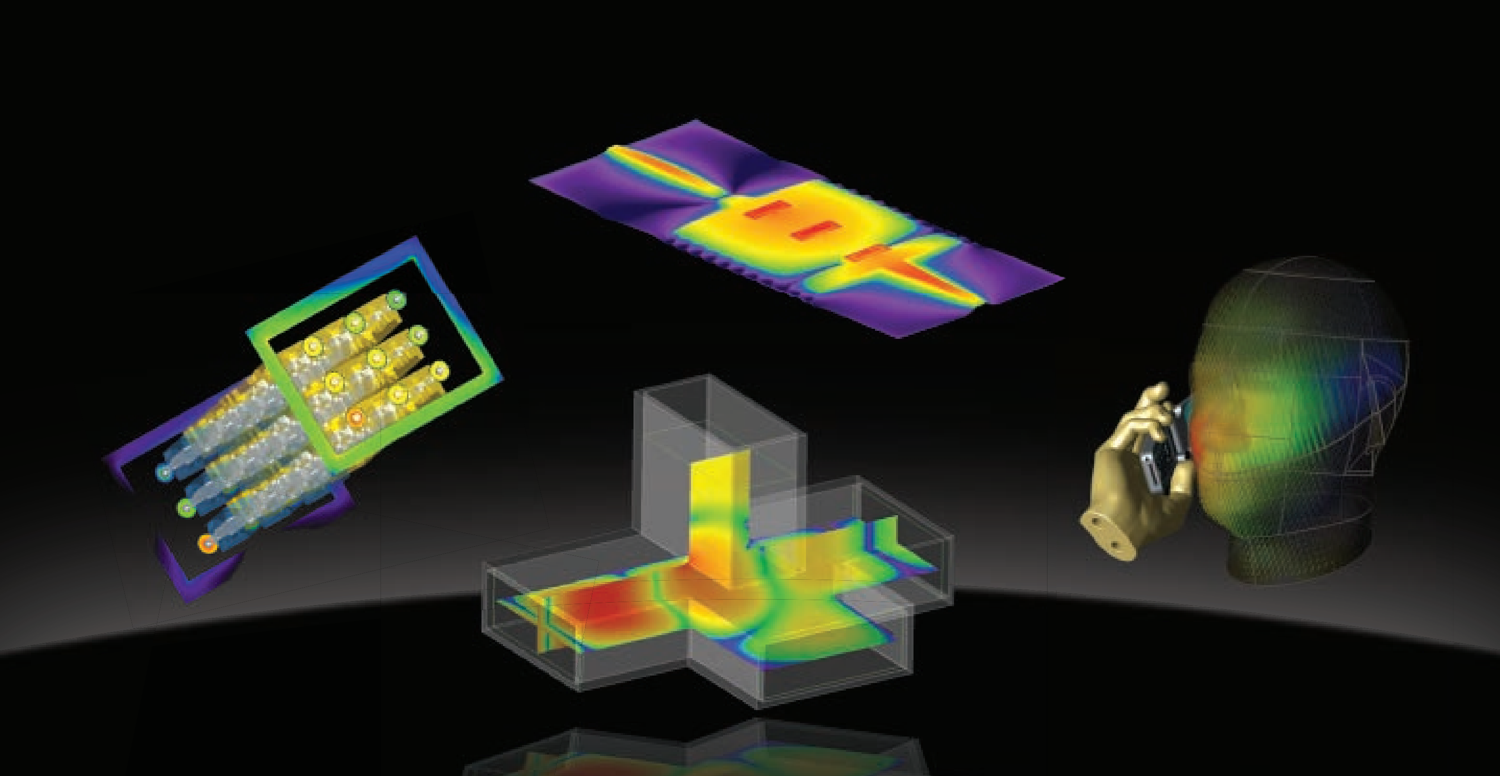

Experience EM Simulation That's Faster, Smarter, More Efficient.

Experience the Newly Enhanced XF7.

Remcom's XF7 is continually evolving to stay ahead of the curve. We push beyond standard updates, adding important functionality and streamlining usability in direct response to our customers' needs. Our goal is to exceed expectations and provide a truly unique experience with each new version.

Download the What's New in XF7 Flyer at: **www.remcom.com/new-xf7**.

REMCOM®
Electromagnetic Simulation Solutions

New features for 2012 include:

- Waveguide ports
- Stretch, twist, bend, and wrap geometry
- XStream® GPU Acceleration for Time-dependent Materials, Magnetized Ferrite, Debye/Drude Dispersive Materials, and more
- Materials database
- ODB++ PCB import within CAD Merge, allowing retention of previous modifications to the PCB
- Time Domain Reflectometry (TDR) and Time Domain Transmission (TDT) output types
- Ability to combine SAR from multiple sources

Visit **www.remcom.com/xf7** to learn more.

+1.888.7.REMCOM (US/CAN) | +1.814.861.1299 | **www.remcom.com**

PA Termination Impedance Selection Utilizing Temperature Contours

A successful power amplifier (PA) design requires an assortment of design tools. Small-signal S-parameters will provide a measure of small signal stability, power gain and the required input and output termination networks to provide a conjugate matched network. These techniques are well suited to device operation in the small signal regime. However, large output power requirements subject the device to operation over a greater range of voltage and current and thus additional measures are required. Further parameters entering the design space include power, efficiency, linearity, harmonic distortion and thermal considerations and their effect on device reliability. These added factors call upon the nonlinear aspects of active load pull[1] and polyharmonic distortion[2] for the measurement and modeling process and device modeling applied to harmonic balance[3] in simulation. However, in all cases, the resulting output of these collective efforts is a set of active device input and output terminations, Z_S and Z_L, provided by input and output matching networks (IMN, OMN). These matching sections satisfy performance criteria while permitting a large power device to conveniently operate in the system impedance. In addition, the networks provide for bias of the active device and collectively form a set of bias tees. The in-situ measurement process of active load pull places the device into large signal operation, stressing both the device thermal and electrical properties. An important first step in PA design is the characterization of a device performance as a function of termination impedance. Active load pull conducted first at small signal input levels provide device information analogous to S-parameter data collection.

THE LOAD PULL SYSTEM AND PROCEDURE

Small-signal S-parameter data collection should precede load pull operation. The device stability and regions of potentially unstable terminations need to be assessed. This cannot be over stressed as power devices, which are permitted to enter uncontrolled oscillation, can be destroyed, leading to erroneous data and damaged test sets. Adding either series or shunt resistive losses to the input or output of the test set will stabilize the active device. Finally, S-parameters will guide the selection of appropriate input and output load pull impedance regions for power gain.

Alan Victor and Walter Nagy
Nitronex Corp., Durham, NC

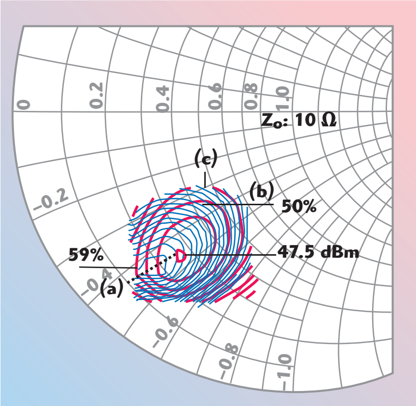

▲ *Fig. 1 Trade-off between power and efficiency for a given termination impedance at 2.2 GHz.*

In large power transistors, the goal is to find the appropriate real and imaginary terminating impedances at the device input and output, which maximize the device output power commensurate with minimum distortion and the deleterious effect of device heating. These terminating impedances are frequency dependent and must be obtained at multiple frequencies in order to map out an impedance trajectory vs. frequency.

The power gain, output power and drain efficiency are parameters provided by the load pull contours. Contours mapping of equal values are useful; however, their dependence and tradeoff is not clear. Instead, a combined relationship between the parameter sets that provides a single concise objective is sought. Such a relationship was outlined previously;[4] however, the approach to generate the contours was based on a simplified model of the intrinsic power device and did not target directly the approach taken in this work: temperature.

COMBINATION SEARCH PARAMETERS FACILITATE LOAD PULL TERMINATION SELECTION

Historically, the output power, drain efficiency and power gain are the three main device parameters provided by the load pull contours. The impedance contours provided by these parameters are useful in themselves; however, it is not necessarily a straightforward process to determine how to trade off these parameters to achieve maximum device performance. Typically a sector line (a) is drawn (see ***Figure 1***) to establish a tradeoff between the output power (b) and the efficiency (c). To address this challenge, the use of a combined relationship between these parameters that provide an additional concise design objective via the dissipated power contours is explored.

Increased operating voltage and the ability to dissipate tremendous amounts of DC power creates an increased concern for device reliability and robustness. A reliable power amplifier design is highly dependent on controlling the output power commensurate with the device junction temperature. For example, an Arrhenius plot for GaN-on-Silicon leads to a MTTF, which improves approximately ten-fold for each 20°C reduction in junction temperature.[5] Therefore any reduction in junction temperature can have a significant impact upon device reliability.

▲ *Fig. 2 Infrared camera used to characterize the temperature rise of a package device.*

The junction temperature, T_J, is dependent on the thermal resistance, device drain efficiency, power output and power gain. In addition, the materials and methods of attaching the transistor to the package affect T_J as well as these items being accounted for in the device thermal impedance, R_{th}. Tying these four parameters together leads to a temperature contour, which reveals the termination minimizing T_J for a specific power output. Determination of the device thermal impedance is the initial key to creating temperature contours. These contours are subsequently mapped against the device termination impedance. The thermal characterization is provided by an infrared (IR) camera, shown in ***Figure 2***. Cooling the camera system is required for its operation and maintaining high optical sensitivity. The clear difference in device temperature profile and thermal impedance influenced by the packaging are shown in the IR camera image of ***Figure 3***. The larger difference in device temperature rise between the two packages is noted in the white spot nearest to the drain terminal of the device b.

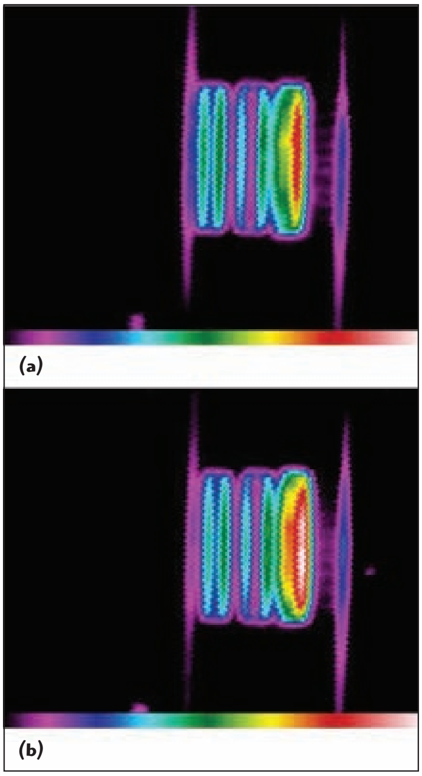

▲ *Fig. 3 Temperature rise for a copper-moly-copper (a) and copper-tungsten (b) package.*

Conservation of energy dictates that the total power into the active device, the RF and the DC input power sum to the total power output, the RF

Technical Feature

power and the power lost as heat or the dissipative power. Therefore,

$$P_{in}^{RF} + P_{in}^{DC} = P_{out}^{RF} + P_{diss} \quad (1)$$

Equation 1 can be rewritten, recognizing that the power gain G_p and the DC-to-RF drain efficiency η are implicit. The power dissipation of the transistor is given by

$$P_{diss} = P_{out}^{RF}\left(\frac{1}{\eta} + \frac{1}{G_p} - 1\right) \quad (2)$$

The junction temperature is related to the product of the dissipated power and the device thermal resistance,

$$T_J = R_{th}P_{diss} + T_0 \quad (3)$$

The parameter T_0 is the base plate temperature. Facilitating these calculations is accomplished if Equation 3 is recast in terms of the power added efficiency (PAE). Using Equation 2 and consolidating the power gain and drain efficiency gives

$$P_{diss} = P_{in}^{DC}(1 - PAE) \quad (4)$$

The load pull data collection provides contours of drain efficiency, output power and power gain vs. impedance. Once the thermal resistance is determined, typically with an IR thermal camera, the temperature rise of the device junction can be calculated.

Using Equations 2 and 3, the junction temperature rise and the resulting thermal contours are calculated, resulting in a fourth parameter being available to select optimum device impedances. The objective in using the thermal contours is to select impedance regions where the desired power, gain and drain efficiency coexist and then focus on the region that provides minimum rise in junction temperature. This methodology will provide the designer with an impedance set that not only optimizes device RF performance, but also maximizes the device reliability. In some cases, the impact can be an order of magnitude increase in device lifetime.

In this work, the definition of optimum load impedance refers to the impedance that minimizes the rise in junction temperature while meeting the targeted output power. In Figure 1, a typical power output and drain efficiency were shown at 2.2 GHz for a 24 mm GaN-on-Si HFET[6] with 40 µm gate pitch, while the profile of T_j for the same frequency is shown in ***Figure 4***. In all cases, the base plate temperature, T_0, is held constant at 25°C and the measured R_{th} is 1.8°C/W.

The efficiency steps are 1 percent, while the temperature steps are 2°C. The range in drain efficiency spans 9 percentage points while the temperature spans a range of 30°C. The power contours consist of the peak power at 47.5 dBm and

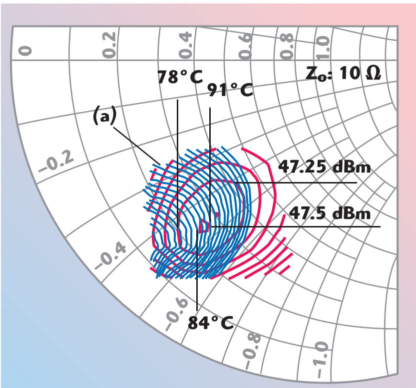

▲ *Fig. 4 Temperature open-contours (a) in 2°C increments and power output closed contours in 0.25 dB steps.*

successive power steps, which are 0.25 dB below the peak. The ability to assess the appropriate load termination impedance, Z_L, and its impact on junction temperature are shown in Figures 4 and 5. A lower T_J of 84°C occurs near the maximum drain efficiency Z_L and has a real termination that is lower in value than for the peak power Z_L. For example, the 47.25 dBm contour in Figure 4 shows a 30°C difference in T_J for the same output power.

APPLICATION TO BROADBAND DESIGN

A temperature gradient vector points in the direction of increasing temperature and in effect consolidates drain efficiency, output power and power gain contours. At different frequencies, the angle of the vector will vary. This is illustrated in ***Figure 5***, where the temperature gradients are shown to rotate in a counter-clockwise direction as the frequency changes from 1 to 2.2 GHz. The temperature

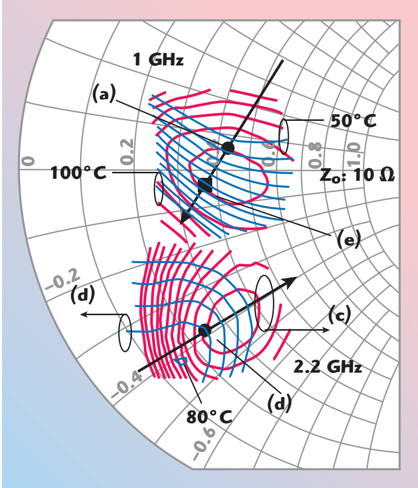

▲ *Fig. 5 Contours of constant temperature (open loci) and output power (closed contours) at 1 GHz (a) and 2.2 GHz (b).*

and power steps are 5°C and 0.5 dB, respectively.

At 1 GHz, a decrease in the real impedance of the termination increases the temperature, while at 2.2 GHz the opposite occurs. For the same output power, there exists multiple impedance points, which provide differing temperature rise. For example, at 1 GHz, Figure 5 (a) is 25° cooler than Figure 5 (e). Broadband application of the amplifier and ease to impedance match requires thermal impedance points vs. frequency not too far apart and closest to the chart center. At 1 GHz, while higher output power is possible, it will be at the risk of higher T_J. In essence, the increase in power output is not complemented by a larger increase in drain efficiency. Furthermore, if the impedance points are constrained by the matching network, an increase in T_J at lower frequency occurs, since these impedance points are not satisfied, see Figure 5 (e) vs. 5 (a). Clustering the impedance values to facilitate broadband matching requires the target impedance set to meet as (b) and (e) of Figure 5 and not (a). The resulting increase in temperature, T_J, at 1 GHz is evident. The optimal thermal drain impedances loci migrate in opposite directions; the lower frequency favoring higher real impedance, the higher frequency favoring lower.

The impact on the selection of terminations is particularly acute when investigating amplifier efficiency alone. It is instructive to look at a device at constant output power as seen

UP TO **100 Watt**

AMPLIFIERS

NOW! **100 kHz to 18 GHz**

from **$945** ea. qty. (1-9)

It's Watts you want? From 3 up to 100 Watts, Mini-Circuits has high-power amplifiers built for rugged, reliable performance in heavy-duty, 100 kHz-18 GHz applications. Each model is available with or without a heat sink/fan, operating on a single integrated DC supply, with surprisingly efficient current consumption. Extensive safety features prevent amplifier damage from over-temperature, over-voltage, or open or short loads. And internal power regulation delivers high performance even when your DC power supply is fluctuating. Our manufacturing controls ensure that quality and reliability are built into every unit, to provide the **truly *robust* amplifiers that our customers demand.**

IN STOCK! FAST DELIVERY!

Mini-Circuits…we're redefining what VALUE is all about!

Model ***With Heat Sink/Fan***	Freq. (MHz) f_L-f_U	Gain (dB) Typ.	P_{out} (dBm) @Comp 1dB Typ.	P_{out} (dBm) @Comp 3dB Typ.	Dynamic Range NF (dB) Typ.	Dynamic Range IP3 (dBm) Typ.	DC Pwr. Volt (V) Nom.	DC Pwr. Current (A) Max	Price $ ea. Qty. 1-9	Price *X suffix*
NEW LZY-22+	0.1-200	43	+42.0	+45.0	8.9	+52	24	6.0	1495	1470
LZY-1+	20-512	43	+45.7	+47.0	8.6	+54	26	7.3	1995	1895
LZY-2+	500-1000	46	+45.0	+45.8	8.0	+54	28	8.0	1995	1895
ZHL-5W-1	5-500	44	+39.5	+40.5	4.0	+49	25	3.3	995	970
ZHL-5W-2G+	800-2000	45	+37.0	+38.0	8.0	+44	24	2.0	995	945
ZHL-10W-2G	800-2000	43	+40.0	+41.0	7.0	+50	24	5.0	1295	1220
ZHL-16W-43+	1800-4000	45	+41.0	+42.0	6.0	+47	28	4.3	1595	1545
• ZHL-20W-13+	20-1000	50	+41.0	+43.0	3.5	+50	24	2.8	1395	1320
ZHL-30W-252+	700-2500	50	+44.0	+46.0	5.5	+52	28	6.3	2995	2920
ZHL-30W-262+	2300-2550	50	+43.0	+45.0	7.0	+50	28	4.3	1995	1920
• ZHL-50W-52	50-500	50	+46.0	+48.0	6.0	+55	24	9.3	1395	1320
• ZHL-100W-52	50-500	50	+47.0	+48.5	6.5	+57	24	10.5	1995	1920
• ZHL-100W-GAN+	20-500	42	+49.0	+50.0	7.0	+60	30	9.5	2395	2320
ZVE-3W-183+	5900-18000	35	+34.0	+35.0	5.5	+44	15	2.2	1295	1220
ZVE-3W-83+	2000-8000	36	+33.0	+35.0	5.8	+42	15	1.5	1295	1220

• ***Protected under U.S. Patent 7,348,854***

*For models without heat sink, add **X suffix** to model No. (Example: LZY-1+, LZY-1X+)*

Mini-Circuits®

ISO 9001 ISO 14001 AS 9100

P.O. Box 350166, Brooklyn, New York 11235-0003 (718) 934-4500 Fax (718) 332-4661

IF/RF MICROWAVE COMPONENTS

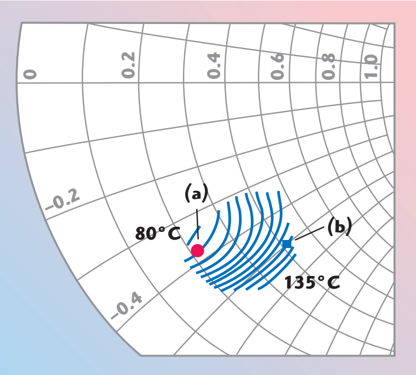

▲ *Fig. 6 Constant output power region at 2.2 GHz display multiple temperature contours ranging from 80° to 135°C.*

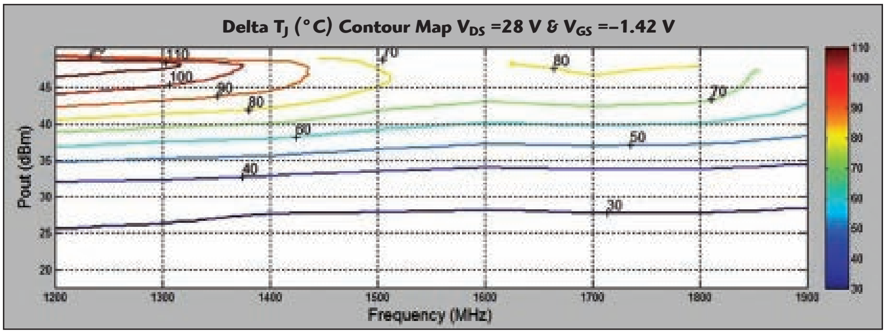

▲ *Fig. 8 Junction temperature rise assembled from measured drive up characteristics of the power amplifier.*

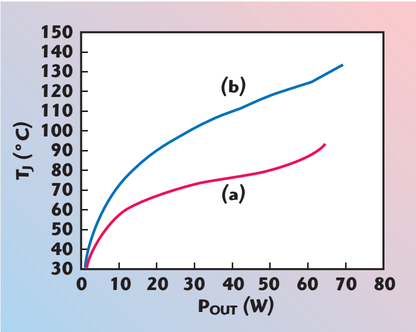

▲ *Fig. 7 Junction temperature rise as a function of output power for two selected drain impedances of 2.2 GHz.*

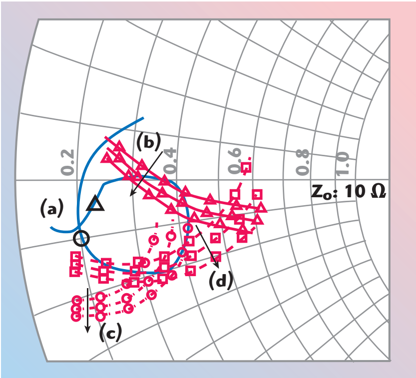

▲ *Fig. 9 Simulated drain port reflection coefficient obtained from measurements vs. frequency, 0.8 to 2.2 GHz (a), triangle point at 1.1 GHz, square at 1.7 GHz and circle at 1.9 GHz.*

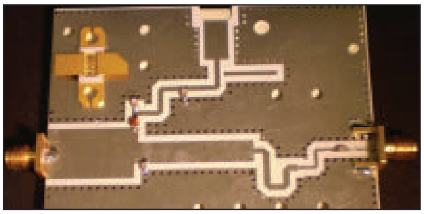

▲ *Fig. 10 Drain side bias line and termination or output matching network with SMA measurement launch on the left.*

in ***Figure 6*** at 2.2 GHz and 47.5 dBm. At constant output power, the power gain is nearly constant and maximum drain efficiency correlates well with the minimum T_J. The value of T_J varies by over 55°C over this power output region. Therefore, the selection of Z_L has a significant impact upon the T_J and hence device reliability. Unlike conventional load pull contours displaying a range of output power, when the output power is held constant, the contours of temperature align well with the contours of drain efficiency. Evidence of the junction temperature difference due to the selection of drain termination (see Figure 6a and b) is apparent in the drive up the curve at a single frequency of 2.2 GHz. Two selected termination impedances are chosen, one at low T_J (a) and one at high T_J (b). The resulting temperature rise vs. power output is shown in ***Figure 7***. At (a) the termination at the device lead is 2.51-j3.72 Ω, while at (b) is 3.68-j5.05 Ω. The T_J difference is at least 30°C at moderate power output.

This work is applicable to power amplifiers operating in the pulse mode. The temperature contours are simply linear scaled from parameters of efficiency, output power and thermal resistance. Although these elements will shift slightly in value from CW operation to pulse operation, the shift will be properly captured during active load pull. However, the value of thermal resistance from IR scans should be captured while the device is operating in the pulse mode and should be no different than the CW mode.

CIRCUIT IMPLEMENTATION AND RESULTS

Application of the design method over a broadband begins with a collection of load pull data spanning 1.2 to 1.9 GHz. During load pull, the maximum power output is limited to 47.5 dBm, nearly 60 W. Measured and calculated load pull parameters and a measured R_{th} are subsequently used to generate optimal impedances at each frequency for a target T_J of 70°C. This constitutes a load impedance table. A source table is found by searching first for maximum G_p at each frequency and moving along the associated constant reactance contour, while aiming to increase the real part of the source. The effect of this approach improves linearity and furthers the ability to broadband the design of the input matching network.

The impedance tables were used in the construction of a broadband amplifier circuit spanning a frequency range of 1.2 to 1.9 GHz. Measured results of P_{out} and T_J vs. frequency of the broadband board are shown in ***Figure 8***. Measurement and co-simulation of the power amplifier drain port impedance via its reflection coefficient, ***Figure 9*** (a), with the overlay of the temperature contours show good agreement with measurements of the completed amplifier, Figure 8. The amplifier reflection coefficient misses the targeted thermal contour at 900 MHz, is properly centered for 1.2 to 1.9 GHz operation and is off target beyond 1.9 GHz.

The measured amplifier OMN, shown in ***Figure 10*** and the drain reflection coefficient require modeling and co-simulation with an electromagnetic simulation (EM) tool. The drain reflection coefficient measurement is facilitated by an SMA connector launch. However, there exists a substantial electrical difference, a 35.2 ps delay, between the connector launch and the power amplifier package lead. Validating card measurements requires VNA calibration. Then, the port extension is enabled in

the VNA and used to account for the SMA delay during measurement. The measured card is modeled completely with both the discrete elements and EM simulation of the transmission lines. This EM simulation is completed using AXIEM.[7] The edge port for launch for this initial simulation of the transmission lines on the card is the width of the SMA pin. Subsequently, after the model and the simulation of the card agree with measurement data, another EM simulation is required where the edge port launch is now the width of the package lead. The resulting final simulation is shown in Figure 9 (a).

CONCLUSION

A PA design technique was presented, which focuses on control of device temperature rise by careful selection of the termination impedance. Thermal contours are assembled from conventional load pull data which is post processed. A measured 1.2 to 1.9 GHz, 60 W amplifier design demonstrates correlation with the method. Circuit measurement and simulation with validation requires co-simulation with EM and modeling of all discrete elements. The technique outlined in this work leads to a favorable selection of terminations which is less prone to error as the objective is concise. ■

ACKNOWLEDGMENT

The authors thank Michael Kendall for his extensive data collection and the post process measurements.

References

1. I. Angelov, H. Zirath and N. Rorman, "A New Empirical Nonlinear Model for HEMT and MESFET Devices," *IEEE Transactions on Microwave Theory and Techniques*, Vol. 40, No. 12, December 1992, pp. 2258-2266.
2. J. Verspecht and D.E. Root, "Polyharmonic Distortion Modeling," *IEEE Microwave Magazine*, Vol. 7, No. 3, June 2006, pp. 44-57.
3. D.E. Root, J. Xu, J. Horn, M. Iwanto and G. Simpson, "Device Modeling with NVNAs and X-Parameters," *2010 IEEE Workshop on Integrated Nonlinear Microwave and Millimeter-wave Circuits (INMMIC)*, pp. 12-15.
4. B.W. Leake, "The Analytical Construction of Power-dissipation and Efficiency-contours from Load Pull Data," *1983 IEEE ARFTG Conference Digest*, Vol. 3, pp. 31-38.
5. S. Singhal, T. Li, A. Chaudhari, A.W. Hanson, R. Therrien, J.W. Johnson, W. Nagy, J. Marquart, P. Rajagopal, J.C. Roberts, E.L. Piner, I.C. Kizilyalli and K.J. Linthicum, "Reliability of Large Periphery GaN-on-Si HFETs," *Microelectronics Reliability*, Vol. 46, No. 8, August 2006, pp. 1247-1253.
6. Nitronex Corp., NPT1014 Data sheet, www.nittronex.com
7. Applied Wave Research, AXIEM, www.awrcorp.com

Alan Victor *received his doctorate from North Carolina State University. He is a principal engineer with the Nitronex Corp., where his current interests are in the development of microwave power amplifiers and MMIC designs utilizing GaN-on-Silicon. Prior to joining Nitronex, Dr. Victor was with the IBM Microelectronics Group, Harris Microwave and the Motorola Communications Sector. He co-founded a wireless data communications company and has 10 issued patents and over 100 publications.*

Walter Nagy *has more than 25 years of microwave experience and is a principal engineer at Nitronex Corp. where he has worked since 2001. In his current role, Nagy is the RF technical lead on Nitronex's 48 V GaN product line and supports advance technology development. He has experience with high power load pull measurements, nonlinear device modeling, device thermal simulations and device level robustness and reliability testing. Nagy's prior role at Nitronex was in applications engineering where he developed evaluation boards and supported customers for wireless infrastructure and broadband military applications.*

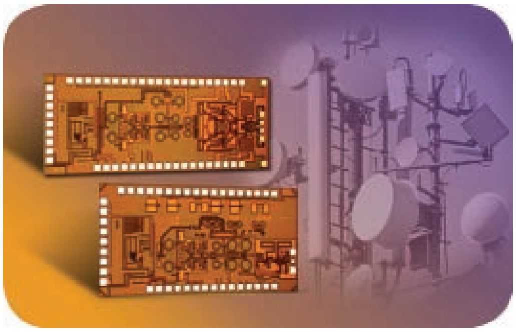

Highly Integrated 60 GHz Radio Transceiver Chipset

The demand for high capacity data continues to increase year over year at significant rates. In an ongoing race, technology and application developers have pushed into higher and higher bandwidths, first with voice, then data and now video is driving the demand. This demand is evident in cellular technology with the migration from AMPS to 3G, and now the rollout of 4G capabilities aimed at the millions of application-rich smartphone and tablet devices. It is also evident in the home, where WiFi has moved from 1 to 54 Mbps and now is pushing into hundreds of Mbps with IEEE 802.11n and 802.11ac. Spectrum availability has been a prime consideration in the development of technologies to meet the data capacity demand. Techniques such as Orthogonal Frequency Division Multiplexing (OFDM), Multiple In Multiple Out (MIMO), higher order modulations and the use of smaller cells have all been effective approaches to increasing data rates and data capacity within a given amount of spectrum.

Recognizing many of the important developments taking place in the 57 to 64 GHz band, Hittite Microwave is now offering a highly integrated silicon chipset solution. Hittite's HMC6000/6001 chipset not only solves many of the key technical challenges encountered at millimeter-wave frequencies, but also enables turn-key multi-Gbps communication links at 60 GHz.

60 GHz APPLICATIONS

The wide bandwidth and high EIRP available in this band, combined with the attenuation properties over long distances, make 60 GHz an attractive solution for short range applications requiring multi-Gbps data capacity. These include outdoor point-to-point radio solutions for metrocell/picocell backhaul, and indoor datalink applications such as wireless Gbps cable replacement (HDMI, USB 3.0, Thunderbolt, etc.), wireless docking stations, and video/magazine kiosks. The wide bandwidth available is also applicable to wireless sensor applications for robotics requiring short range with high precision.

Hittite Microwave Corp.
Chelmsford, MA

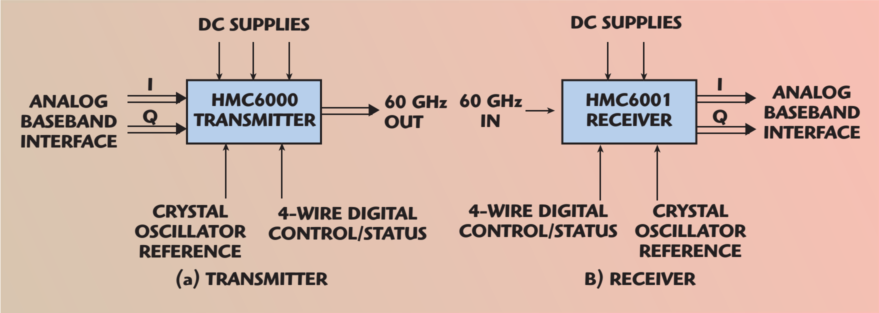

▲ *Fig. 1 Hittite's 60 GHz transceiver chip set.*

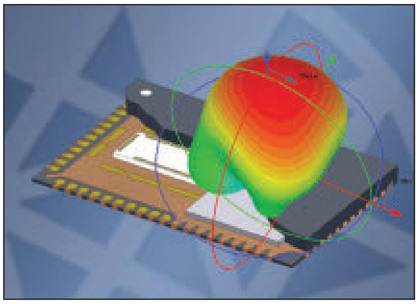

▲ *Fig. 2 Hittite's 60 GHz antenna-in-package (AiP) solution.*

TABLE I

TYPICAL PERFORMANCE CHARACTERISTICS OF HITTITE'S 60 GHz TRANSCEIVER CHIPSET

Key Feature	HMC6000 mmW Transmitter IC	HMC6001 mmW Receiver IC
Operating Frequency Range	57 to 64 GHz (supports IEEE channel plan)	
Linear Output Power (dBm)	+12	—
Noise Figure (dB)	—	6
Maximum Gain (dB)	38	67
Gain Control Range (dB)	17	65 / 1 dB steps
Phase Noise @ 1 MHz Offset (dBc/Hz)	– 86	– 86

the millimeter-wave interconnects are incorporated into the chips and/or packaged parts. Hittite Microwave, a contributing member of WiGig, solves this challenge with an integrated silicon chipset that translates standard baseband signals directly to and from 60 GHz, minimizing the need for high frequency component interconnects on the PCB.

Several standards and industry groups have emerged to address the use of 60 GHz including the IEEE 802.11ad and 802.15.3c standards, and the WirelessHD and Wireless Gigabit Alliance (WiGig) consortiums. The many benefits of 60 GHz come with significant challenges. Interconnecting components on a printed circuit board at these frequencies is quite difficult and requires expensive board materials. Low-cost solutions can only exist if

Hittite's HMC6000 transmitter (***Figure 1a***) includes all the functionality required to translate a baseband analog I and Q signal up to a selected channel in the 60 GHz band, requiring only a low frequency external reference clock. Constructed in SiGe BiCMOS, it has analog I and Q (differential) inputs with DC coupling to enable cancellation of DC offsets and carrier feedthrough. It includes a low phase-noise frequency synthesizer

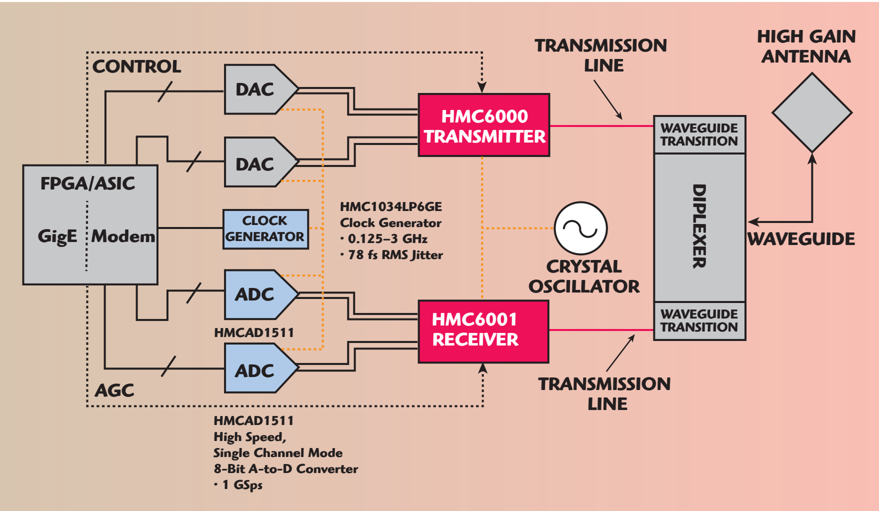

▲ *Fig. 3 60 GHz Gigabit Ethernet point-to-point microwave backhaul solution.*

which allows tuning across the 57 to 64 GHz ISM band with a step-size of 500 or 540 MHz (one quarter of the IEEE channel spacing) depending on the reference input frequency. The HMC6000 also provides up to 38 dB of variable gain to achieve a saturated output power of 17 dBm and a linear power of up to 12 dBm, which is significantly higher than what is currently achievable in CMOS. The differential RF output provides a low-loss RF transition with high output efficiency.

The HMC6001 receiver chip (***Figure 1b***) accepts the millimeter-wave signal at a selected channel in the 60 GHz band and translates this down to differential analog baseband I and Q. All the necessary frequency generation, filtering and gain control is on-chip, including a programmable high-pass filter corner to help remove residual DC offset and LO feedthrough. The HMC6001 receiver achieves a 6 dB noise figure at maximum gain. See ***Table 1*** for a performance summary of the transceiver chipset. A simple 4-wire digital serial interface provides all control and status of the chips including frequency channel selection, gain control, circuit biases and filter bandwidths.

Phase noise can be a significant challenge at 60 GHz since the reference and VCO phase noise is multiplied up to this high frequency. To avoid degrading the receiver noise figure, the integrated phase noise is typically 10 dB below the required SNR of the modulation. Fortunately, with the faster symbol rates used at 60 GHz, the integrated phase noise of concern is much further away from the carrier. For example, with the 1.76 GHz symbol rates of WiGig, phase noise below 1 MHz offset has insignificant impact. For the WiGig symbol rates, the HMC6000 and HMC6001 have an integrated phase noise of roughly

Fairview Microwave Inc.
ADAPTERS
SM5250 $58.16
SMA SWEPT 27 GHZ
SM4979 $38.77
SMA 27 GHZ
SM4923 $97.25
SMA FLANGE 27 GHZ
SM3224 $226.17
2.92 BULKHEAD 40 GHZ
SM3221 $148.48
3.5-3.5 34 GHZ
SM3935 $440.50
1.85-1.85 65 GHZ
SM8867 $195.00
SMP-2.4 40 GHZ
SM2927 $138.94
GMS-SMA 23 GHZ
SM3358 $226.17
7mm-3.5 18 GHZ
SM3397 $51.76
7/16 90° 6 GHZ
SM4531 $172.00
N 90° 18 GHZ
SM3547 $38.77
TNC-BNC 8 GHZ
SM5514 $145.40
ZMA-SMA 18 GHZ
SMW75ACN $297.95
WR75-N 10-15 GHZ
28AC206 $363.60
WR28-2.92 26-40 GHZ
SM4835 $172.53
SSMA-2.92 40 GHZ
ATTENUATORS
SA18N5WA $60.17
N 5W 18 GHZ
SA18N25WA $232.24
N 25 W 18 GHZ
SA18N507 $343.09
N 50 W 18 GHZ
SA3015 $13.55
SMA 2 W 3 GHZ
SA18S50W $337.81
SMA 50 W 18 GHZ
SA3N511 $162.41
N 50 W 3 GHZ
SA4020 $738.96
2.92 10 W 40 GHZ
SA5074 $274.47
2.4 1 W 50 GHZ
COUPLERS, POWER DIVIDERS
MC0626 $1,045.15
2.92 COUPLER 6-26 GHZ
MC0618 $341.38
SMA COUPLER 6-18 GHZ
MC4061 $757.50
N-SMA COUPLER 1-12 GHZ
SMC4037 $52.52
N COUPLER 700-2700 MHZ
MP0218-4 $600.95
SMA 4-WAY 2-18 GHZ
MP1540-2 $1,045.15
2.92 2-WAY 15-40 GHZ
MP8769 $472.68
N 2-WAY 2-8 GHZ
MP8758-4 $82.98
N 4-WAY 800-2500 MHZ
TERMINATIONS
ST27N301 $434.98
N 700-700 MHZ LOW PIM
ST3N501 $129.56
N 50 W 3 GHZ
ST3D-50 $206.96
7/16 50 W 3 GHZ
ST1831 $19.57
SMA PUSH ON 1 W 18 GHZ
ST2671 $51.11
SMA 2 W 27 GHZ
ST6T-5W $53.29
TNC 5 W 6 GHZ
ST4021 $521.98
2.92 5 W 40 GHZ
ST5038 $299.05
2.4 1 W 50 GHZ
INTRODUCING NEW PRODUCTS: GAIN HORNS AND LOW PIM SERIES
MasterCard
VISA
FAST DELIVERY!
CHECK OUT OUR INVENTORY LEVELS, PRICING, DATA SHEETS, & PLACE ORDERS ONLINE AT
WWW.FAIRVIEWMICROWAVE.COM 1-800-715-4396
1130 JUNCTION DR. STE 100 ALLEN, TX 75013 1-800-715-4396 FAX: 972-649-6689 EMAIL:SALES@FAIRVIEWMICROWAVE.COM

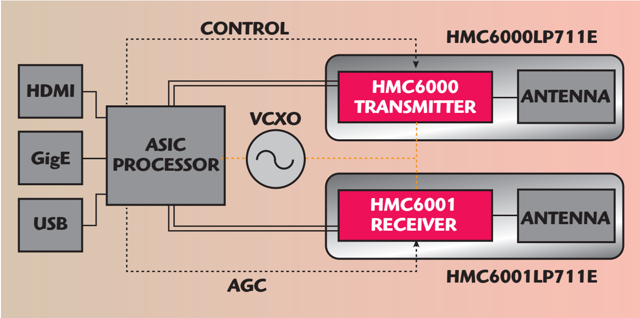

▲ *Fig. 4 Consumer-oriented multi-gbps solution adhering to the WiGig standard.*

-25 dBc enabling up to 16 QAM modulation.

Hittite offers both connectorized and antenna-in-package (AiP) solutions using these chips to facilitate customer integration of 60 GHz into their product. For example, Hittite's HMC6000LP711E solution (shown in ***Figure 2***) combines a 60 GHz antenna with the millimeter-wave transmitter chip in a low cost 7 × 11 mm QFN plastic package. This enables a surface-mount compatible solution using standard low cost PCB assembly techniques and requires no millimeter-wave experience. The HMC60001LP711E solution combines the millimeter-wave receiver chip with an antenna in an identical package.

SOLUTION SETS

The Hittite HMC6000/6001 chipset and packaged parts are ideal for emerging 60 GHz applications, including outdoor point-to-point links and indoor consumer devices. ***Figure 3*** is a block diagram of a typical point-to-point microwave radio transporting one or more Gigabit Ethernet data streams over a 60 GHz link. These are full-duplex connections so a diplexer is commonly used to provide the necessary isolation between the transmit and receive channels while sharing a common, high gain antenna. Earlier 60 GHz point-to-point systems required numerous discrete components to build the radio which was expensive, large and power hungry. Hittite's integrated chipset solution reduces the radio portion of the design to two chips and a crystal oscillator, and the interconnect challenge is reduced to two short transmission lines to the diplexer.

Figure 4 is a block diagram of a consumer-oriented multi-Gbps device adhering to the WiGig standard. A variety of high speed digital interfaces can be used including GigE, USB, HDMI or even PCIe. In order to meet the price point of the consumer market, all of the network processing, Media Access Control and Physical Layer functionality would be integrated into a single ASIC. The ADCs and DACs will typically operate at multi-Gbps sampling rates, of at least twice the symbol rate of the modulation used. To minimize power and cost, these data converters would also likely be integrated as part of the baseband ASIC. A diplexer is not required for this application since WiGig uses Time-Division Duplex (TDD) multiplexing. The high gain antenna needed for point-to-point links can

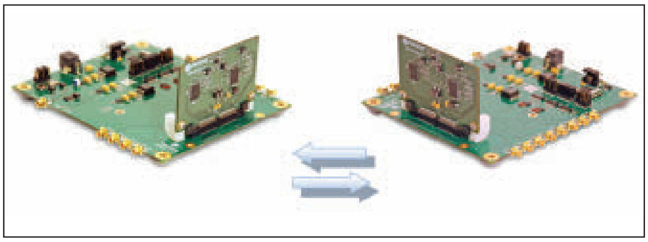

Fig. 5 *HMC6450 antenna-in-package transceiver evaluation kit.*

be replaced by a much smaller, lower gain antenna since the path distance is limited to the size of a room.

To minimize the loss due to the 60 GHz transmission lines to the antenna, the ideal location for the radio is next to, or integrated with the antenna, and not necessarily co-located with the desired location for the baseband processing. The differential baseband interface provided with Hittite's integrated chipset is desirable to allow for possible separation between the ASIC and the optimal antenna location.

TRANSCEIVER EVALUATION KITS

To facilitate rapid evaluation of Hittite's 60 GHz chipsets and customer prototyping for system development, Hittite is offering evaluation kits for both connectorized and AiP configurations. The HMC6450 is a 60 GHz AiP Transceiver Evaluation Kit and is shown in ***Figure 5***. The HMC6450 includes two boards each with the HMC6000LP711E transmitter and HMC6001LP711E receiver. Together with configuration software, this provides everything needed to quickly set up a bi-directional link at 60 GHz with a universal analog baseband I and Q interface. The HMC6451 is a 60 GHz MMPX Transceiver Evaluation Kit and provides the same functionality with snap-on MMPX connectorized 60 GHz interfaces.

The unlicensed 60 GHz spectrum provides an excellent opportunity to meet today's ever-growing demand for data capacity. Hittite Microwave now offers a highly integrated HMC6000/6001 silicon transceiver chipset targeting 60 GHz applications such as picocell backhaul and short-range multi-Gbps data rate indoor communication links. The 60 GHz chipset provides all the necessary functionality to translate I and Q baseband analog signals to a selected channel in the 60 GHz ISM band, using only an external low-frequency reference clock oscillator. For ease of use, the chips are also offered in connectorized packages and antenna-in-package solutions. The HMC6000/6001LP711E antenna-in-package solution combines a 60 GHz antenna with 60 GHz transmitter/receiver chips in a low-cost, plastic QFN package.

VENDORVIEW

Hittite Microwave Corp.,
Chelmsford, MA,
sales@hittite.com,
www.hittite.com.

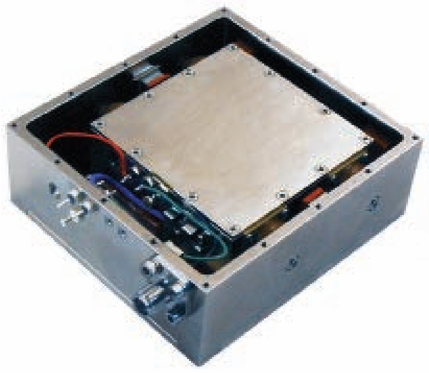

1 to 650 MHz Ultra Low Noise OCXOs

Liz Ronchetti,
Owner of Wenzel Associates
Visit mwjournal.com to read this in-depth interview.

Executive Interview

Precision crystal oscillators, which are at the heart of many high level electronic systems, are often the most susceptible component in the system to acceleration, vibration, shock and acoustic environments. These dynamic conditions are common in airborne, ground and shipboard applications and significant degradation of the entire system can occur as a result. For these systems, it is imperative for designers to select a crystal oscillator that has been designed to minimize the effects of the crystal's acceleration sensitivity.

REDUCING ACCELERATION SENSITIVITY

Three approaches are used to improve the crystal oscillator's performance when exposed to dynamic conditions: minimize the crystal's intrinsic acceleration sensitivity, vibration isolate the crystal and apply active compensation (as in Wenzel's Bootstrap Series). These techniques have been successfully implemented in many cases. The most common approaches using inherent low-g sensitivity crystals and vibration isolation is available in Wenzel's Citrine Series.

Vibration mounts must be chosen carefully since many materials exhibit substantial stiffness changes over temperature and have direction-dependent isolation. When size is critical, small, omni-directional shock mounts are contained within the oscillator package. For lower resonant frequencies, larger mounts supporting heavier isolated masses are used, increasing the size of the outer chassis.

CITRINE SERIES CRYSTAL OSCILLATORS

The new Citrine Series crystal oscillators were developed specifically to provide a broad product offering for the most demanding applications requiring low phase noise performance in both static and dynamic conditions. The Citrine oscillators can be configured at any fixed frequency between 1 and 650 MHz.

The Citrine Series is available in eight configurations. Both low frequency HF oscillators and VHF oscillators are available with and without

Wenzel Associates Inc.
Austin, TX

Phase Adjusters

Part Number	Con-nectors	Frequency Range (GHz)	VSWR max.	Insertion Loss max. (dB)	Phase Shift min. (°)	No. of Turns	Phase Shift Deg/GHz/Turn	Time Delay min. (psec.)	Time Delay max. (psec.)	Temperature (°C)	Weight max. (g)
LS-0002-YYYY[1]	div.	DC - 2	1.2:1	0.3	85	37		393	516		98-220[2]
LS-0103-6161	Nf	DC - 3	1.15	0.4	540	cont.	1.15	1826	2328	-65 to +125	700
LS-0203-6161				0.8	1080			3693	4694		1200
LS-0012-YYYY[1]	div.	DC - 12	1.3:1	0.8	520	37		406	530		114-234[2]
LS-0112-XXXX[3]	SMA	DC-12.0	1.25:1	0.4	230	16.5	1.2	238	293	-65 to +125	70
LS-A112-XXXX[3]											47
LS-0212-1121											70
LS-A212-1121											47
LS-0118-XXXX[3]		DC-18.0		0.6	350						70
LS-A118-XXXX[3]											47
LS-0218-1121											70
LS-A218-1121											47
LS-0118-5161	N							300	355	-65/+70	105
LS-U118-5161										-65/+165	
LS-0018-YYYY[1]	div.	DC - 18	1.5:1	1.0	770	37	1.15	406	530		114
LS-0121-XXXX[3]	SMA	DC-26.0	1.30:1	0.8	500	16.5	1.2	238	293	-65 to +125	70
LS-A121-XXXX[3]											47
LS-0221-1121											70
LS-A221-1121											47
LS-0321-1121			1.31:1		500	35	0.6	236.7	290.5		30
LS-0170-1121			1.26:1	0.26	127	13.5	0.36	109.2	122.8		9
LS-S008-1121			1.50:1	0.4	155	10	0.6	118.6	135.1		20
LS-P140-KFKM	2.92 mm	DC-40.0	1.2:1	0.6	590	12	1.2	168	208	-65 to +65	51
LS-0140-KFKM			1.4:1								49
LS-P150-HFHM	2.40 mm	DC-50.0	1.3	0.8	400	7		172	195		55
LS-0150-HFHM			1.5								53
LS-P165-VFVM	1.85 mm	DC-63.0	1.4	0.8	600	8		167	195		55
LS-0165-VFVM			1.5								53

[1]div.: Connector Configuration available: SMA, male and female; N, male and female; TNC male and female
[2]Weight depends on connector configuration
[3]SMA Connector Configuration available: male/female; male/male; female/female; female/male

Spectrum Elektrotechnik GmbH **when Quality is needed**

80905 Munich, Germany **P.O. Box 450533**
Telephone: +49-89-3548-040 **Facsimile: +49-89-3548-0490**
www.spectrum-et.com * **Email: sales@spectrum-et.com**

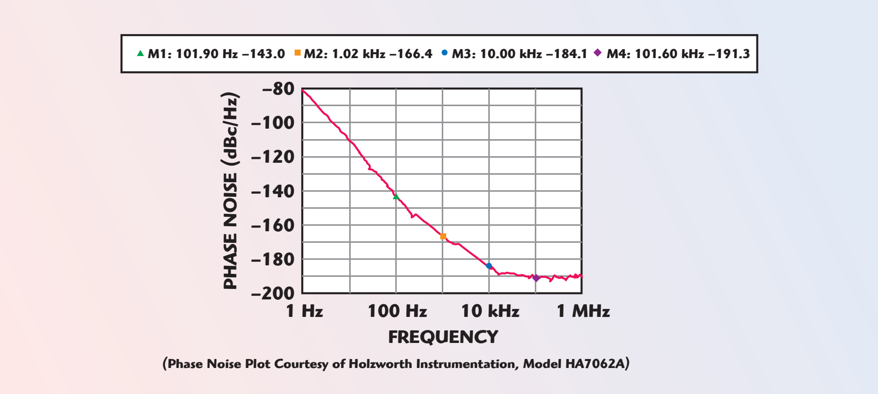

▲ *Fig. 1 Static phase noise for the 100 MHz Golden Citrine Oscillator P/N: 501-25900.*

a vibration isolation system. And, both the HF and VHF Citrines are available in the "PLUS" series, which adds multipliers, dividers, amplifiers, filters and dual outputs, when the application demands something extra.

The Citrine Series comes in a variety of package configurations that are selected depending on the frequency, options desired, performance specifications and other application considerations. See ***Table 1*** for standard Citrine configurations and performance options.

CITRINE STATIC PHASE NOISE PERFORMANCE

Phase noise floor performance for both HF and VHF frequency ranges can be specified for the oscillator as Standard at -165 dBc/Hz or Premium at -176 dBc/Hz at a fixed frequency within the range. The close-to-the-carrier phase noise performance below 100 Hz is primarily a function of the quartz crystal used in the oscillator, and can be selected based on the system's requirement.

The Golden Citrine option is now available within the VHF frequency range, which offers typical phase noise performance to -183 dBc/Hz at 10 kHz offset and -190 dBc/Hz at and beyond the 100 kHz offset. See ***Figure 1*** for a static phase noise plot of the 100 MHz Golden Citrine crystal oscillator.

CITRINE DYNAMIC PHASE NOISE PERFORMANCE

Dynamic phase noise performance of an oscillator can be improved with careful selection of a low-g crystal depending on the application specifi-

TABLE I

CITRINE CONFIGURATION, PERFORMANCE AND PLUS OPTIONS

Frequency	*Citrine Model*	*Case Size*	*Phase Noise Floor, Static*	*Temperature Stability Ref: +25°C*	*Aging*
HARD MOUNTED - TYPICAL					
5 to 25 MHz	HF Citrine	2.25" × 2.25" × 0.8"	Standard <-165 dBc/Hz at 100 kHz Premium <-176 dBc/Hz at 100 kHz	±5e-8,0t o+ 50°C ±1e-7,-20°t o+ 70°C ±2e-7, -40° to +85°C	2e-8/year
1 to 125 MHz	HF Citrine Plus*	2.25" × 2.25" × 1.3"	20log(N) of Base HF Citrine		
25 to 130 MHz	VHF Citrine	2.0" × 2.0" × 0.7"	Standard <-165d Bc/Hz at100k Hz Premium <-176d Bc/Hza t 100 kHz Golden < -190 dBc/Hz at 100 kHz	±5e-7, 0 to +50°C ±8e-7,-20° to+ 70°C ±1.5e-6, -40° to +85°C	5e-7/year
25 to 650 MHz	VHF Citrine Plus*	2.0" × 2.0" × 1.3"	20log(N) of Base VHF Citrine		
VIBRATION ISOLATED - TYPICAL					
5 to 25 MHz	HF Citrine	3.25" × 3.05" × 1.25"	Standard <-165d Bc/Hz at100k Hz Premium <-176 dBc/Hz at 100 kHz	±5e-8,0t o+ 50°C ±1e-7,-20°t o+ 70°C ±2e-7, -40° to +85°C	2e-8/year
1 to 125 MHz	HF Citrine Plus*	3.25" × 3.05" × 1.75"	20log(N) of Base HF Citrine		
25 to 130 MHz	VHF Citrine	3.0" × 2.0"× 1.3"	Standard <-165d Bc/Hz at100k Hz Premium <-176d Bc/Hza t 100 kHz Golden < -190 dBc/Hz at 100 kHz	±5e-7,0t o +50°C ±8e-7,-20° to+ 70°C ±1.5e-6, -40° to +85°C	5e-7/year
25 to 650 MHz	HF Citrine Plus*	3.0" × 2.8" × 1.75"	20log(N) of Base VHF Citrine		

** Citrine Plus Options*	*Acceleration Sensitivity*
• Amplifier (to +21 dBm) • Divider (Divide by 2 to 256, -168 dBc/Hz floor) • Regen Divider (Divide by 2, -172 dBc/Hz floor) • Multiplier (×2, ×3, ×4, ×5) • RF Filter (Harmonics to -60 dBc) • Phase Lock Loop (PLL)	• ≤ 5E-10/g, typical • ≤ 2E-10/g at select frequencies • Natural mount resonant frequency between 30 to 70 Hz depending on vibration levels and isolated configuration. • Compensated g-sensitivity of a 100 MHz Citrine when isolated with vibration levels at 0.01 g²/Hz from 10 Hz to 2 kHz: 100 Hz 5e-11/g 1 kHz 4e-12/g 2 kHz 2e-12/g

PERFECTION

When you need perfection in satellite high frequency communication.

Family of Broadband High Frequency Coaxial Rotary Joints

Single Channel & Dual Channel Rotary Joints — Frequency DC to 40.0 GHZ
MDL's short low torque, high performance coaxial rotary joints as well as our extensive line of waveguide rotary joints have set the standards of the industry .

You've never been in better hands.
Quality from CAD to crate, quick turnaround, and tight economy is what we're all about.
Call an MDL specialist today at 800-383-8057 or visit us at mdllab.com.
You'll find that we specialize in perfection.

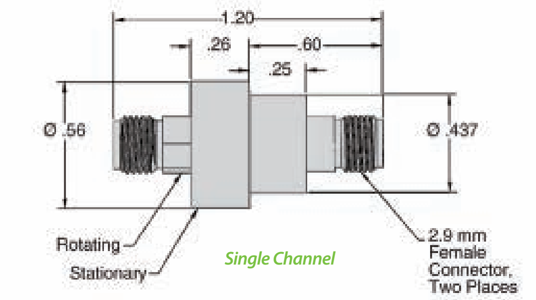

Single Channel

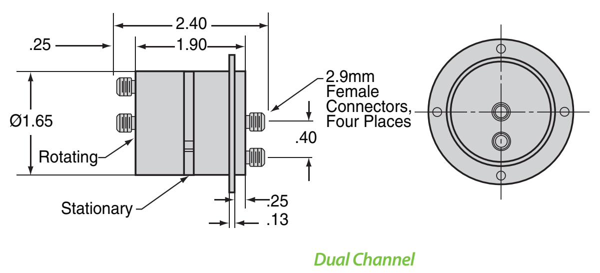

Dual Channel

SINGLE CHANNEL SPECIFICATIONS:

ELECTRICAL

FREQUENCY	DC - 18 GHz	
VSWR	DC - 10 GHz	1.20 : 1 MAX.
	10 - 26 GHz	1.35 : 1 MAX.
	26 - 40 GHz	1.75 : 1 MAX.
WOW	1.05 MAX.	
INSERTION LOSS	DC - 10 GHz	0.2 dB MAX.
	10 - 26 GHz	0.4 dB MAX.
	26 - 40 GHz	0.6 dB MAX.
PEAK POWER	Equal to connector rating	

DUAL CHANNEL SPECIFICATIONS:

ELECTRICAL	Channel 1	Channel 2
FREQUENCY	7.0 - 22.0 GHz	29.0 - 31.0 GHz
VSWR	1.50:1 MAX.	1.70:1 MAX.
WOW	0.15	0.25
INSERTION LOSS	0.5 dB MAX.	1.0 dB MAX.
ISOLATION	Channel to Channel	50.0 dB MIN.

Scan here to visit our website

Microwave Development Laboratories, 135 Crescent Road, Needham Heights, MA 02494
V: 781-292-6680/6684 • F: 781-453-8629 • E-mail: mdlsales@mdllab.com • www.mdllab.com

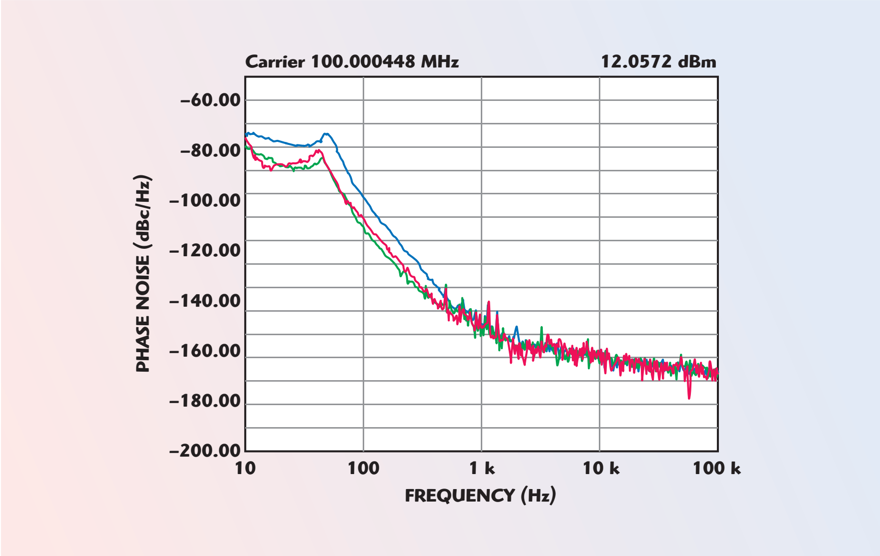

▲ *Fig. 2 Phase noise performance under vibration for a 100 MHz vibration isolated Citrine P/N: 501-24942 Rev. B. (Vibration Profile: 10 Hz to 2 kHz, 0.01 g^2/Hz, natural resonance is ~50 Hz).*

cations. Although typical low-g crystals have acceleration sensitivity at 5E-10/g per axis, they can be specified at 3E-10/g per axis and as low as 2E-10/g per axis at some frequencies. Specifying the right crystal for each requirement can be a difficult task considering some are better for static performance and others are best for dynamic conditions.

Dynamic phase noise performance can be improved further by using shock mounts. Although vibration isolation may not be a viable solution for applications where vibration is significant below 100 Hz offsets and performance is critical in this region, it works well for minimizing vibration beyond the natural resonant frequency of the isolated unit. In the Citrine Series, isolator resonance can be optimized in the range of 30 to 70 Hz, and performance varies depending on the weight of the isolated unit and vibration profile.

Figure 2 shows the dynamic phase noise measurement of a Premium 100 MHz vibration isolated Citrine, P/N 501-24942 Rev. B, during a vibration profile of 10 Hz to 2 KHz at 0.01 g^2/Hz. This oscillator has a natural resonance of ~50 Hz. To mitigate vibration at frequencies lower than ~30 Hz such as in shipboard applications, selecting the best low-g crystal and using a hard-mounted option may be the best solution. Regardless of the application, Wenzel's Application Engineers study each requirement carefully to configure the best solution possible for each customer.

CITRINE PLUS OPTIONS

Since many applications require high quality signals at frequencies or stabilities that cannot be created by the oscillator alone, several additional circuits are available to satisfy this demand. The Citrine Plus, with a slightly larger housing, has several standard options. These additional circuits are based on our Blue Tops RF Modules product line and include multipliers, dividers, amplifiers, filters and a PLL option, all integrated into the Citrine Plus packaging along with the oscillator to create the desired final frequency or function. The Citrine Plus models can also be provided in a vibration isolated configuration. See Table 1 for additional details about the Citrine Plus options.

The Citrine Series product line offers a wide variety of standard oscillators that provide extremely high performance in high vibration and benign environments. Low phase noise, high stability and customized outputs are available on a standard COTS delivery schedule. Since the series is configurable for many applications, very few compromises are required.

Wenzel Associates Inc.
Austin, TX (512) 835-2038,
www.wenzel.com.

New Thermal Solver for RF Applications

With its latest release, the EMPIRE XCcel 3D EM solver now features a novel thermal solver for the simulation of the temperature distribution of power electronics, RF circuits and integrated circuits, as well as electromagnetic heating in the human body. The thermal simulation includes thermal conductivities of materials, surface convection and radiation cooling. It also supports heat sources and heat sinks for heating and cooling mechanisms.

With the increased packaging density of RF circuits, heating can become a severe problem for the lifetime of critical components such as diodes (also LEDs), transistors, resistors and ICs. Also passive structures such as filters, couplers or resonators can exhibit high currents in small areas where the temperature can rise to a critical level. Also, with regards to electromagnetic radiation the prediction of thermal heating inside human bodies (e.g. handheld antenna next to a human head) is necessary to prevent hazards.

TEMPERATURE DISTRIBUTION PREDICTION

The accurate prediction of the temperature distribution is now possible with EMPIRE XCcel 6.0. The geometry can be imported or is created within the GUI where properties such as thermal conductivity and heat transfer rates can be entered similarly to electromagnetic properties. A large database is equipped with known parameters and thermal sources can be set directly, e.g. by entering a thermal power in watts for a lumped element such as a transistor.

Thermal sources can be determined by an EM simulation, too. With a combined EM and thermal simulation the RF losses are calculated in a first EM simulation run, which will be used as a source for subsequent thermal simulations. Cooling elements can be defined as surfaces with a specific thermal resistivity. In the case of human body thermal modelling, the blood perfusion rate can also be taken into account. In addition, known thermal properties are available in a tissue database.

The simulation engine automatically identifies the surface to air interfaces and invokes the heat transfer mechanisms such as radiation and convection. With this method, cells filled with air do not need to be part of the solution, thus minimizing the number of cells to be simulated for the temperature distribution.

FAST SIMULATION

A robust and efficient solver kernel is used for the fast solution of the thermal equations. An adaptive scheme optimizes the over-relaxation factor during the iteration process for maximum simulation speed. After simulation the temperature distribution can be displayed together with the structure. The temperature can be displayed as distinct planes, as maximum or minimum of each plane or as top and bottom temperature distribution. The latter is especially intended for comparison with infrared camera images.

IMST GmbH
Kamp-Lintfort, Germany

■ Six Days ■ Three Conferences ■ One Exhibition

Europe's Premier Microwave, RF, Wireless and Radar Event

EUROPEAN MICROWAVE WEEK
RAI Amsterdam
EuMW 2012
28 October – 2 November 2012
www.eumweek.com

Space for Microwaves

EXHIBITION & CONFERENCE REGISTRATION INFORMATION

October 28th - November 2nd 2012
Amsterdam RAI, The Netherlands

EuMA
European Microwave Association

Official Publication: Microwave Journal

Organised by: horizon house

Supported by: IET The Institution of Engineering and Technology

Co-sponsored by: MTT-S

Co-sponsored by: IEEE

EuRAD 2012
The 9th European Radar Conference
Co-sponsored by: AESS

42ND EUROPEAN MICROWAVE CONFERENCE 2012
The 42nd European Microwave Conference
Co-sponsored by:

EuMIC 2012
The 7th European Microwave Integrated Circuits Conference
Co-sponsored by: Electron Devices Society, GAAS

Register online at:
www.eumweek.com

EUROPEAN MICROWAVE WEEK
RAI Amsterdam
28 October – 2 November 2012
EuMW 2012
www.eumweek.com

EUROPEAN MICROWAVE WEEK 2012
THE CONFERENCES

Don't miss Europe's premier microwave conference event. The 2012 week consists of three conferences and associated workshops:

- **European Microwave Integrated Circuits Conference (EuMIC) – 29th – 30th October 2012**
- **European Microwave Conference (EuMC) – 29th October - 1st November 2012**
- **European Radar Conference (EuRAD) – 31st October - 2nd November 2012**
- **Workshops – 28th - 29th October and 1st - 2nd November 2012**

The three conferences specifically target ground breaking innovation in microwave research through a call for papers explicitly inviting the submission of presentations on the latest trends in the field, driven by industry roadmaps. The result is three superb conferences created from the very best papers, carefully selected from close to 1,000 submissions from all over the world. Special rates are available for EuMW delegates. For a detailed description of the conferences, workshops and short courses please visit www.eumweek.com. The full conference programme can be downloaded from there.

Fast Track
Badge Retrieval

Register online and print out your badge in seconds onsite at the Fast Track Check In Desk

Conference Prices

There are TWO different rates available for the EuMW conferences:

- **ADVANCE DISCOUNTED RATE** – for all registrations made online before 27th September
- **STANDARD RATE** – for all registrations made online after 27th September and onsite

Please see the Conference Registration Rates table on the back page for complete pricing information.
All payments must be in € euro – cards will be debited in € euro.

Online registration is open now, up to and during the event until 2nd November 2012

DELEGATES

Registering for the Conference

- Register online at www.eumweek.com
- Receive a confirmation email receipt with barcode
- Bring your email, barcode and photo ID with you to the Event
- Go to the Fast Track Check In Desk and print out your delegates badge
- Alternatively, you can register Onsite at the self service terminals during the registration opening times below:
  - Saturday 27th October (16.00 – 19.00)
  - Sunday 28th October (07.30 – 17.00)
  - Monday 29th October (07.30 – 17.00)
  - Tuesday 30th October (07.30 – 17.00)
  - Wednesday 31st October (07.30 – 17.00)
  - Thursday 1st November (07.30 – 17.00)
  - Friday 2nd November (07.30 - 10.00)

Once you have collected your badge, you can collect the conference proceedings on USB stick and delegate bag for the conferences from the specified delegate bag area by scanning your badge.

CONFERENCE PRICING AND INFORMATION

EUROPEAN MICROWAVE WEEK 2012, 28th October - 2nd November, Amsterdam, The Netherlands

Register Online at www.eumweek.com
ONLINE registration is open from 12th June 2012 up to and during the event until 2nd November 2012.
ONSITE registration is open from 4pm on 27th October 2012.
ADVANCE DISCOUNTED RATE (before 27 Sept), STANDARD RATE (after 27 Sept & Onsite)

Reduced rates are offered if you have society membership to any of the following: Eu*M*A, gaas, iet or ieee
Eu*M*A membership costs: Professional: € 20/year Student € 10/year
Reduced Rates for the conferences are also offered if you are a Student/Senior (Full-time students less than 30 yrs of age and Seniors 65 or older as of 2nd November 2012)

ADVANCE REGISTRATION CONFERENCE FEES (BEFORE 27 SEPT)

CONFERENCE FEES	ADVANCE DISCOUNTED RATE			
	Society Member (*any of above)		Non-member	
1 Conference	Standard	Student/Sr.	Standard	Student/Sr.
EuMC	€ 420	€ 100	€ 550	€ 130
EuMIC	€ 325	€ 90	€ 430	€ 120
EuRAD	€ 255	€ 80	€ 340	€ 110
2 Conferences				
EuMC + EuMIC	€ 600	€ 190	€ 790	€ 250
EuMC + EuRAD	€ 550	€ 180	€ 720	€ 240
EuMIC + EuRAD	€ 470	€ 170	€ 630	€ 230
3 Conferences				
EuMC + EuMIC + EuRAD	€ 710	€ 270	€ 940	€ 360

STANDARD REGISTRATION CONFERENCE FEES (AFTER 27 SEPT AND ONSITE)

CONFERENCE FEES	ADVANCE DISCOUNTED RATE			
	Society Member (*any of above)		Non-member	
1 Conference	Standard	Student/Sr.	Standard	Student/Sr.
EuMC	€ 550	€ 130	€ 720	€ 170
EuMIC	€ 430	€ 120	€ 560	€ 160
EuRAD	€ 340	€ 110	€ 450	€ 150
2 Conferences				
EuMC + EuMIC	€ 790	€ 250	€ 1030	€ 330
EuMC + EuRAD	€ 720	€ 240	€ 940	€ 320
EuMIC + EuRAD	€ 630	€ 230	€ 810	€ 310
3 Conferences				
EuMC + EuMIC + EuRAD	€ 940	€ 360	€ 1230	€ 480

WORKSHOP AND SHORT COURSE FEES (ONE STANDARD RATE THROUGHOUT)

For full details & titles of Workshops & Short Courses, visit www.eumweek.com

FEES	ADVANCE DISCOUNTED RATE			
	Society Member (*any of above)		Non-member	
	Standard	Student/Sr.	Standard	Student/Sr.
1/2 day WITH Conference registration	€ 80	€ 60	€ 110	€ 80
1/2 day WITHOUT Conference registration	€ 110	€ 80	€ 150	€ 110
Full day WITH Conference registration	€ 120	€ 90	€ 160	€ 110
Full day WITHOUT Conference registration	€ 160	€ 120	€ 210	€ 150

Proceedings on USB stick

All papers published for presentation at each conference will be on a USB stick, given out FREE with the delegate bags to those attending conferences. For additional USB sticks the cost is € 50

Hotel & Travel Service

Amsterdam RAI Hotel & Travel Service has enormous experience and can offer you considerable savings in money, time and hassle. Visit www.rai.nl/hotelservice

DVD Archive EuMC	
DVD Archive EuMC 1969-2003	€ 10
DVD Archive EuMC 2004-2008	€ 35

FREE SPECIAL FORUMS & SESSIONS

Date	Time	Title	Location	No. of Days	Cost
Weds 31st Oct	08:30 - 19:00	The 2012 Defence, Security and Space Forum	Auditorium	1	FREE
Thurs 1st & Fri 2nd Nov	08:30 - 17:00	Doctoral School of Microwaves	Room G001	2	€ 80

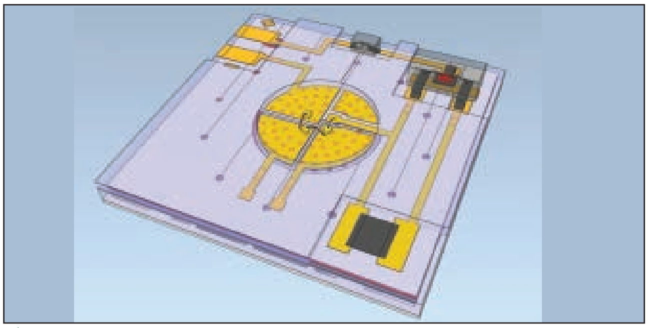

Fig. 1 *LTCC module with LEDs and driver circuit.*

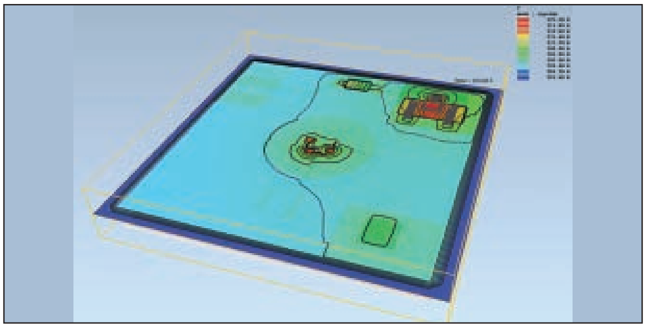

Fig. 2 *Temperature distribution on the LTCC module.*

As an application example, ***Figure 1*** shows an LTCC module which has been developed in a joint project of German companies: odelo LED GmbH, IGOS GmbH and IMST GmbH. It contains three LED chips on top which are die-bonded and wire-bonded to the top metallization. A small driver circuit with a Schottky diode, transistor and resistor is also placed on top. Many thermal vias are integrated beneath the active elements to transfer the heat from the top to the heatsink at the bottom. In this case the power loss is known and entered as lumped and distributed heat sources.

Figure 2 shows the temperature distribution of the top obtained with EMPIRE XCcel 6.0. The module is subdivided into 10.3 million cells and an accuracy of 0.6 mK has been obtained after 2700 iterations. The simulation time needed is about three minutes on a notebook with Intel Core i7-2620M CPU at 2.7 GHz. For this size the memory requirement is about 1 GB. The temperature rise is about 40°K above ambient temperature with the maximum inside the transistor package. As can be seen a temperature distribution for a complex structure is obtained with the EMPIRE XCcel 6.0, which provides valuable input for the thermal design.

The new EMPIRE XCcel 6.0 3D EM solver has been designed to cover nearly all today's design challenges for RF designers, like antennas, passive circuits, packages, waveguides or EMC/EMI problems including thermal examination of the human body. The new thermal solver has also been optimized with respect to solution speed thus giving reliable results within the minimum solution time.

IMST GmbH,
Kamp-Lintfort, Germany
+49 (0) 2842 9810,
www.empire.de,
empire@imst.com.

Catalog Update

DesignCon Material

VENDORVIEW

Agilent offers a composite of the 2012 DesignCon educational forums and workshops. This new DVD showcases tools, demos, videos, and presentations including those on design and simulation; validation of a model; debug, validate and characterize; system test; compliance testing; and compliance standards information. The DVD is available now at www.agilent.com/find/HSD-Pinpoint. Additional information can be found at www.agilent.com/find/HSD.

**Agilent Technologies Inc.,
Santa Clara, CA (800) 829-4444, www.agilent.com.**

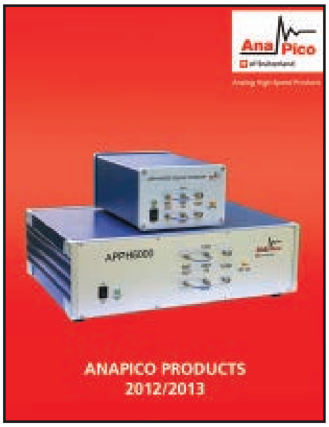

Product Catalog

AnaPico's new product catalog for 2012 and 2013 is now available from your local AnaPico representative. It gives an overview of the latest developments, especially highlighting the various models of RF and microwave signal generators and phase noise test systems up to 6 and 21 GHz. The catalogue is also available in full for free download at www.anapico.com.

**AnaPico AG,
Zurich, Switzerland +41 44 440 00 51, www.anapico.com.**

EMC & RF Testing Catalog

VENDORVIEW

AR's new product catalog is now available from your local AR sales associate. The catalog is easy to use, with "find-it-fast" charts and color coding to help get right to whatever you need for RF and EMC testing. It is available for free download, either in full or by section, at www.arworld.us.

**AR RF/Microwave Instrumentation,
Souderton, PA (215) 723-8181, www.ar-worldwide.com.**

Build-to-Print Brochure

DLI offers thin film build-to-print services designed to meet the advanced needs of today's customers. Product design, manufacturing and testing capabilities; DLI can offer customers prototype to high volume manufacturing for simple designs to high frequency (> 40 GHz) complex filters offering some or all. Manufacture on standard ceramics (Al_2O_3, AlN) or high K materials offering temperature stability over frequency. Combining all of DLI's unique capabilities and offering one-of-a-kind service to meet your needs and exceed your expectations.

**Dielectric Laboratories Inc.,
Cazenovia, NY (315) 655-8710, www.dilabs.com.**

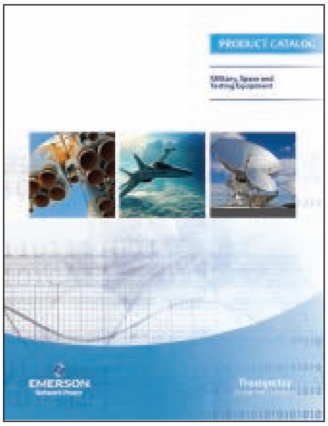

Trompeter T24 Catalog

Emerson Network Power Connectivity Solutions announces the new Trompeter T24 catalog highlighting products for military, space and testing applications. The catalog features a new 1023 series of DIN Connectors, which are 45 percent smaller than the company's DIN 1.6/5.6 connectors and are ideal for higher density patching requirements. This line of 1.0/2.3 series 75 Ohm connectors delivers the same quality performance of the 220 Series BNC range. The T24 catalog also includes an updated QPL list of 70/370 connectors that meet the requirements of MIL-C-49142.

**Emerson Network Power Connectivity Solutions Inc.,
Bannockburn, IL (847) 739-0300,
www.emersonnetworkpower.com.**

Selection Guide

VENDORVIEW

Hittite releases the May 2012 selection guide that summarizes over 1025 products, including 21 new products. New for this publication is a 60 GHz Tx/Rx Chipset which supports WiGig and IEEE 802.11ad multi-Gbps solutions. The selection guide is organized by RF & microwave, analog & mixed signal, clocks & timing and LO frequency generation IC sections along with modules and instrumentation. The new & expanded product line section includes a new programmable harmonic filter, MMIC 2W PA with on chip power detector, dual channel downconverter, A/D converter, and clock generator with Integer-N PLL.

**Hittite Microwave Corp.,
Chelmsford, MA (978) 250-3343, www.hittite.com.**

Catalog Update

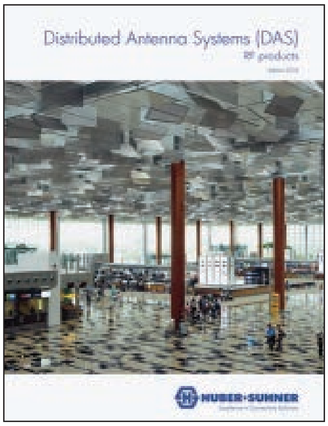

Distributed Antenna Systems

When it comes to the availability and quality of wireless voice and data communication services, the high coverage requirements apply equally both outside and inside buildings. The shielding effect of the building's front and structure on radio signals often is reason for insufficient service quality. With the implementation of dedicated solutions in the form of systems with distributed antennas, the internal coverage required can be achieved in every case. The new HUBER+SUHNER catalogue offers the relevant solutions. You can access the catalog at http://ipaper.ipapercms.dk/hubersuhner/marketsegments/communication/distributedantennasystemsendas/.

HUBER+SUHNER AG,
Herisau, Switzerland +41 71 353-4111, www.hubersuhner.com.

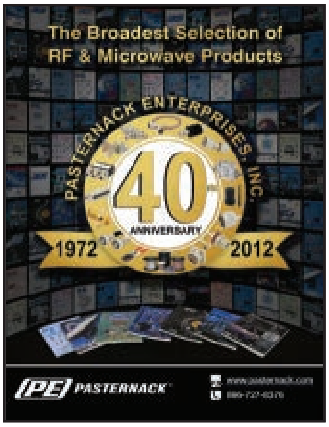

RF and Microwave Catalog

Pasternack's interactive catalog contains all of the same content as the printed catalog, but offers additional capabilities such as single-page or double-page viewing options, zoom capabilities and a product search bar. Page-turning animation simulates the look and feel of a tangible catalog, while the interactive version allows the user to click on any product inside the 296-page online book and go directly to the product page on Pasternack's new website. The catalog is optimized for usage on all mobile devices and can be found at www.pasternackcatalog.com.

Pasternack Enterprises Inc.,
Irvine, CA (866) 727-8376, www.pasternack.com.

Test & Measurement Catalog

VENDORVIEW

Rohde & Schwarz set standards in research, development, production and service. As a key partner of industry, network operators and public institutions, they offer a broad spectrum of market-leading solutions for state-of-the-art technologies, including LTE-Advanced, the mobile radio standard of the next generation, as well as for extremely high-frequency applications up to 500 GHz. Rohde & Schwarz meets the growing demand by offering cutting-edge products for signal generation, signal analysis, network analysis and power measurement.

Rohde & Schwarz,
Munich, Germany +49 89 41 29 0, www2.rohde-schwarz.com.

The 2012 Defence, Security and Space Forum

At European Microwave Week

Microwave Journal
Frequency Matters.

EuMA
European Microwave Association

Wednesday 31 October 2012 • Auditorium 8:30 to 19:00

A full-day Forum, focusing on Space and Defence issues, incorporating the EuRAD Opening Session and featuring the EuMW Defence and Security Executive Forum.

The 2012 EuMW Defence, Security and Space Forum will feature:

EARLY MORNING SESSION: 08:30–10:10
Focuses on Defence, Security and Space from an industrial perspective and considers the application of the microwave technology that is being developed to address pivotal issues.

LATE MORNING SESSION: 10:40 – 12:20
For the first time the EuMW Defence, Security and Space Forum incorporates the EuRAD Opening Session, which offers an overview of prevalent defence and security issues and highlights synergies between the industrial defence and space sector.

LUNCH AND LEARN: 12:30 – 13:30
Provided to all attendees, courtesy of *Strategy Analytics*, who will present market data and analysis of the global defence market.

AFTERNOON SESSION: 13:50 – 15:30
Tutorials by industry and agency experts will give an insight into the latest Defence and Space developments.

EVENING EXECUTIVE FORUM: 16:00 – 18:00
Executives from space and defence agencies and leading defence/space contractors will consider the issues that their organizations are currently addressing and the role that technology has to play. A Q&A session will conclude the forum.

COCKTAIL RECEPTION: 18:00 – 19:00
Offers delegates the unique opportunity to network and discuss the issues raised throughout the Forum in an informal setting.

Sponsorship Opportunities

Sponsorship Includes:

- ✓ Literature distribution at the event
- ✓ Sponsor designation in the official show guide
- ✓ Full list of attendees with contact information
- ✓ Video of event posted on MWJ and EuMW websites with sponsor recognition
- ✓ Logo placement on all promotions, in official Show Guide and on event signage

Promotional Activity will Include:

- ✓ Multiple full page advertisements in Microwave Journal with sponsor recognition
- ✓ Multiple email broadcasts to the MWJ database of 50,000+ subscribers
- ✓ Full page ad in the official EuMW Show Guide
- ✓ Featured listing on MWJ and EuMW websites

Cost: $5,000 (Net)

Contact your sales representative for more information or to reserve your sponsorship.

Components

Waveguide Filter

Delta Microwave announced delivery of the X1980 High-Q TE111 dual-mode cylindrical cavity Waveguide filter for the X-Band data link for a space observatory application. The X1980 bandpass filter has a passband from 8.00 to 8.30 GHz with a maximum insertion loss of 0.5 dB and a maximum return loss of 20 dB. The unit has a minimum rejection of 40 dB from 6.9 to 7.9 and 8.4 to 9.4 GHz.

Delta Microwave,
Oxnard, CA (805) 751-1100,
www.deltamicrowave.com.

Cavity Filter

This 3-section narrowband cavity filter has a center frequency of 1817.5 MHz with an equiripple bandwidth of 17.4 MHz minimum, yielding an insertion loss of 1.5 dB maximum. The out-of-band attenuation for this 3-pole filter is 30 dB minimum from DC to 1767.5 MHz and from 1867.5 MHz. The group delay variation is less than 2 ns maximum over 1812.5 to 1822.5 MHz. The input/output return loss is 14 dB minimum over the 1807.5 to 1827.5 MHz passband.

K&L Microwave Inc.,
Salisbury, MD (410) 749-2424,
www.klmicrowave.com.

Directional Coupler

Krytar's model 180120 is a multi-purpose, stripline design that exhibits excellent coupling over the 1 to 18 GHz frequency band. Krytar's technological advances has extended the frequency range of this single unit from 1 to 18 GHz with coupling (with respect to output) of 20 dB ±1.0 dB, frequency sensitivity of ±0.3 dB (1 to 12.4 GHz), ±0.4 dB (1 to 18 GHz), and directivity of > 16 dB. The directional coupler exhibits insertion loss (including coupled power) of less than 0.95 dB across the frequency range.

Krytar Inc.,
Sunnyvale, CA (408) 734-5999,
www.krytar.com.

I/Q Demodulator

The LTC5584 is an ultrawide bandwidth direct conversion I/Q demodulator with linearity of 31 dBm IIP3 and 70 dBm IIP2. The device offers demodulation bandwidth of over 530 MHz and operates over a wide frequency range from 30 MHz to 1.4 GHz, covering a broad range of VHF and UHF radios and the 450/700 MHz LTE frequency bands. Unique to the LTC5584 are two built-in calibration features: advanced circuitry and on-chip circuitry. Combined with a 9.9 dB noise figure, these features enhance the dynamic range performance in receivers.

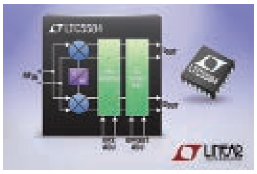

Linear Technology,
Milpitas, CA (408) 432-1900,
www.linear.com.

Power Divider/Combiners

VENDORVIEW

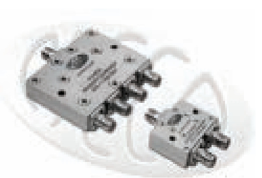

Compact, high-performance Wilkinson power divider/combiners ideally suited for C-, X- and Ku-Band systems applications. Two-way and four-way SMA-female models feature high isolation, low insertion loss, exceptional VSWR and excellent phase/amplitude balance. Available in octave bands and also broadband designs including 2 to 18 GHz. Delivery from stock – four weeks ARO. Made in USA – 36 month warranty.

MECA Electronics Inc.,
Denville, NJ (973) 625-0733,
www.e-MECA.com.

Transformer

VENDORVIEW

Mini-Circuits new TCM2-33X+ transformer is ideal for impedance-matching push-pull amplifiers across all major cellular frequencies and for many WLAN systems. This patent-pending dual output autotransformer offers an excellent return loss of 20 dB typical, across its entire frequency range, for 2:1 balanced-to-unbalanced transformations in 50 Ω applications. It has a wide bandwidth of 30 to 3000 MHz. The aqueous washable case includes Mini-Circuits unique Top Hat™ feature to help speed customer pick-and-place, and is available on small quantity reels (20 pieces and up) at no extra cost.

Mini-Circuits,
Brooklyn, NY (718) 934-4500,
www.minicircuits.com.

LC Filter

VENDORVIEW

NIC introduced a high frequency LC filter at 5252 MHz, designed for use in Hi-Rel C-Band application. This filter offers high performance in a low profile (0.2" & up) hermetically sealed package. It features low insertion loss and high rejection, as well as a ruggedized package for Hi-Rel environments.

Networks International Corp.,
Overland Park, KS (913) 685-3400,
http://nickc.com.

Single Sideband Modulator

VENDORVIEW

Model PSM-0R5G2R5G-CD-1 is a single sideband modulator that operates over the 500 MHz to 2.5 GHz frequency range. The input P1dB is +5 dBm typical and has an IF modulation range of DC to 500 MHz. The IF modulation power range is +7 dBm minimum and +13 dBm maximum into 50 ohms. The conversion loss is 13.5 dB maximum and this model provides carrier suppression of 23 dBc typically. The Quadrature phase accuracy is ±10 degrees maximum with a Quadrature amplitude accuracy of ±2.0 dB maximum.

Planar Monolithics Industries Inc.,
Frederick, MD (301) 662-5019,
http://pmi-rf.com.

90° Quadrature Hybrid

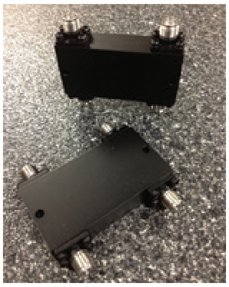

Response Microwave Inc. announced the availability of its new broadband 3 dB, 90° quadrature hybrid for use in automated test and production applications. The new RMHY3.18000Sf covers the 2 to 18 GHz band offering typical electrical performance of 1.5 dB insertion loss, VSWR of 1.50:1, minimum isolation of 16 dB. Average power handling is 50 W and the unit is operational over the –55° to +85°C range.

Response Microwave Inc.,
Devens, MA (978) 772-3767,
www.responsemicrowave.com.

Bessel Lowpass Filters

RLC Electronics now offers 4th order tubular Bessel lowpass filters with 3 dB cutoffs from 1 to 22 GHz. Computer design and tubular construction allow RLC to maintain excellent group delay characteristics with reasonable rejection while extending RLC's 3 dB cutoff approaching 30 Giga bits. These filters should be regarded as compromise designs for pulsed systems where truthful reproduction of the pulse shape is important.

RLC Electronics Inc.,
Mount Kisco, NY (914) 241-1334,
www.rlcelectronics.com.

Smart SYNTHESIZED SIGNAL GENERATORS 250-4000 MHz

WOW! only $1995.00 ea.

Rugged, portable, production test workhorses

Sweep or hop across wide frequency and power bands, use a pair for third-order intercept tests, or slip one into your laptop case and take it on the road! Our easy-to-use GUI will have you up and running in minutes. Compatible with most test software,* they add capabilities and increase efficiency, all without busting your budget!

*See data sheets for an extensive list of compatible software.

Accurate, reliable results at high speed

Signals within 1 ppm for frequency and 0.25 dBm for power, low harmonics, a resolution of 5 kHz, and 5-msec settling times help you get the data you need from complex, high-speed testing plans. Just go to minicircuits.com for specifications, performance data, and everything you need to make your choice — and get it in your hands as soon as tomorrow!

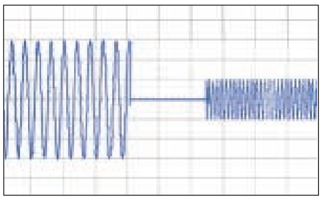

Frequency and power hopping.

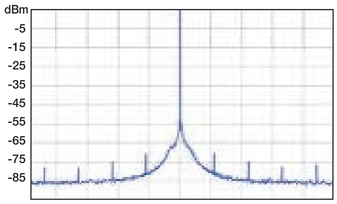

Low spurious.

Model	Frequency (MHz)	Power (dBm)	Harmonics (dBc typ.)	Price ($ ea.)
SSG-4000HP	250-4000	-50 to +20	-40	1995.00
SSG-4000LH	250-4000	-60 to +10	-66	2395.00

Mini-Circuits...we're redefining what VALUE is all about!

SP4T Switch

VENDORVIEW

Skyworks introduced a 0.1 to 2.7 GHz SP4T switch with integrated logic decoder for GSM quad-band receive and diversity-antenna applications. The 2 × 2 mm SKY13388-465LF is controlled with 1.8 V logic and is ideal for 3G handsets and data cards. It delivers low-insertion loss, does not require any DC blocks or external components for operation, and its high-compression point leads to better linearity, lower-harmonic generation, and less stringent harmonic filtering.

Skyworks Solutions Inc.,
Woburn, MA (781) 376-3000,
www.skyworksinc.com.

Power Doubler

The TAT8857 is ideal for use as a 'green doubler' in typical 75 Ohm line amplifier systems where it reduces power consumption 20% compared to existing MMIC solutions in standard 24 V operation. It is versatile, designed for distribution node applications from 40 to 1002 MHz; it can also be operated on 12 V for optimal efficiency. The TAT8857 utilizes on-chip linearized, integrated PHEMT and MESFET technology to provide low distortion configurable gain from 22 to 27 dB. The device comes in a standard SOIC-16 package.

TriQuint Semiconductor,
Hillsboro, OR (503) 615-9000,
www.triquint.com.

Dual Directional Coupler

VENDORVIEW

Werlatone's new 40 dB dual directional coupler, model C8998, offers exceptional performance while covering a full 100 to 3000 MHz band and is rated for 250 W CW. Operating with only 0.4 dB of insertion loss, this compact design measures just 3" × 2.2" × 1.1" and is designed for commercial and military applications. It has an operating temperature of -55° to +85°C and is available with N female and SMA female connectors.

Werlatone Inc.,
Patterson, NY (845) 278-2238,
www.werlatone.com.

Amplifiers

Solid-State Power Amplifiers

CTT Inc. announced a new family of 39 compact, GaN-based SSPAs operating in the 6.4 to 11 GHz frequency range. CTT's latest

compact SSPA designs offer as much as 160 W of output power in a compact package. They include 15 models for narrow-band applications operating from 7.8 to 10.7 GHz in CW mode. For wideband and ultra-wideband applications, there are 12 models that operate from 6.4 to 11 GHz in CW mode.

CTT Inc.,
Sunnyvale, CA (408) 541-0596,
www.cttinc.com.

Optical Modulator Driver

VENDORVIEW

Hittite Microwave Corp. released the industry's lowest power and smallest form factor SMT packaged optical modulator driver. It operates from DC to 30 GHz and is designed for 40 and 100 Gbps Mach-Zehnder optical modulator driver applications. The HMC5850BG features high gain across a wide frequency range, low power dissipation, very compact size, integrated peak detector function, fast rise/fall time and integrated bias-tee inductor. The driver provides 8 Vp-p saturated output swing up to 32 Gbps and features output swing cross point adjustment.

Hittite Microwave Corp.,
Chelmsford, MA (978) 250-3343,
www.hittite.com.

CMOS Driver

The MADR-010410 is an efficient CMOS driver and ideal for logic control of GaAs based T/R modules as well as a 6-Bit S/P driver for attenuators or phase shifters. High speed analog CMOS technology is utilized to achieve low

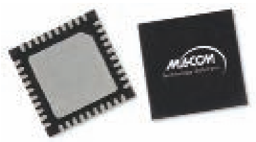

power consumption at moderate to high speeds. The MADR-010410 boasts low power dissipation and translates CMOS/LVCMOS input controls to negative gate control voltages for GaAs FETs. Packaged in a 5 mm 40-Lead PQFN, the CMOS driver allows a high output voltage of -0.1 V and a low output voltage of 0.1 V.

M/A-COM Technology Solutions Inc.,
Lowell, MA (978) 656-2896,
www.macomtech.com.

X-Band Amplifier

Microsemi announced the availability of a low noise X-Band amplifier, model number AML812L3003. This LNA operates in the frequency range of 8 to 12 GHz with small signal gain over 30 dB and a noise figure of 1.1 dB typical. Output P1dB is +10 dBm min. This amplifier is available in a SMA connectorized housing with internal voltage regulation and reverse voltage protection.

Microsemi Corp.,
Santa Clara, CA (805) 388-1345,
www.microsemi.com/rfis.

Power Amplifier

VENDORVIEW

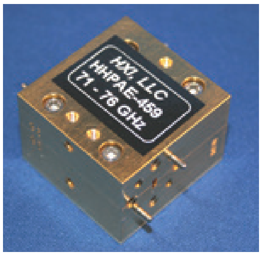

The HHPAE-459 power amplifier covers the frequency range from 71 to 76 GHz. The amplifier has an output P1dB of +18 dBm with small signal gain of 29 dB. MMIC technology is employed for high reliability and repeatability. A single +6.5 V DC bias feeds an internal voltage regulator and bias sequencer to power the amplifier, freeing the user from the complications of a dual bias configuration. The amplifier was designed for use in transmitters for E-Band radio communications systems.

Renaissance Electronics/HXI,
Harvard, MA (978) 772-7774,
www.rec-usa.com.

Wideband Power Amplifier

VENDORVIEW

Using an advanced high power density GaN semiconductor process, RFMD's new RFHA1006 high-performance amplifier achieves high efficiency, flat gain, and large instantaneous bandwidth in a single amplifier design. This input-matched GaN transistor is packaged in an air cavity ceramic package for excellent thermal stability through the use of advanced heat sink and power dissipation technologies. Ease of integration is accomplished through the incorporation of optimized input matching network within the package that provides wideband gain and power performance in a single amplifier.

RFMD,
Greensboro, NC
(336) 664-1233,
www.rfmd.com.

Software

3D Simulation Platform

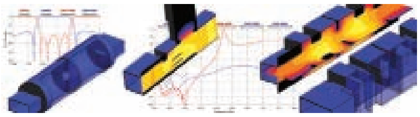

SPEAG's latest release of SEMCAD X provides users the unique capability to combine a new solver based on the Mode Matching Technique with proven FDTD techniques for the accurate and fast simulation of passive waveguide structures. The new solver has been integrated into the existing SEMCAD X framework to solve complex EM challenges in the microwave industry. Together with the EM and Thermal solvers, SEMCAD X Microwave can be successfully applied to a wide variety of electromagnetic problems ranging from microwave devices, EMC, optics, to bio-medical applications.

Schmid & Partner Engineering AG,
Zurich, Switzerland
+41-44-2459700,
www.speag.com.

Sources

Locked Oscillators

API Technologies Corp. announced a new line of multiplied phase locked oscillators from the Spectrum Microwave family of products. Phase noise performance is -175 dBc/Hz (at 100 kHz offset) and can use its internal or external 10 MHz reference. The line has an output range of 80 to 1600 MHz and deliver spurious performance of -60 dBc when powered by a +12 V supply. Additional features include: DC voltage regulation, automatic reference sensing, low current consumption and multiple RF outputs.

API Technologies Corp., Orlando , FL (855) 294-3800, http://apitech.com.

Clock Oscillator

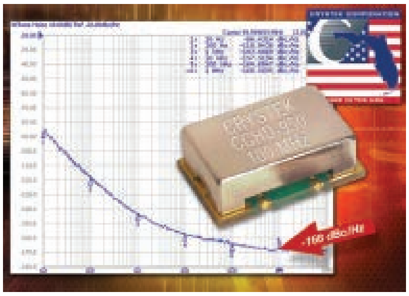

Crystek Corp.'s CCHD-950 Series HCMOS clock oscillator has a -168 dBc/Hz noise floor (100 MHz model). The CCHD-950 generates frequencies between 45 and 130 MHz, with 50, 80, 100 and 130 MHz offered as standard. A high-Q crystal and 3rd overtone technology provide the ultra-low phase noise and low-jitter performance. Generating no sub-harmonics, the CCHD-950 requires an input supply voltage of 3.3 V DC consuming 15 mA of current. It is available in an FR5 9 × 14 mm SMD package.

Crystek Corp., Fort Myers, FL (800) 237-3061, www.crystek.com.

Voltage-Controlled Oscillator

The USSP2350-LF covers the frequency range of 2300 to 2400 MHz in 0.5 to 3 V of tuning voltage. This high performance VCO comes available in a compact surface-mount package measuring 0.2" × 0.2" × 0.04" while operating off 2.7 V and drawing 6 mA, typically. The USSP2350-LF provides a spectral purity of –82 dBc/Hz, typically, at 10 kHz from the carrier and is designed to operate over the commercial temperature range of –20° to 70°C. This VCO delivers 0±4 dBm of output power into a 50 ohm load and suppresses the 2nd harmonic to better than -13 dBc.

Z-Communications Inc., Poway, CA (858) 621-2700, www.zcomm.com.

MICRO-ADS

The Book End

Microwave and RF Engineering: An Electronic Design Automation Approach, Vol. 1

Ali A. Behagi and
Stephen D. Turner

Unlike many traditional textbooks on microwave and RF engineering written mainly for the classroom, *Microwave and RF Engineering, Vol. 1* adopts a practical, hands-on approach to introduce and familiarize students and engineers new to the field. Topics range from an introduction of lumped elements and transmission line components to multi-stage amplifier design. Theoretical concepts are explained through real world computer models. The authors extensively include the use of electronic design automation tools to illustrate the foundation principles of microwave and RF engineering.

This book introduces not only a solid understanding of microwave and RF engineering concepts, but also more importantly how to use design automation tools to analyze, synthesize, simulate, tune and optimize these essential components in a design flow as practiced in the industry. The book covers RF and microwave concepts such as the Smith Chart, S-parameters, transmission lines, impedance matching, filters and amplifiers. The text is designed to be a 'hands-on' book with practical examples. It stresses the importance of design automation techniques with an emphasis on Agilent's Genesys Linear Software Suite.

In addition to university and college students, engineers and technicians will find this text to be a valuable reference. Practicing engineers can find it helps them set up various circuit models very quickly, while students can solve practical examples and learn the theory by modeling problems using CAD. This first volume teaches the basics of RF and microwave engineering with a tight integration of linear CAD techniques and is a very good reference book for both students and engineers to have on their bookshelf. The second volume will focus more on nonlinear CAD techniques.

To order this book, contact:

BT Microwave LLC
www.amazon.com

464 pages, $95
ISBN: 978-0-98354-601-6

eLEARNING center

July Short Course Webinars

Innovations in Signal Analysis
Presented by: Agilent Technologies
Wireless Site Survey Using a Handheld Spectrum Analyzer
Live webcast: 7/11/12, 1:00 PM ET

Agilent in Aerospace/Defense Series
Phase Noise Measurement Methods and Techniques
Live webcast: 7/19/12, 1:00 PM ET

Agilent in LTE
Wideband Digital Pre-Distortion Modeling for LTE-Advanced
Presented by: Agilent Technologies
Live webcast: 7/26/12, 1:00 PM ET

COMING IN AUGUST
Innovations in EDA
Live Webcast: 8/1/12, 1:00 PM ET

Past Webinars On Demand

Masters of MIMO Series
- Over-the-Air (OTA) Signal Challenges and Implications – Recommendation for LTE RAN
- MIMO OTA Measurements – The Next Generation Platform for Wireless Testing

THE MASTERS OF MIMO SERIES

MicroApps Expert Forum
- Device Characterization Methods & Advanced RF/Microwave Design

RF/Microwave Training Series
Presented by: Besser Associates
- Mixers and Frequency Conversion
- LTE Broadband Wireless Access

Market Research Series
Presented by: Strategy Analytics
- AESA Radar Market Trends: Fast-Jets and Beyond

Technical Education Series
- Improving GaN HEMT PA Design with Cree's Large Signal Models and AWR's Microwave Office™
- Understanding Radio Channel - Part 2: Reaching a Data Rate of 100 Mbit/s with LTE
- RF and Microwave Heating with COMSOL Multiphysics

Innovations in EDA/Signal Generation & Analysis Series
Presented by: Agilent EEsof EDA/Agilent Technologies
- System-level Design and Verification for Advanced Satellite Comms
- Hybrid-Active Load Pull with PNA-X and Maury Microwave
- Comprehensive mmWave Design Solutions for TSMC's 60 GHz CMOS RDK
- Fast Characterization of Power Amplifier Performance with Modulated Signals
- Multi-Signal, Multi-Format Analysis with the 89600 VSA
- Nonlinear Characterization and Modeling Through Pulsed IV/S-Parameters

Agilent in Aerospace/Defense Series
Presented by: Agilent Technologies
- Simulating Power Transients and Noise
- Mixed Signal Testing Challenges in FPGA-based Radar Systems
- Fast and Accurate Frequency Converter Characterization
- RF Streaming, Analysis and Playback in Aerospace & Defense Applications

Agilent in LTE/Wireless Communications Series
Presented by: Agilent Technologies
- MSR Base Station Introduction and Measurement Challenges
- Next Generation 802.11ac WLAN MIMO Design and Test Challenges
- LTE Channel State Testing: An Overview of CQI, PMI, and RI for LTE
- Optimize UE Design for Greater Battery Run-Time

Register to attend at mwjournal.com/webinars

Microwave Journal
Frequency Matters.

Advertising Index

Advertiser	Page No.
Advanced Switch Technology	125
Agilent Technologies, Inc.	21, 105
Anaren Microwave	33
Anatech Electronics, Inc.	80
Ansys, Inc.	37
AR RF/Microwave Instrumentation	39
Artech House	120
ASB, Inc.	38
AWR	11
AWT Co., Ltd.	84
B&Z Technologies, LLC	29
Bonding Source	35
Boonton Electronics (a Wireless Telecom Group Company)	COV 2
Carlisle Interconnect Technologies	13
Cernex, Inc.	32
Ciao Wireless, Inc.	40
Coilcraft	15
COMSOL, Inc.	25
Copper Mountain Technologies	94
CPI Beverly Microwave Division	83
Cree, Inc.	57
CST of America, Inc.	23
dBm, LLC	58
Eastern Wireless TeleComm, Inc.	97
EDICON 2013	44
Empower RF Systems, Inc.	93
ES Microwave, LLC	112
ET Industries	28, 72
EuMW 2012	115
Fairview Microwave	103
Feko	116
Frontlynk Technologies Inc.	86
G.T. Microwave Inc.	62
Herotek, Inc.	34
Hittite Microwave Corporation	71, 73
Huber + Suhner AG	59
K&L Microwave, Inc.	7
Linear Technology Corporation	51
Maury Microwave Corporation	60
MECA Electronics, Inc.	6
Mercury Computer Systems	42
Microtool, Inc.	120
Microwave Development Laboratories	111
Microwave Journal	121, 126, 127

Advertiser	Page No.
Mini-Circuits	4-5, 16, 47, 48, 55, 69, 95, 107, 123, 129
MITEQ Inc.	3, 113
Modco, Inc.	125
Modpak, Inc.	125
Munich International Trade Fairs, German American Chamber of Commerce, Inc. (Electronica 2012)	36
Narda Microwave-East, an L3 Communications Co.	24, 106
National Instruments	27
NoiseWave Corp.	8
Norden Millimeter Inc.	30
OML Inc.	101
Pascall Electronics Limited	46
Pico Technology	92
Pivotone Communication Technologies, Inc.	79
Planar Monolithic Industries, Inc.	75
Programmed Test Sources, Inc.	COV 3
Pulsar Microwave Corporation	50
R&K Company Limited	112
Reactel, Incorporated	43
Remcom	87
RFHIC	63, 82, 104, 119
RFMD	61
Richardson RFPD Inc.	18, 19
Rogers Corporation	65
Rohde & Schwarz GmbH	31
Rosenberger	77
RT Logic	99
Sector Microwave Industries, Inc.	125
SGMC Microwave	91
Sivers IMA AB	98
Skyworks Solutions, Inc.	85
Sonnet Software, Inc.	81
Special Hermetic Products, Inc.	125
Spectrum Elektrotechnik GmbH	109
Synergy Microwave Corporation	53, 117
Tru Corporation	67
Universal Microwave Components Corporation	68
Virginia Diodes, Inc.	89
Waveline Inc.	70
Weinschel Associates	66
Werlatone, Inc.	COV 4
Win Semiconductors Corp.	9
Wright Technologies	125

Coming in August:

Satellite and Radio Communications

- **Wireless Sensor Network Challenges and Solutions**
- **Tackling Satellite Interference**
- **Antennas, The mm-Wave Advantage**
- **Military Microwaves Supplement**

Sales Representatives

Microwave Journal — Frequency Matters.

Carl Sheffres, Publisher

Ed Kiessling, Traffic Manager

Eastern and Central Time Zones
Chuck Boyd
Northeast Reg. Sales Mgr.
(New England, New York, Eastern Canada)
685 Canton Street
Norwood, MA 02062
Tel: (781) 769-9750
FAX: (781) 769-5037
cboyd@mwjournal.com

Michael Hallman
Eastern Reg. Sales Mgr.
(Mid-Atlantic, Southeast, Midwest)
4 Valley View Court
Middletown, MD 21769
Tel: (301) 371-8830
FAX: (301) 371-8832
mhallman@mwjournal.com

Pacific and Mountain Time Zones
Carl Sheffres
685 Canton Street
Norwood, MA 02062
Tel: (781) 619-1949
FAX: (781) 769-5037
csheffres@mwjournal.com

International Sales
Richard Vaughan
International Sales Manager
16 Sussex Street
London SW1V 4RW, England
Tel: +44 207 596 8742
FAX: +44 207 596 8749
rvaughan@horizonhouse.co.uk

Germany, Austria, and Switzerland (German-speaking)
WMS.Werbe- und Media Service
Brigitte Beranek
Gerhart-Hauptmann-Street 33,
D-72574 Bad Urach
Germany
Tel: +49 7125 407 31 18
FAX: +49 7125 407 31 08
bberanek@horizonhouse.com

Israel
Oreet Ben Yaacov
Oreet International Media
15 Kineret Street
51201 Bene-Berak, Israel
Tel: +972 3 570 6527
FAX: +972 3 570 6526
obenyaacov@horizonhouse.com

Korea
Young-Seoh Chinn
JES Media International
2nd Floor, ANA Bldg.
257-1, Myungil-Dong
Kangdong-Gu
Seoul, 134-070 Korea
Tel: +82 2 481-3411
FAX: +82 2 481-3414
yschinn@horizonhouse.com

Japan
Katsuhiro Ishii
Ace Media Service Inc.
12-6, 4-Chome,
Nishiiko, Adachi-Ku
Tokyo 121-0824, Japan
Tel: +81 3 5691 3335
FAX: +81 3 5691 3336
amskatsu@dream.com

China
Michael Tsui
ACT International
Tel: 86-755-25988571
Tel: 86-21-62511200
FAX: 86-10-58607751
michaelT@actintl.com.hk

Hong Kong
Mark Mak
ACT International
Tel: 852-28386298
markm@actintl.com.hk

MWJ Puzzler

RF/MICROWAVE SOFTWARE AND DESIGN

ANSWERS AVAILABLE AT WWW.MWJOURNAL.COM

FILL IN THE MISSING VARIABLE IN THE PINK SHADED BOX.

Z_0 CHARACTERISTIC IMPEDANCE [Ω]

The characteristic impedance is the resistance initially seen when a signal is applied to the line. It is a physical characteristic resulting from the materials and geometry of the line.

Lossless line:

$$Z_0 = \sqrt{\frac{\boxed{}}{C}} = \frac{V_+}{I_+} = -\frac{V_-}{I_-}$$

δ SKIN DEPTH [CM]

The depth into a material at which a wave is attenuated by 1/e (about 36.8%) of its original intensity. This is not the same δ that appears in the loss tangent, tan δ.

$$\delta = \frac{1}{\alpha} = \sqrt{\frac{2}{\omega \boxed{} \sigma}}$$

TAN δ LOSS TANGENT

The loss tangent, a value between 0 and 1, is the loss coefficient of a wave after it has traveled one wavelength. This is the way data is usually presented in texts.

$$\tan\delta = \frac{\boxed{}}{\omega\varepsilon}$$

V_ρ VELOCITY OF PROPAGATION [CM/S]

The velocity of propagation is the speed at which a wave moves down a transmission line. The velocity approaches the speed of light but may not exceed the speed of light since this is the maximum speed at which information can be transmitted.

$$v_p = \frac{1}{\sqrt{LC}} = \frac{1}{\sqrt{\boxed{}\mu}} = \frac{\omega}{\beta}$$

ρ REFLECTION COEFFICIENT

The reflection coefficient is the ratio of reflected voltage to the forward-traveling voltage, a value ranging from –1 to +1 which, when multiplied by the wave voltage, determines the amount of voltage reflected at one end of the transmission line.

$$\rho = \frac{V_-}{V_+} = -\frac{\boxed{}}{I_+}$$